STUDIES OF INFRARED SPECTRA OF ISOLATED BIOMOLECULES

By

Ismael Scott-Lebron

A DISSERTATION PRESENTED TO THE GRADUATE SCHOOL
OF THE UNIVERSITY OF FLORIDA IN
PARTIAL FULFILLMENT OF THE REQUIREMENTS
FOR THE DEGREE OF DOCTOR OF PHILOSOPHY

UNIVERSITY OF FLORIDA
1986

To

Evelyn, Christian and Krystina

ACKNOWLEDGMENTS

I would like to express my sincerest appreciation to Professor Willis B. Person for his guidance, encouragement, and patience through the course of this research.

I am grateful to Dr. Krystyna Szczepaniak of the Polish Academy of Sciences (Warsaw, Poland) for providing matrix-isolation infrared spectra of uracils and also for her friendship and helpful discussions. Thanks are due to Dr. Steven Chin for doing the ab initio calculation for the atomic polar tensors of uracil.

I wish to thank also the past and present members of Dr. Person's research group for their friendship and moral support over the past few years. Special thanks are due to Mr. Luis A. Hernandez for helping with the typing of this manuscript.

The support from the Graduate School of the University of Florida (G-POP program) is gratefully acknowledged, as well as the support from the National Institutes of Health (Grant No. GM32988) and from the National Science Foundation (Grant No. CHE 81-01131).

TABLE OF CONTENTS

LIST OF TABLES

LIST OF FIGURES

Abstract of Dissertation Presented to the Graduate School
of the University of Florida in Partial Fulfillment of the
Requirements for the Degree of Doctor of Philosophy

STUDIES OF INFRARED SPECTRA OF
ISOLATED BIOMOLECULES

By

Ismael Scott-Lebron

May 1986

Chairman: Willis B. Person
Major Department: Chemistry

The infrared spectra of uracil and methylated uracils have been interpreted by carrying out theoretical predictions of these spectra for such biomolecular systems. The infrared spectra for these molecules isolated in noble gas matrices are interpreted by comparison with the predicted spectra. These predictions are made using force constants and intensity parameters (Atomic Polar Tensors) from quantum mechanical ab initio calculations with a 4-31G basis set for the in-plane modes of these uracils.

The infrared frequencies and intensities of the methylated uracils are predicted transferring vibrational parameters from other molecules. The absolute intensities predicted for these molecules are compared with the experimental relative intensities, which were obtained in matrices. Comparisons of ab initio and semi-empirical force constants are discussed, as well as intensity parameters.

The comparison of the transferred atomic polar tensors and of the force constants from quantum mechanical calculations is discussed for each of the following molecules: 1-methyluracil, 1-methyl-3-D-uracil, 3-methyluracil, and 1,3-dimethyluracil. This comparison shows that atomic polar tensors transferred from uracil, acetone and N-methyl-acetamide predict the observed intensities of the methylated uracils within the usual "factor-of-two". Also, the scaled ab initio force constants reproduce the experimental wavenumbers of a molecule within about 20 cm^{-1}.

CHAPTER 1
INTRODUCTION

In recent years, vibrational spectroscopy has proven to be a powerful tool in biophysical research on nucleic acids (1-6). In particular, infrared and Raman spectra have played a critical role in the study of molecular structures and dynamical properties of nucleosides, nucleotides, and the constituent bases of nucleic acids (2,4,6). However, the full power of infrared and Raman spectroscopy depends not only on obtaining spectra of such biomolecules, but on the most accurate interpretation of their spectra. In order to properly accomplish this purpose, it is essential first to obtain, and then to understand, the details of the spectra for the isolated non-interacting monomeric molecules. It is then required that these experimental data be complemented with theoretical calculations. This procedure leads to the establishment of correlations between spectral changes which occur from the isolated molecule to molecules placed in more and more strongly interacting environments.

It is well known that nucleic acids are important constituents of all living cells because they are the biomolecules which carry and transmit genetic information used in the synthesis of the cellular proteins (7,8). Depending upon the molecular structure of their constituent sugars, nucleic acids may be divided into two distinct classes, ribonucleic acid (RNA) or deoxyribonucleic acid (DNA). In RNA the sugar is D-ribofuranose and in DNA is 2-deoxy-D-ribofuranose. Both RNA and

DNA are the result of successive linking of alternating simple units consisting of phosphoric acid, sugar residues, and purine or pyrimidine bases (7). These simple units, which are called nucleotides, have the general structure given in Fig. 1-1(a) for a ribonucleotide. For a deoxyribonucleotide the OH group attached to C2' in the ribose ring is replaced by an H atom. Thus, a nucleotide is a phosphate ester of a nucleoside, like uridine (Fig. 1-1(b)).

It is known that the genetic code consists of 64 triplet combinations (codons) of nucleotides, as shown in Fig. 1-2. Of the 64 possible combinations, 61 of them specify particular amino acids (7). The sequence of codons in messenger-RNA (mRNA) is translated to the sequence of amino acids in the protein biosynthesis, making possible the biological process of transmission of genetic information. If one of the bases in a codon is substituted by another, (e.g., CGU is changed to CAG (Fig. 1-2)), then a mutation occurs because this new codon would code for a different amino acid in the cell (8).

As seen in Fig. 1-2 one very important nucleoside in the genetic code is uridine (base = uracil) which is present in 37 of the 64 possible codons. Because of the central role that uridine plays on the transmission of genetic information, it is essential to understand its molecular structure in complete detail. For this it is important to carry out studies of its isolated molecular components in order to understand their interactions with other molecules. Further, the systematic study of the structural and dynamical properties of these molecules represents an interesting problem in its own rights.

We shall be concerned in this dissertation with the study of the uracil base and some of its methylated derivatives. Specifically we

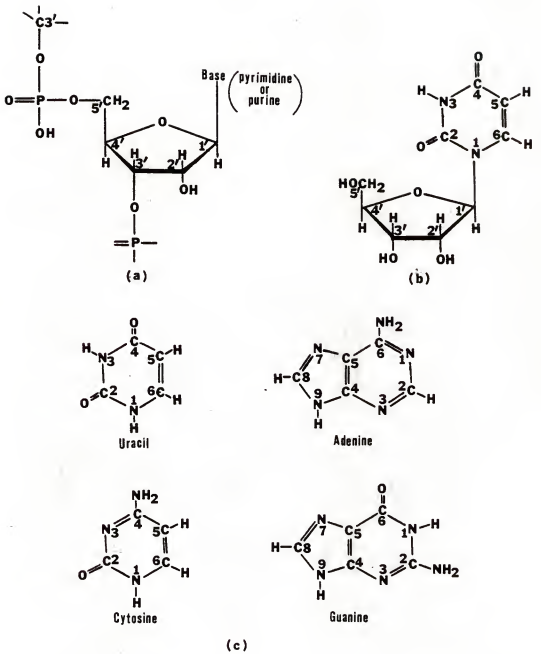

Figure 1-1. Molecular structures of nucleic acid constituents.
(a) General structure of a ribonucleotide. When the OH group in position C2' of the ring system is replaced by H, then it is a deoxyribonucleotide.
(b) Structure of uridine (a ribonucleoside).
(c) Usual pyrimidine (uracil and cytosine) and purine (adenine and guanine) bases. To form the nucleotide or nucleoside, the N1 atom of the pyrimidine or the N9 atom of the purine is attached to the C1' atom of the ribose sugar.

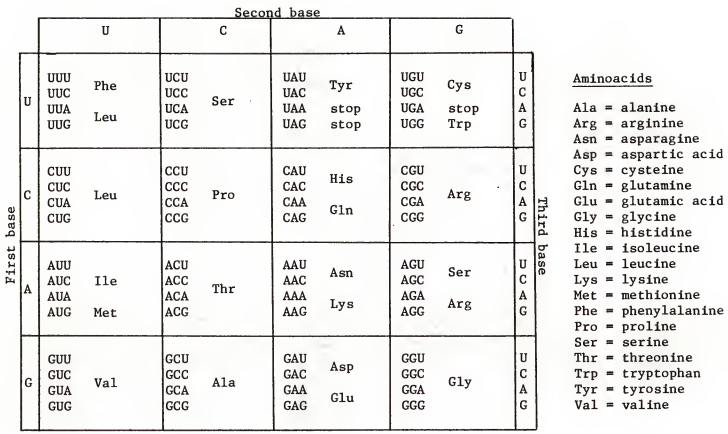

Figure 1-2. The genetic code. Here U, C, A, and G stand for uracil, cytosine, adenine, and guanine bases, respectively. These are the bases in the nucleotides, which constitute the codons.

shall be concerned with the infrared frequencies and intensities of isolated uracils, and in particular we shall carry out normal coordinate analysis calculations for the in-plane vibrations of these molecules, using these together with the dipole moment derivatives to predict quantitatively their infrared spectra. Then the calculated and experimental spectra for the isolated molecules will be compared so that more reliable assignments can be made for the observed spectra.

We believe the study of the methylated uracils to be of considerable importance; in particular 1-methyluracil, because this molecule is more representative spectroscopically of the base in the uridylate nucleotide or uridine nucleoside than uracil itself, since the heavy methyl group has almost the same effect on the uracil base vibrations as does the ribose sugar. The study of the other methylated uracils is also of importance because they provide useful tests of the procedure used for assignment of 1-methyluracil and their spectra provide insight as to changes expected when the structure changes slightly. Also, the changes in the spectrum of 1,3-dimethyluracil from matrix-isolated molecule to solid provide some insight as to the effect of stacking interactions, since this molecule is free of hydrogen bonding, which dominates the same changes in the spectra of the other molecules.

Historical Perspective

A considerable number of studies dealing with the infrared and Raman spectra of uracil, its isotopic derivatives (deuterated, ^{15}N and ^{18}O), and its methylated derivatives have been reported (1-6,8-20). We shall review here briefly some of these studies, in particular those in which an interpretation of the spectra has been made by means of normal coordinate analyses (NCAs).

An extensive study by Angell (9) reported the infrared spectra in the solid state of uracil, cytosine, adenine, and guanine bases, of ribose and deoxyribose nucleosides derived from these bases, and of some mononucleotides. He found that in the case of uracil and cytosine, only small changes occurred in the part of the spectrum from the base residue when a sugar group was added. He observed a number of strong bands in the spectrum of the nucleoside between 900 - 1200 cm^{-1} which are characteristic of the sugar residue. Upon addition of phosphate group to uridine there was relatively little change in the bands due to the uridine. He also found that the spectra of uridine, cytidine, adenosine and thymidine do not change from that for the solid when the compounds are dissolved in water. According to Angell (9) this finding is important when one attempts to extend the results from simple compounds in the solid state to the spectra of nucleic acids that usually exist in a highly hydrated state.

The rather exhaustive Raman spectral studies of Lord and Thomas (10,11) showed that uracil and its derivatives in any given environment have similar Raman lines in the 1500 - 1800 cm^{-1} region regardless of the substituents at position N_1 (see Fig. 1-1(c)). They interpreted the Raman spectra of these molecules in terms of changes in molecular structure produced by changes in pH, pD and state of aggregation. In this study an analogy was established between the observed Raman spectra of uridine, 1-methyluracil and 1,3-dimethyluracil. They found that the Raman spectra as a function of pH of these methylated uracils resemble those of uridine.

In the study by Susi and Ard (12) laser-Raman and infrared spectra of polycrystalline uracil, N,N-dideutero-, C,C-dideutero-, and perdeu-

tero uracil were obtained. In order to make assignments of these spectra, they carried out NCAs for the planar modes, which were described in terms of potential energy distributions and Cartesian displacements. For this calculation they constructed a 23 parameter valence force field by a least-squares refinement procedure, starting by transferring force constants from other molecules, for example acetone, to uracil. This force field reproduced 83 observed frequencies for uracil and its deuterated derivatives, with an average error of 8 cm^{-1}.

More NCAs were carried out for pyrimidine derivatives by Susi and Ard (13). These included cytosine, thymine, 1-methyluracil, and some deutero derivatives of these molecules. Again, as they did in their uracil study, a refinement of 42 force constants was made to fit observed frequencies, and the average frequency error ranged from 12 - 18 cm^{-1}. They pointed out that an empirical assignment for methylated pyrimidine derivatives is next to impossible because of pronounced coupling between ring stretching modes and methyl group stretching and deformation modes.

Detailed studies on pyrimidine bases were conducted by Tsuboi, Takahashi, and Harada (1). For uracil, cytosine, adenine and guanine bases, as well as for some of their methylated and methylated-deuterated derivatives, they obtained Raman, preresonance Raman and infrared spectra. These experimental spectra were then compared with those of different types of uridine phosphoric acids, for example, ß-uridine-5'-phosphoric acid. Also, they carried out NCAs for these molecules, including ^{15}N and ^{18}O isotopic shifts, at two different levels of approximation assuming that some groups behave as single dynamical

units. The purpose of these approximations was to simplify the vibrational problem to one with less atoms. They were able to characterize Raman lines or infrared bands describing the normal modes in terms of potential energy distributions. The force constants which they used in their calculation were obtained by a refinement procedure.

In their study of the normal modes of vibration in the uracil residue of β-uridine-5'-phosphoric acid Nishimura, Hirakawa, and Tsuboi (6) used frequency shifts measured for a set of ^{15}N isotope derivatives to interpret the observed vibrational spectrum of uracil. They found that the N-H in-plane deformations are extremely sensitive to the ^{15}N substitution. The agreement between the observed and calculated ^{15}N-isotope shifts was good except for the 1397, 1689, 1464, and 1402 cm^{-1} resonance Raman lines of uracil. They explained that this disagreement in ^{15}N-shifts for these four lines could be attributed to anharmonicity, Fermi resonance, and vibrational couplings with the solvent molecules, factors which were not taken into consideration in their calculation. For their NCA this time they began with force constants transferred to uracil from benzene.

Very recently, a study of the in-plane vibrational modes in uracil using an ab initio quantum mechanical calculation was made by Nishimura, Tsuboi, Kato, and Morokuma (14). A force field was obtained with calculation using the STO-3G basis set, which was then scaled to that expected for a 4-31G basis set, using various scaling factors estimated from results for other molecules (acrolein, urea, and formamide). In their NCA calculation this "corrected to 4-31G force field" could reproduce observed frequencies of uracil, 1,3-dideutero-, 5,6-dideu-

tero-, and perdeutero-uracil, except that the calculated normal frequencies are 8 % (on the average) greater than the observed frequencies. However, they found that all of the 21 in-plane calculated frequencies were readily correlated with the observed frequencies, and that the calculated normal modes of vibrations were not contradictory with the available experimental data.

In order to study the band-splittings in the double bond region of the spectra of uracil and methylated uracils, Bandekar and Zundel (3) obtained the infrared and Raman spectra of these molecules in solution and solid phase. Then they carried out a NCA calculation to assign these spectra, using a force field obtained by a least-squares refinement procedure. They proposed that the concept of transition dipole-dipole coupling (3) could explain the observed splitting of the C=O double bond stretching mode in these molecules.

Another NCA was made by Bowman and Spiro (15) on the in-plane vibrations of uracil and three isotopic molecules (N,N-dideutero-, C,C-dideutero-, and perdeutero-uracil) using a semi-empirical molecular orbital calculation (MNDO) to obtain a force field for uracil. This was refined to reproduce 81 observed frequencies with a mean error of 9.7 cm^{-1}. Then they applied this force field to interpret the vibrational spectra of the isoalloxazine ring of flavin.

Recently, experimental infrared spectral studies of uracil and some of its deuterated derivatives have been made for the matrix-isolated molecules by Maltese, Passerini, Nunziante-Cesaro, Dobos and Harsanyi (2), by Barnes, Stuckey, and Le Gall (5), and by Szczesniak, Nowak, Rostkowska, Szczepaniak, Person, and Shugar (16). Matrix isolation spectroscopy provides a unique method for study of vibra-

tional spectra of monomeric uracil molecules under conditions where interaction between molecules, and their rotational motions, are minimized (16-20). This technique consists in trapping the uracil molecule in an inert solid matrix (argon, xenon, krypton or nitrogen) at 10 K, and obtaining its spectrum. Raising the concentration allows the changes in the spectrum resulting from intermolecular hydrogen bonding to be observed (20). The assignments to the spectra by Maltese et al. (2), Barnes et al. (5) and Szczesniak et al. (16) will be considered in detail and compared in Chapter 4.

Finally, in a recent study Lewis, Miles, and Becker (4) obtained the infrared and Raman spectra in solid phase of 1-methyluracil and seven isotopic derivatives (^{2}H and ^{18}O). In an attempt to distinguish in-plane and out-of-plane modes they studied polarized Raman and infrared spectra of single crystals. Their vibrational assignments are in quite good agreement with previous studies.

Features of the Present Study

In this study we shall attempt to interpret the experimental matrix-isolated spectra of uracils, including some methylated derivatives, by carrying out NCA calculations using force constants obtained at the ab initio level. In the past, as described in the previous section, most of the spectroscopic studies of uracils were made on solid samples or solutions, resulting in broad infrared spectra in which overlapping bands are not resolved, due to intermolecular hydrogen bonding, interactions with polar solvents, etc. The advantage of using matrix-isolation infrared spectroscopic data is that the spectra of uracils are expected in general to be equivalent to the pure vibrational spectra for the isolated monomeric molecules; hence they

can be compared directly with vibrational spectra predicted theoretically for the isolated molecule. Also, the use of complete force fields obtained at the ab initio level is more reliable for this calculation of theoretical spectra. This procedure is different from many of the previous studies of uracils, where valence force constants were in some instances arbitrary values forced to fit the experimental frequencies. Evenmore, very few interaction force constants could be evaluated in those studies. All these aspects will be considered in great detail in Chapters 2 and 4.

A very important aspect of this dissertation involves the transfer of vibrational parameters -- force constants and atomic polar tensors (APTs). The APTs are intensity parameters which relate the dipole moment derivatives, obtained in an ab initio calculation, and the absolute infrared intensities, as will be discussed in Chapters 2 and 3. We transfer ab initio force constants and APTs obtained for uracil and other molecules (acetone, N-methylformamide, and N-methylacetamide) to make predictions of frequencies and intensities of the methylated uracil molecules. This calculation will be carried at two levels of approximation: one in which the methyl group is treated as a single dynamical unit, and other in which it is properly treated as a four-atom unit. We will compare the predicted results with the experimental infrared spectra. In Chapter 5 we will examine the transfer of vibrational parameters, and in Chapter 6 we will apply the transfer of these parameters to predict the spectra of the methylated uracils.

Another feature of the present study is that we predict the absolute infrared intensities in the infrared spectra. Then, we are able to compare the observed spectra of the uracils with both calculated

frequencies and intensities. Therefore, we can be confident that most of our assignments are correct. An illustration of the calculations for uracil will be given in Chapters 3 and 4.

CHAPTER 2
TECHNIQUES

This chapter deals with the experimental as well as with the theoretical methods followed in the present study. We shall first describe the experimental procedures that were used to obtain the infrared-active frequencies and intensities of matrix isolated uracil and its derivatives. This is followed by a brief description of the calculation for predicting the vibrational spectra of the same molecules. Since these experimental and theoretical techniques have been discussed in detail elsewhere (explicit references are given later in this chapter) our presentation will emphasize only those considerations that apply to the present work.

Experimental Studies of Infrared Spectra of Matrix-Isolated Species

The experimental matrix isolation infrared spectroscopic data used in this study were obtained by K. Szczepaniak and coworkers (M. J. Nowak, M. Szczesniak and H. Rostkowska) in their laboratory at the Institute of Physics of the Polish Academy of Sciences in Warsaw, Poland. The experimental procedure which they employed to obtain the observed frequencies and relative intensities of the infrared spectrum of uracil and its methylated derivatives isolated in noble gas matrices has been described in Refs. 16 to 20.

A brief qualitative summary is that uracil was isolated in different matrices (argon, krypton, xenon, and nitrogen), and methylated uracils in

argon and nitrogen, at matrix-to-solute ratios of about 1000 : 1, at a temperature of approximately 10 K. Then the infrared spectra of these matrices were recorded on a Perkin-Elmer 580B spectrometer at a resolution of 1 cm^{-1}. No evidence of H-bonding (for example, to form dimers) was found in these spectra, indicating that the species present in these matrices are the isolated monomers.

Calculation of Vibrational Spectra

In order to calculate the vibrational frequencies of a molecule, the vibrational eigenvalue secular equation must be solved:

$$\underset{\sim}{GFL} = \underset{\sim}{L\Lambda} \quad . \tag{2-1}$$

Here $\underset{\sim}{G}$ is the inverse kinetic energy matrix, $\underset{\sim}{F}$ the force constants matrix, $\underset{\sim}{L}$ the tranformation matrix between the internal coordinates and the normal coordinates, and $\underset{\sim}{\Lambda}$ the eigenvalue matrix of the frequency parameters ($\lambda_i = 4\pi^2c^2\nu_i^2$, where c is the speed of light constant in cm sec^{-1} and ν_i the wavenumber in cm^{-1}; it follows that $\nu_i(cm^{-1}) = 1303.1\sqrt{\lambda_i}$). Here the secular equation (Eq. (2-1)) has been set-up following the well-known GF matrix method by Wilson, Decius and Cross (21), and it can be solved by methods they described. Alternatively, Miyazawa (22) has described a simpler method to solve this equation based on symmetry considerations. In our discussion we shall follow Miyazawa's method.

While we calculate the vibrational frequencies of the molecule under study, by finding the eigenvalues of Eq. (2-1), it is desirable, as well, to obtain some prediction of the absolute infrared intensities for each fundamental band. Comparison of both the calculated frequencies and intensities with the observed spectrum will aid in the correct assignment of the latter.

The atomic polar tensors (APTs) for the atoms in the molecule being studied are the parameters that determine the infrared intensities. These APTs are the derivatives of the dipole moment with respect to displacements of the atoms in a fixed-Cartesian coordinate system (23). In this section we shall describe the use of the APTs to calculate the absolute infrared intensities for the fundamental vibrational modes of a molecule.

Vibrational Frequencies

The fundamental frequencies of a molecule are calculated by a normal coordinate analysis (NCA) to obtain the solution of the secular Eq. (2-1). The NCA is a rather involved subject which has been discussed elsewhere in great detail (21,24-26), so here only the general procedure will be described. For a nonlinear polyatomic molecule with N atoms there are 3N - 6 normal modes of vibration (3N - 5 if the molecule is linear). By using the molecular symmetry it is possible to identify and classify these modes of vibration into their symmetry group species (24), as will be considered below.

It will be convenient to point out several important coordinate transformations that appear in the NCA. These have been summarized in Table 2-1. For example, it is shown there that the transformation from space-fixed Cartesian displacement coordinates, $\underset{\sim}{X}$, to molecule-fixed internal displacement coordinates, $\underset{\sim}{R}$, is given by

$$\underset{\sim}{R} = \underset{\sim\sim}{B}\underset{\sim}{X} \qquad (2\text{-}2)$$

where $\underset{\sim\sim}{B}$ is a (3N - 6) x 3N matrix. Taking advantage of any symmetry that the molecule may have, and using the sets of $\underset{\sim}{R}$ internal coordinates as basis functions, we apply the projection operator technique (27) to set up linear combinations of the internal coordinates that are proper

TABLE 2-1
COORDINATE TRANSFORMATIONS

	Cartesian	Internal	Symmetry	Normal
Coordinates	$\underset{\sim}{X}$	$\underset{\sim}{R}$	$\underset{\sim}{S}$	Q
	$\underset{\sim}{R} = \underset{\sim}{B}\underset{\sim}{X}$	$\underset{\sim}{S} = \underset{\sim}{U}\underset{\sim}{R}$	$Q = \underset{\sim}{L}^{-1}\underset{\sim}{S}$; $\underset{\sim}{S} = \underset{\sim}{L}Q$	
	$\underset{\sim}{X} = \underset{\sim}{A}\underset{\sim}{R}$		$Q = \underset{\sim}{L}^{-1}\underset{\sim}{U}\underset{\sim}{R} = \ell_s^{-1}R$	
			$Q = \underset{\sim}{L}^{-1}\underset{\sim}{U}\underset{\sim}{B}\underset{\sim}{X} = \underset{\sim}{\ell}^{\dagger}\underset{\sim}{q}$	
			$= \underset{\sim}{\ell}^{\dagger}\underset{\sim}{M}^{\frac{1}{2}}\underset{\sim}{X}$	
Kinetic Energy $2T$ =	$\dot{\underset{\sim}{X}}^{\dagger}\underset{\sim}{M}\dot{\underset{\sim}{X}}$	$\dot{\underset{\sim}{R}}^{\dagger}\underset{\sim}{G}^{-1}\dot{\underset{\sim}{R}}$	$\dot{\underset{\sim}{S}}^{\dagger}\underset{\sim}{G}_s^{-1}\dot{\underset{\sim}{S}}$	$\dot{Q}^{\dagger}\dot{Q}$
	$\underset{\sim}{G}_I = \underset{\sim}{B}\underset{\sim}{M}^{-1}\underset{\sim}{B}^{\dagger}$	$\underset{\sim}{G}_s = \underset{\sim}{U}\underset{\sim}{G}_I\underset{\sim}{U}^{\dagger}$	$\underset{\sim}{A} = \underset{\sim}{M}^{-1}\underset{\sim}{B}^{\dagger}\underset{\sim}{G}^{-1}$	
			$\underset{\sim}{A}\underset{\sim}{B} = \underset{\sim}{E}$	
Potential Energy $2V$ =	$\underset{\sim}{x}^{\dagger}\underset{\sim}{F}_x\underset{\sim}{X}$	$\underset{\sim}{R}^{\dagger}\underset{\sim}{F}_r\underset{\sim}{R}$	$\underset{\sim}{S}^{\dagger}\underset{\sim}{F}_s\underset{\sim}{S}$	$Q^{\dagger}\Lambda Q$

symmetry adapted functions transforming according to the appropriate irreducible representations of the symmetry point group of the molecule. The transformation from the internal coordinates $\underset{\sim}{R}$ to the symmetry coordinates $\underset{\sim}{S}$ is then expressed as

$$\underset{\sim}{S} = \underset{\sim}{U}\underset{\sim}{R} \tag{2-3}$$

where $\underset{\sim}{U}$ is a (3N - 6) x (3N - 6) orthogonal matrix, when existing redundancies have been eliminated. The redundancy problem will be explicitly dealt with when we describe the in-plane symmetry coordinates of uracil and of the methylated uracils. In terms of the $\underset{\sim}{S}$ symmetry coordinates, the $\underset{\sim}{G}_S$ and $\underset{\sim}{F}_S$ matrices of the vibrational equation (Eq. (2-1)) are block factored, where each symmetry block is associated only with the subset of symmetry coordinates which transform according to the same irreducible representation of the molecular point group.

Another important relation shown in Table 2-1 is

$$\underset{\sim}{Q} = \underset{\sim}{L}_S^{-1}\underset{\sim}{S} \tag{2-4}$$

where the symmetry coordinates $\underset{\sim}{S}$ are transformed to normal coordinates $\underset{\sim}{Q}$ by $\underset{\sim}{L}_S^{-1}$, which is the inverse of the normal coordinate transformation matrix $\underset{\sim}{L}_S$. From Eq. (2-1) it can be seen that this $\underset{\sim}{L}_S$ matrix is the eigenvector matrix obtained from the solution of the vibrational secular equation.

Overall transformations between coordinates are also given in Table 2-1. For example, the transformation from Cartesian coordinates $\underset{\sim}{X}$ to normal coordinates $\underset{\sim}{Q}$ is

$$\underset{\sim}{Q} = \underset{\sim}{L}_S^{-1}\underset{\sim}{U}\underset{\sim}{B}\underset{\sim}{X} = \underset{\sim}{\ell}^{\dagger}\underset{\sim}{M}^{\frac{1}{2}}\underset{\sim}{X} \tag{2-5}$$

where the matrices in the first part have been defined previously in this section, and $\underset{\sim}{\ell}^{\dagger}$ is the transpose (equal to the inverse since $\underset{\sim}{\ell}$ is orthogonal) of the normal coordinate transformation matrix $\underset{\sim}{\ell}$ from

mass-weighted Cartesian coordinates $\underset{\sim}{q}$ to normal coordinates $\underset{\sim}{Q}$, and $\underset{\sim}{M}^{\frac{1}{2}}$ is a diagonal matrix whose elements are the square roots of the mass of each atom (28). Also found in this table are expressions for the kinetic and potential energy functions in terms of the various coordinate systems. For example, the relation

$$2T = \dot{\underset{\sim}{X}}^{+}\underset{\sim}{M}\dot{\underset{\sim}{X}} \qquad (2\text{-}6)$$

gives the kinetic energy in terms of the time derivatives (velocities) of the Cartesian coordinates $\dot{\underset{\sim}{X}}$, the diagonal $\underset{\sim}{M}$ matrix defined above, and the transpose of $\dot{\underset{\sim}{X}}$, written as $\dot{\underset{\sim}{X}}^{+}$.

Two important matrices in the NCA are the $\underset{\sim}{G}$ and the $\underset{\sim}{A}$ matrices. The first one is defined as

$$\underset{\sim}{G} = \underset{\sim}{B}\underset{\sim}{M}^{-1}\underset{\sim}{B}^{+} \quad . \qquad (2\text{-}7)$$

Here $\underset{\sim}{B}$ is the transformation matrix given by Eq. (2-2), $\underset{\sim}{B}^{+}$ its transpose and $\underset{\sim}{M}^{-1}$ the inverse of the diagonal $\underset{\sim}{M}$ matrix. The dimensions for the unsymmetrized $\underset{\sim}{G}$ matrix are (3N - 6) x (3N - 6). The $\underset{\sim}{A}$ matrix, of dimensions 3N x (3N - 6), transforms the internal coordinates $\underset{\sim}{R}$ into the Cartesian coordinates $\underset{\sim}{X}$

$$\underset{\sim}{X} = \underset{\sim}{A}\underset{\sim}{R} \quad . \qquad (2\text{-}8)$$

Substitution of $\underset{\sim}{R} = \underset{\sim}{B}\underset{\sim}{X}$ (Eq. (2-2)) gives

$$\underset{\sim}{X} = \underset{\sim}{A}\underset{\sim}{B}\underset{\sim}{X} \quad . \qquad (2\text{-}9)$$

Therefore,

$$\underset{\sim}{A}\underset{\sim}{B} = \underset{\sim}{I} \qquad (2\text{-}10)$$

where $\underset{\sim}{I}$ is the 3N x 3N unit matrix. Premultiplying $\underset{\sim}{G}$ in Eq. (2-7) by $\underset{\sim}{A}$ gives

$$\underset{\sim}{A}\underset{\sim}{G} = \underset{\sim}{A}\underset{\sim}{B}\underset{\sim}{M}^{-1}\underset{\sim}{B}^{+} = \underset{\sim}{M}^{-1}\underset{\sim}{B}^{+} \qquad (2\text{-}11)$$

or

$$\underset{\sim}{A} = \underset{\sim}{M}^{-1}\underset{\sim}{B}^{+}\underset{\sim}{G}^{-1} \quad . \qquad (2\text{-}12)$$

The vibrational secular equation in terms of internal coordinates (Eq. (2-1)) is most conveniently set-up in symmetric form according to Miyazawa's method (22). The geometrical basis for this method was discussed by Person and Crawford (29). According to this method, first consider the equation

$$\underset{\sim}{G}\underset{\sim}{Y} = \underset{\sim}{Y}\underset{\sim}{T} \tag{2-13}$$

where $\underset{\sim}{Y}$ is the matrix of the eigenvectors, and $\underset{\sim}{T}$ is the diagonal eigenvalue matrix, of $\underset{\sim}{G}$. Since $\underset{\sim}{G}$ is a real symmetric matrix, $\underset{\sim}{Y}$ is orthogonal; thus

$$\underset{\sim}{G} = \underset{\sim}{Y}\underset{\sim}{T}\underset{\sim}{Y}^{\dagger} = \underset{\sim}{Y}\underset{\sim}{T}^{\frac{1}{2}}\underset{\sim}{T}^{\frac{1}{2}}\underset{\sim}{Y} = \underset{\sim}{W}\underset{\sim}{W}^{\dagger} \quad . \tag{2-14}$$

Here we have defined the (3N - 6) x (3N - 6) matrix $\underset{\sim}{W} = \underset{\sim}{Y}\underset{\sim}{T}^{\frac{1}{2}}$. Using Eq. (2-14) the secular equation in Eq. (2-1) can be written in the form

$$\underset{\sim}{W}\underset{\sim}{W}^{\dagger}\underset{\sim}{F}\underset{\sim}{L} = \underset{\sim}{L}\Lambda \tag{2-15}$$

or

$$\underset{\sim}{W}^{\dagger}\underset{\sim}{F}\underset{\sim}{W}(\underset{\sim}{W}^{-1}\underset{\sim}{L}) = (\underset{\sim}{W}^{-1}\underset{\sim}{L})\Lambda \quad . \tag{2-16}$$

If we define a new matrix $\underset{\sim}{C}$ as

$$\underset{\sim}{C} = \underset{\sim}{W}^{-1}\underset{\sim}{L} \quad , \tag{2-17}$$

Eq. (2-16) takes the form

$$\underset{\sim}{W}^{\dagger}\underset{\sim}{F}\underset{\sim}{W}\underset{\sim}{C} = \underset{\sim}{C}\Lambda \quad . \tag{2-18}$$

Defining also $\underset{\sim}{H}$ as

$$\underset{\sim}{H} = \underset{\sim}{W}^{\dagger}\underset{\sim}{F}\underset{\sim}{W} \quad , \tag{2-19}$$

Eq. (2-18) becomes

$$\underset{\sim}{H}\underset{\sim}{C} = \underset{\sim}{C}\Lambda \quad . \tag{2-20}$$

Hence, the solution of the secular equation (Eq. (2-1)) is simplified to finding an orthogonal matrix $\underset{\sim}{C}$ which diagonalizes the symmetric $\underset{\sim}{H}$

matrix, since it follows from Eq. (2-20) that

$$\underset{\sim}{\Lambda} = \underset{\sim}{C}^{+}\underset{\sim}{H}\underset{\sim}{C} \quad . \tag{2-21}$$

The solution of Eq. (2-1) is thus reduced to diagonalization first of the symmetric $\underset{\sim}{G}$ matrix (Eq. (2-14)), calculating $\underset{\sim}{W}$ and then $\underset{\sim}{H}$, and diagonalizing that symmetric matrix. Diagonalization methods for symmetrical matrices, based on iterative methods like Jacobi's (30), are very well suited for computer programs.

It is interesting to note that once the secular equation in symmetric form has been solved, the $\underset{\sim}{L}_S$ transformation matrix can be obtained from Eq. (2-17)

$$\underset{\sim}{L}_S = \underset{\sim}{W}_S\underset{\sim}{C}_S = \underset{\sim}{Y}_S\underset{\sim}{T}_S^{\frac{1}{2}}\underset{\sim}{C}_S \quad . \tag{2-22}$$

And from Eqs. (2-18) and (2-22)

$$\underset{\sim}{L}_S^{-1} = \underset{\sim}{\Lambda}_S^{-1}\underset{\sim}{L}_S^{+}\underset{\sim}{F}_S \quad . \tag{2-23}$$

The units that we use in the NCA deserve some discussion. The Cartesian displacement coordinates of the atoms are expressed in angstroms (Å, 1 Å = 10^{-8} cm), so the internal displacement coordinates for bond stretches (Δr) have units of Å and the internal coordinates for angle bends ($\Delta\theta$) are in radians. Hence, the $\underset{\sim}{B}$ matrix element for a bond stretch is dimensionless, while that for a bending internal coordinate will have units of $Å^{-1}$. Since we use atomic mass units (u, 1 u = 1.66056 x 10^{-27} kg) for the masses, the $\underset{\sim}{G}$ matrix elements all have units of u^{-1}. The units of the $\underset{\sim}{F}$ matrix are mdyne $Å^{-1}$ (= aJ $Å^{-2}$) for the force constants involving two stretches, mdyne Å for bend-bend elements, and mdyne for bend-stretch elements.

Potential Energy Distributions

After having carried out the NCA, it is useful to calculate what percentage of the potential energy associated with a given normal

coordinate is contributed by each symmetry coordinate. From Table 2-1, the potential energy 2V is given by

$$2V = \underset{\sim}{Q}^{\dagger}\underset{\sim}{\Lambda}\underset{\sim}{Q} \quad . \tag{2-24}$$

Since the eigenvalue matrix $\underset{\sim}{\Lambda}$ is given by

$$\underset{\sim}{\Lambda} = \underset{\sim}{L}^{\dagger}\underset{\sim}{F}\underset{\sim}{L} \quad , \tag{2-25}$$

substitution of this relation into Eq. (2-24) gives

$$2V = \underset{\sim}{Q}^{\dagger}\underset{\sim}{L}^{\dagger}\underset{\sim}{F}\underset{\sim}{L}\underset{\sim}{Q} \quad . \tag{2-26}$$

For the kth normal coordinate, whose frequency parameter is λ_k,

$$\lambda_k = \sum_{i,j} L_{ki}^{\dagger} F_{ij} L_{jk} = \sum_{i,j} F_{ij} L_{ik} L_{jk} \quad . \tag{2-27}$$

The total potential energy distribution (PED) for the kth normal coordinate Q_k was defined by Morino and Kuchitsu (31) as

$$V(Q_k) = (\tfrac{1}{2}) Q_k^2 \sum_{i,j} F_{ij} L_{ik} L_{jk} \quad , \tag{2-28}$$

using Eqs. (2-24) and (2-27). Examining the magnitudes of the terms contributing to the sum in Eq. (2-28), it is argued that in general, the value of $F_{ij}L_{ik}L_{jk}$ is large only when i = j. Thus, the $F_{ii}L_{ik}^2$ terms are usually the most important in determining the PEDs. Therefore, it has become conventional to define the percentage PED from the ith symmetry coordinate to be given by the ratio of $F_{ii}L_{ik}^2$ to the total sum $\sum_{i,j} F_{ij}L_{ik}L_{jk}$ (this sum is equal to λ_k) times 100

$$PED_{ik} = (F_{ii}L_{ik}^2/\lambda_k) \times 100 \quad . \tag{2-29}$$

Here, F_{ii} is the diagonal force field element associated with the ith symmetry coordinate, λ_k is the eigenvalue of the kth normal coordinate, and L_{ik} is an element from the normal coordinate transformation matrix $\underset{\sim}{L}$.

The PEDs provide information about the contribution of each symmetry coordinate i to the potential energy for the kth normal mode of vibration. With the aid of Eq. (2-29), we can determine whether all the symmetry coordinates contribute equally to the total potential energy of

a given normal coordinate or whether just a few predominate. It is a valuable guide to the interpretation of results from the NCA.

Infrared Intensities

The other aspect of the vibrational spectra that we want to consider is the absolute infrared intensity of each absorption band. For a normal vibrational mode k the absolute infrared intensity is proportional to the square of the molecular dipole moment derivative with respect to the kth normal coordinate (23). The components along the space-fixed Cartesian axes of the dipole moment derivatives with respect to the normal coordinates can be written as a 3 x (3N - 6) tensor, designated as $\underset{\sim}{P}_Q$. In order to interpret or to predict these values, the first thing to do is to calculate the APTs $\underset{\sim}{P}_X$ in the space-fixed Cartesian coordinate system. In the next section we will describe the method used to calculate $\underset{\sim}{P}_X$. Let us now describe the relationship between these tensors and the absolute infrared intensities.

The relation between $\underset{\sim}{P}_Q$ and $\underset{\sim}{P}_X$ is given by (32)

$$\underset{\sim}{P}_Q = \underset{\sim}{P}_X \underset{\sim}{A}\underset{\sim}{L} \qquad (2\text{-}30)$$

where the $\underset{\sim}{A}$ and $\underset{\sim}{L}$ matrices are obtained through the NCA, as previously described. The elements in $\underset{\sim}{P}_X$ have units of electrons (e), those in $\underset{\sim}{A}$ are unitless and those in $\underset{\sim}{L}$ have units of $u^{-\frac{1}{2}}$. The resulting units of $\underset{\sim}{P}_Q$ are $eu^{-\frac{1}{2}}$.

For absorption of light by a molecule during a transition from the i to the i + 1 vibrational state of the sth normal mode, the absolute absorption coefficient A_s is given by (33)

$$A_s = (8\pi^2 N_o \nu_s / 3hc) \sum_{i}^{g_s} |\langle i+1|\vec{p}|i\rangle|^2 \qquad (2\text{-}31)$$

where N_o is Avogadro's number, ν_s is the transition frequency in cm^{-1}, h is Planck's constant, c is the speed of light in cm sec^{-1}, $\vec{p}$ is the

dipole moment operator, and $\langle i+1|\vec{p}|i\rangle$ is the transition moment integral. The sum on $\underline{i}$ is over the g_s degenerate states; all of the vibrational modes in the uracils are singly degenerate ($g_s = 1$). Under the assumption that mechanical anharmonicity is small, the wavefunctions are perfect harmonic oscillator functions. After expanding the dipole moment in a Taylor's series in the normal coordinates Q

$$\vec{p} = \vec{p}^{\,o} + \sum_s (\partial\vec{p}/\partial Q_s)Q_s + \tfrac{1}{2}\sum_s\sum_j (\partial^2\vec{p}/\partial Q_s \partial Q_j)Q_s Q_j + \ldots \quad (2\text{-}32)$$

the second and higher order terms are neglected (assumption that there is no electrical anharmonicity), so

$$A_s = (N_o \pi g_s/3c^2)\,|\partial\vec{p}/\partial Q_s|^2 \quad . \quad (2\text{-}33)$$

Here $|\partial\vec{p}/\partial Q_s|^2$ is given by

$$|\partial\vec{p}/\partial Q_s|^2 = (\partial\vec{p}_x/\partial Q_s)^2 + (\partial\vec{p}_y/\partial Q_s)^2 + (\partial\vec{p}_z/\partial Q_s)^2 \quad (2\text{-}34)$$

where $|\partial\vec{p}/\partial Q_s|$ is the absolute value of the dipole moment vector derivative with respect to the sth normal coordinate, and $\partial\vec{p}_x/\partial Q_s$, $\partial\vec{p}_y/\partial Q_s$ and $\partial\vec{p}_z/\partial Q_s$ are the components of $\partial\vec{p}/\partial Q_s$ along each of the x, y and z space-fixed Cartesian axes.

Evaluation of the constants in Eq. (2-33) when A_s is in km mol^{-1} and $\partial\vec{p}/\partial Q_s$ in $eu^{-\frac{1}{2}}$ units gives (32)

$$A_s(\text{km mol}^{-1}) = 974.9\; g_s|\partial\vec{p}/\partial Q_s|^2 \quad . \quad (2\text{-}35)$$

Now the calculation of the absolute infrared intensities is straightforward. The calculated APTs in space-fixed Cartesian system ($\underline{P}_X$) are transformed into normal coordinate space ($\underline{P}_Q$) with the use of Eq. (2-30), where the $\underline{A}$ and $\underline{L}$ matrices have been obtained from the NCA. Then the $\underline{P}_Q$ values are substituted in Eq. (2-35) to get the $\underline{A}$ values in km mol^{-1}.

Calculation of Atomic Polar Tensors

The atomic polar tensors (APTs) for uracil were calculated by S. Chin using ab initio quantum mechanical methods (17,18). To summarize briefly, what was done was to calculate the wavefunctions, energy, and dipole moment components of uracil at the experimental equilibrium configuration (17) and then to repeat the calculation at the distorted geometries to obtain the dipole moment derivatives $\underset{\sim}{P}_S$ by the method of finite differences (34). These dipole derivatives are calculated with respect to a set of mass-weighted, molecule-fixed, principal Cartesian displacement coordinates $\underset{\sim}{S}$ orthogonal to the translations and rotations and reflecting the molecular symmetry (28). The orthogonality of the $\underset{\sim}{S}$ coordinates is ensured by defining them to be orthogonal to each other and to the six Eckart conditions (35,36), which define three translations ρ_t of the entire molecule, and three rotations ρ_r.

The APTs in the principal Cartesian coordinate system are given by the following equation (28,37)

$$\underset{\sim}{P}_x = (\underset{\sim}{P}_\rho | \underset{\sim}{P}_S) \underset{\sim}{LM}^{\frac{1}{2}} \tag{2-36}$$

where $\underset{\sim}{P}_\rho$ is a 3 x 6 matrix that consists of the translational and rotational corrections to the dipole moment derivatives (38), and is equal to

$$\underset{\sim}{P}_\rho = \begin{pmatrix} 0 & 0 & 0 & 0 & p^o{}_z/I_{yy}^{\frac{1}{2}} & -p^o{}_y/I_{zz}^{\frac{1}{2}} \\ 0 & 0 & 0 & -p^o{}_z/I_{xx}^{\frac{1}{2}} & 0 & p^o{}_x/I_{zz}^{\frac{1}{2}} \\ 0 & 0 & 0 & p^o{}_y/I_{xx}^{\frac{1}{2}} & -p^o{}_x/I_{yy}^{\frac{1}{2}} & 0 \end{pmatrix}. \tag{2-37}$$

Here, the p^os are the components of the permanent dipole moment along the principal Cartesian coordinate axes at equilibrium configuration; and I_{xx}, I_{yy} and I_{zz} are the principal moments of inertia. Also, in

Eq. (2-36) $\underset{\sim}{P}_S$ refers to the dipole derivatives with respect to the $\underset{\sim}{S}$ coordinates, defined as (28)

$$\underset{\sim}{P}_S = \begin{pmatrix} \partial p_x/\partial S_7 & \partial p_x/\partial S_8 & \partial p_x/\partial S_9 & \cdots & \partial p_x/\partial S_{3N} \\ \partial p_y/\partial S_7 & \partial p_y/\partial S_8 & \partial p_y/\partial S_9 & \cdots & \partial p_y/\partial S_{3N} \\ \partial p_z/\partial S_7 & \partial p_z/\partial S_8 & \partial p_z/\partial S_9 & \cdots & \partial p_z/\partial S_{3N} \end{pmatrix} \quad (2\text{-}38)$$

The $\underset{\sim}{U}$ matrix in Eq. (2-36) is the 3N x 3N orthogonal transformation matrix that transforms the mass-weighted principal Cartesian coordinates $\underset{\sim}{q}$ into the $\underset{\sim}{S}$ and $\underset{\sim}{\rho}$ coordinates, according to

$$\begin{pmatrix} \underset{\sim}{\rho} \\ \underset{\sim}{S} \end{pmatrix} = \underset{\sim}{U}\, \underset{\sim}{q} \quad . \quad (2\text{-}39)$$

The $\underset{\sim}{M}$ matrix has been defined previously.

Finally, the full polar tensor $\underset{\sim}{P}_x$ calculated by Eq. (2-36) is given by this general form (23,28,39)

$$\underset{\sim}{P}_x = \begin{pmatrix} \partial p_x/\partial X_1 & \partial p_x/\partial Y_1 & \partial p_x/\partial Z_1 & \partial p_x/\partial X_2 & \partial p_x/\partial Y_2 & \cdots & \partial p_x/\partial Z_N \\ \partial p_y/\partial X_1 & \partial p_y/\partial Y_1 & \partial p_y/\partial Z_1 & \partial p_y/\partial X_2 & \partial p_y/\partial Y_2 & \cdots & \partial p_y/\partial Z_N \\ \partial p_z/\partial X_1 & \partial p_z/\partial Y_1 & \partial p_z/\partial Z_1 & \partial p_z/\partial X_2 & \partial p_z/\partial Y_2 & \cdots & \partial p_z/\partial Z_N \end{pmatrix} \quad (2\text{-}40)$$

In this arrangement the first three columns contain the APT of the first atom, the next three the APT of the second, and so on.

A full account on the calculation of APTs can be found in references 38 and 39. We will describe some properties of APTs for uracil in Chapter 3.

Transfer of Parameters to Predict Infrared Spectra

Since we are interested in making quantitative predictions of the infrared spectra of the polyatomic methylated uracil molecules, we are particularly interested in the possibility of transferring vibrational parameters from similar smaller molecules or molecular fragments to succesfully achieve this purpose. The molecular parameters that may be

transferred are the force constants and the APTs. In the following discussion we shall describe how this technique was applied to the 1-methyluracil (1-Me U) molecule, as an illustration. First we will address the problem of the transfer of force constants, and later the transfer of APTs.

Transfer of ab initio force constants

Let us first consider a simple scheme to show how the transfer of vibrational parameters should work. In principle, we want to transfer the parameters from some molecules with similar structural fragments to the molecule under study. For the specific case of 1-Me U, Fig. 2-1 depicts in a schematic way the strategy to be followed in the transfer of parameters when the H_7 atom in uracil is replaced by a methyl group to form 1-Me U.

As seen in Fig. 2-1, two simple approaches, indicated as Calculation I and Calculation II, can be followed in the procedure. In Calculation I the methyl group is considered to be just a single dynamical unit of mass 15 u. In other words, 1-Me U is regarded as a 12 atom molecule, similar to the calculation of 1-deuterouracil (17). In Calculation II the methyl group is properly treated as a four-atom CH_3 unit, and the predictions for 1-Me U include the vibrations of the methyl group as well as those of the ring.

The force constants that we used in Calculation I, except for the N_1-Me values, were transferred from the ab initio calculation with the STO-3G basis set "converted" to values expected at the 4-31G level for uracil obtained (and described) by Nishimura, Tsuboi, Kato, and Morokuma (14). Of course, we expect that the force constants for the bonds in both rings (in uracil and 1-Me U) will have nearly the same

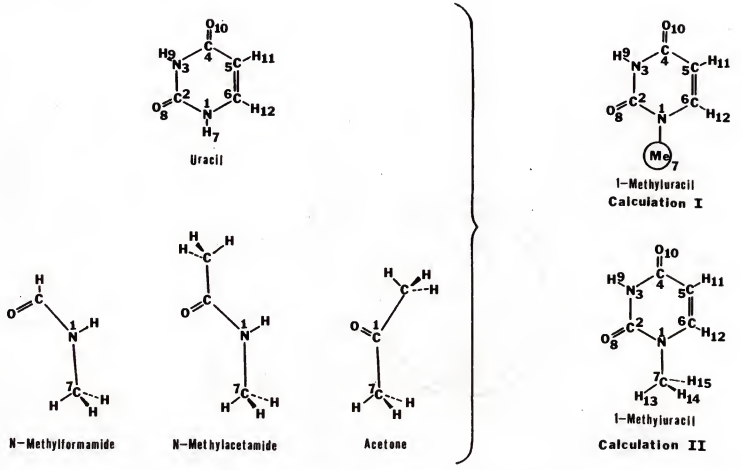

Figure 2-1. Scheme for Calculations I and II of 1-Methyluracil (1-Me U). Vibrational parameters (ab initio force constants and APTs) are transferred to 1-Me U from uracil, N-Methylformamide, N-Methylacetamide and/or acetone.

values, given their structural similarity. We assumed also that the structural parameters (bond distances and angles) of both rings are the same. For the N_1-Me bond the values for the stretching and bending force constants were transferred directly from the N_1-C_7 bond of N-methylformamide, from the ab initio calculation by Sugawara, Hirakawa, Tsuboi, Kato, and Morokuma (40). Also, we used the N_1-Me bond length that they reported as the experimental value. The interaction force constant values for the N_1-Me stretch with the ring stretches in 1-Me U were assumed to be the same as those between N_1-C_7 and the OCN group in N-methylformamide. In Chapter 4 we present the "ab initio STO-3G converted to 4-31G" force constants for uracil obtained by Nishimura et al. (14), and in Chapter 6 all the force constants (transferred from uracil and N-methylformamide) for the methylated uracils will be given.

In Calculation II the force constants for the pyrimidine ring of 1-Me U were again taken from the ab initio calculation by Nishimura et al. (14). For the sake of consistency, we decided to use force constants for the N_1-CH_3 fragment obtained by ab initio methods. For this purpose, the values that Sugawara et al. (40) obtained for N-methylformamide at the 4-31G level seemed very appropriate to use. Therefore, the set of force constants for the N_1-CH_3 group in N-methylformamide from their ab initio calculation (40) were transferred to the N_1-CH_3 group in 1-Me U.

The procedure just described was also used for 3-methyluracil and 1,3-dimethyluracil. All the resulting force fields are given in Chapter 6.

Transfer of APTs

For Calculation I we transferred directly all the atomic polar tensors from uracil to 1-Me U, including the APT for the Me unit, which is that for H_7 of uracil, so that the APTs satisfy the null condition (the sum of all the APTs of a molecule is the null tensor). Therefore, the problem of predicting intensities for 1-Me U in Calculation I is similar to that of predicting the intensities for one of the deuterated derivatives of uracil (17).

It should be pointed out that the assumption that the APT for H_7 atom of uracil is the same as that for the methyl group is not very realistic, so that Calculation I is expected to give only approximate results, for predicted intensities as well as for frequencies.

For Calculation II the H_7 atom in uracil is replaced by a CH_3 group to form 1-Me U. In doing this we considered that the APTs for the methyl ($—CH_3$) fragment could be taken from the atoms in the methyl group attached to the nitrogen atom in N-methylacetamide. Among other things, the CH_3 group in both molecules (1-Me U and N-methylacetamide) is attached to a nitrogen atom, with a C=O group as a neighbor bond. Also, the well known conjugate character of the C_7-N_1 bond in N-methylacetamide could be expected to give almost the same rigidity to that molecule as is found in the N_1-C_7 bond of 1-Me U (see scheme in Fig. 2-1 for the numbering of atoms). Accordingly, we decided to undertake a separate study of N-methylacetamide in order to obtain its APTs, and then transfer the APTs for the N-CH_3 group of this molecule to the N-CH_3 group of 1-Me U. We present the APTs for N-methylacetamide in Chapter 5.

As is also illustrated in the scheme in Fig. 2-1, we also tested the sensitivity of the predicted intensities to the APTs by calculating the intensities using the APTs of the $C-CH_3$ group of N-methylacetamide for the intensity parameters assumed for the N_1-CH_3 group of 1-Me U. Another calculation was done using the APTs transferred from the $C-CH_3$ groups of acetone, taken from Rogers (39).

Because the null condition must be satisfied in all the intensity predictions of Calculation II described above, we chose the APT for either N_1 or C_7 in order to satisfy it, transferring all other APTs from uracil, N-methylacetamide or acetone, and then compared the calculated intensities with the observed spectrum. Applying the appropriate rotation of the coordinates to these APTs made them transferable to 3-Me U and 1,3-di Me U. The different sets of APTs that were obtained for all these molecules will be given in Chapter 6.

CHAPTER 3
ATOMIC POLAR TENSORS

This chapter deals with the atomic polar tensors (APTs) for the uracil molecule and their use in the prediction of absolute infrared intensities for this molecule. Before considering any specific data, we shall review some additional aspects of atomic polar tensor theory. Then we shall present the calculated APTs for uracil, and review the predicted absolute infrared intensities for uracil and examine some sum rules. In particular we shall examine separately the total intensity for the in-plane modes and that for the out-of-plane vibrational modes, compared with the calculated ratio and with the experimental value of this ratio.

Further Theory of Infrared Intensities

As discussed in Chapter 2, the set of normal coordinates Q_δ describes the vibrational modes, and can be expressed in terms of symmetry coordinates (38) as

$$\partial\vec{p}/\partial Q_\delta = \sum_{i=1}^{3N-6} L_{i\delta}(\partial\vec{p}/\partial S_i) \qquad (3\text{-}1)$$

or conversely

$$\partial\vec{p}/\partial S_i = \sum_{i=1}^{3N-6} L_{\delta i}^{-1}(\partial\vec{p}/\partial Q_\delta) \qquad (3\text{-}2)$$

where $L_{i\delta}$ is the i,δ th element of the $\underset{\sim}{L}$ matrix, and $L_{\delta i}^{-1}$ is the δ,ith element of the inverse matrix of $\underset{\sim}{L}$.

Since we cannot determine the sign of $\partial\vec{p}/\partial Q_\delta$ by experiment, the use of Eq. (3-2) leads to more than one possible set of values for the dipole derivatives $\partial\vec{p}/\partial S_i$ (in fact to 2^{k-1} values, where k is the

number of terms (3N - 6) in the summation). The summation in Eq. (3-2) is made separately for all modes of a given symmetry; for a symmetry block with $\underline{k}$ modes, there will be 2^{k-1} possible sets of $\partial\vec{p}/\partial S_i$ values. In order to obtain information for the determination of the correct signs for these values, intensity data from isotopically substituted molecules are usually used (41). Also, the analysis of the Coriolis interactions of the molecule sometimes offers valuable information about such signs (42,43). Different research groups have demonstrated that one possible method of overcoming this signs problem lies in the use of quantum-mechanical calculations (38,44-47). In this dissertation we are using calculated APTs, with the signs from their calculation, to predict the derivatives in Eq. (3-1), so we do not have this sign problem, which arises when we use experimental intensities to derive values of $\partial\vec{p}/\partial S_i$.

A number of theories have been proposed for expressing $\partial\vec{p}/\partial Q_\delta$ in terms of parameters characterizing the individual bonds or atoms of the molecule. A great deal of interest during the last decade has concerned the development and application of such approaches to molecules in the gas phase (48). These include the valence-optical theory, developed by Gribov (49), Sverdlov et al. (50), Gussoni (51), and other workers (52-54). Here, the dipole moment is expressed as a sum of bond dipole moments all directed along their respective bonds. The components of these bond dipole moments and their derivatives with respect to the internal coordinates are called electrooptical parameters (eop's). The major problem with this approach is that it contains too many parameters (greater than the number of independent equations) to be evaluated from experiment, when used in its purest form. It can be

simplified, however, to give considerable insight for the interpretation of intensities (55). For a review on eop's see Ref. 51.

Some modifications to the valence-optical theory have been suggested (56-58). For example, in the hybrid orbital rehybridization model of Wiberg and Wendoloski (56) the $\partial\vec{p}/\partial Q_\delta$ values are described in terms of a contribution resulting from a geometric reorientation of the bond dipole moment, and a second term which describes the change in bond dipole moment due to orbital rehybridization. All the parameters involved in such terms are expressed as simple functions of the bond hybridization.

Other similar theories based on effective charges of bonds or atoms have been proposed (57,58). The bond dipole moment, as defined in the valence-optical theory, can be expressed as a product between an effective bond charge and the bond vector. Then, differentiation of the bond dipole moment with respect to the internal coordinates gives a bond charge derivative. This theory has been extensively developed and applied by Smit and van Straten (58).

Another intensity theory which has had considerable impact during recent years is the Atomic Polar Tensor theory (APT). It was suggested by Biarge, Herranz and Morcillo in 1961 (59), and reviewed, reformulated and extensively applied by Person and Newton (23,32,60). Reviews on the formulism and applications of this theory are found in Refs. 38, 48, and 54, and we shall summarize some aspects in the following discussion.

In the APT theory the components of the dipole moment derivatives are evaluated with respect to a space-fixed Cartesian coordinate system (Eq. (2-40)). An advantage with APTs is that, because they are expressed in space-fixed coordinates, they are now invariant to

isotopic substitution, so we can expect the APTs to transfer from one isotopic form of a molecule to another (38). Also, the APTs are calculated directly in the quantum mechanical calculations, which are usually made in a space-fixed coordinate system. A distinction between APTs and eop's is that APTs are "intensity parameters" that have a one-to-one relationship to the experimental intensity values. On the other hand, the eop's are useful to interpret these intensity parameters. Using group theory, Decius and Mast (57) proved that the number of independent parameters in the APTs for a molecule is the same as the number of equations used to determine them from the experimental data. This aspect of APTs has been discussed by Person (38) in more detail.

The APTs for each atom α (Eq. (2-40)), in a molecule composed of N atoms, are collected in the full 3 x 3N polar tensor $\underset{\sim}{P}_x$

$$\underset{\sim}{P}_x = \left[\underset{\sim}{P}_x^{\,1} \,\vdots\, \underset{\sim}{P}_x^{\,2} \,\vdots\, \underset{\sim}{P}_x^{\,\alpha} \,\vdots\, \ldots \,\vdots\, \underset{\sim}{P}_x^{\,N} \right] \quad . \qquad (3\text{-}3)$$

The expression of the APTs in space-fixed coordinates ($\underset{\sim}{P}_x$) is particularly useful because it is possible to transform them into normal coordinate space ($\underset{\sim}{P}_Q$) according to Eq. (2-30), and thus to obtain the predicted absolute intensities from $\underset{\sim}{P}_x$.

The APTs are always expressed relative to a particular Cartesian coordinate system. If the APT for an atom in one molecule is to be compared or transferred to the same kind of atom in another molecule, it is necessary to express both APTs in the same coordinate system. The "bond coordinate system" has proven to be a useful system for such purposes (60). In this system we define the positive x, y, or z direction to be along the bond in the direction from the central to the terminal atom for the two bonds in consideration.

In general, by applying an orthogonal rotation transformation $\underset{\sim}{T}$ the "bond coordinate axes" can be rotated with respect to the "molecular coordinate axes"; hence the APTs in one axes system are related to the APTs in the other system by (28)

$$\underset{\sim}{P}_x^{\alpha}(\text{new}) = \underset{\sim}{T}\{\underset{\sim}{P}_x^{\alpha}(\text{old})\}\underset{\sim}{T}^{\dagger} \quad . \tag{3-4}$$

Here $\underset{\sim}{T}$ is a transformation matrix ($\underset{\sim}{T}^{\dagger}$ is its transpose) whose elements are the cosines between the old and new axes.

In addition, the APTs for the N atoms in a molecule are also related through the null condition

$$\sum_{\alpha=1}^{N} \underset{\sim}{P}_x = \underset{\sim}{0} \tag{3-5}$$

which arises because the pure translation of a molecule does not alter the dipole moment vector of the molecule and hence a vanishing sum results (23).

The invariant APT properties (32,28,61) associated with absolute infrared intensities are the effective atomic charge χ_α, the mean dipole moment derivative $\bar{P}_\alpha$, and the atomic anisotropy β_α^2. An APT invariant is independent of the choice of the Cartesian coordinate system used. The effective charge χ_α is related to the APT by the following relation (32,61)

$$\chi_\alpha^2 = (1/3)\text{Tr}\{\underset{\sim}{P}_x^{\alpha}(\underset{\sim}{P}_x^{\alpha})^{\dagger}\} \tag{3-6}$$

where $\underset{\sim}{P}_x^{\alpha}$ is the APT for atom α, $(\underset{\sim}{P}_x^{\alpha})^{\dagger}$ its transposed form, and $\text{Tr}\{\underset{\sim}{A}\}$ designates the trace of the $\underset{\sim}{A}$ tensor. Actually, the right-hand-side of Eq. (3-6) is just one-third of the sum of the squares of all elements of the $\underset{\sim}{P}_x^{\alpha}$ tensor for the α atom.

The mean dipole moment derivative $\bar{P}_\alpha$ is given by (28,61)

$$\bar{P}_\alpha = (1/3)\text{Tr}\{\underset{\sim}{P}_x^{\alpha}\} \quad . \tag{3-7}$$

Also, the anisotropy β_α^2, which measures the deviation of $\underset{\sim}{P}_x$ from a

constant diagonal tensor of value $\bar{p}_\alpha$ is given by the following relationship (61)

$$\beta_\alpha^2 = (\tfrac{1}{2})\left[(p_{xx} - p_{yy})^2 + (p_{yy} - p_{zz})^2 + (p_{zz} - p_{xx})^2 + 3(p_{xy}^2 + p_{yz}^2 + p_{zx}^2 + p_{zy}^2 + p_{xz}^2 + p_{yx}^2)\right] \quad (3\text{-}8)$$

where, for example, p_{xz} stands for $\partial p_x/\partial Z$. The relation between χ_α, $\bar{p}_\alpha$ and β_α^2 is (61)

$$\chi_\alpha^2 = (\bar{p}_\alpha)^2 + (2/9)(\beta_\alpha)^2 \quad . \quad (3\text{-}9)$$

It has been found that χ_α is nearly the same for all hydrogen atoms of a number of hydrocarbons, with some exceptions (61). Indeed, King, Mast and Blanchette (62) suggested that the effective charge for an atom may be a transferable intensity parameter. Subsequent work (32,45,55) suggests this idea may be somewhat simplified, but it may be true for atoms in similar chemical environments. In a comparative study of effective atomic charges for hydrogen, fluorine and oxygen atoms in a series of compounds, King (61) concluded that χ_α values for these atoms in such diverse compounds do fall within a narrow ranges of values. These ranges are $\chi_H = 0.101 \pm 0.005$ e in all hydrocarbons except HCCH, $\chi_H = 0.072 \pm 0.012$ e in the methyl halides, $\chi_F = 0.595 \pm 0.039$ e, and $\chi_O = 0.624 \pm 0.099$ e. He pointed out that these results suggest that χ_α represents a particularly localized combination of chemical bond properties.

A useful expression relating the χ_α values for the atoms in a molecule to the sum of the absolute intensities for all the vibrational modes of that molecule, was derived by King, Mast and Blanchette (62)

$$\sum_{s=1}^{3N-6} A_s = (N_o\pi/3c^2)\left\{\sum_{\alpha=1}^{N} 3\chi_\alpha^2/m_\alpha - \Omega\right\} \quad . \quad (3\text{-}10)$$

Here, m_α is the mass of atom α, and Ω is the rotational correction (62)

$$\Omega = \mathrm{Tr}\left[\underline{P}_\rho(\underline{P}_\rho)^\dagger\right] \quad (3\text{-}11)$$

where $\underset{\sim}{P}_\rho$ was previously defined in Eq. (2-37). Evaluating Eq. (3-11), we find

$$\Omega = \left\{(p_z^o)^2/I_{xx} + (p_z^o)^2/I_{yy} + [(p_x^o)^2 + (p_y^o)^2]/I_{zz}\right\} + \left\{(p_y^o)^2/I_{xx} + (p_x^o)^2/I_{yy}\right\} \quad . \tag{3-12}$$

Each one of these quantities was defined earlier when we introduced Eq. (2-37).

In Eq. (3-10) the values of χ_α^2/m_α are usually in e^2u^{-1} units when the APT values are expressed in e units, and masses in atomic mass units (u). Hence, the terms in Ω must be evaluated using dipole moments in $e\mathring{A}$ ($1e\mathring{A}$ = 4.8 Debye) and moments of inertia in $u\mathring{A}^2$. When A_s is in units of km mol^{-1} King's intensity sum rule (Eq. (3-10)) becomes (32)

$$\sum_{s=1}^{3N-6} A_s \text{ (km mol}^{-1}) = 974.9\left\{\sum_\alpha 3\chi_\alpha^2/m_\alpha - \Omega\right\} \quad . \tag{3-13}$$

We can use a relationship similar to Eq. (3-13) for the sum of the infrared intensities of modes belonging to each species contained in the symmetry group to which the molecule belongs (63,64). We shall discuss this topic in more detail after presenting the APTs for uracil.

Finally, we should consider the quantum-mechanical description of the APTs given by King and Mast (65). They interpreted the APTs as the sum of three contributions: a net charge (calculated as the Mulliken charge), the charge flux, and the "interference", which is now called the "overlap" term (66). This treatment has been slightly modified by Zilles (66) to obtain this expression

$$\underset{\sim}{P}_x^\alpha = \underset{\sim}{P}_x^\alpha\text{(charge)} + \underset{\sim}{P}_x^\alpha\text{(charge flux)} + \underset{\sim}{P}_x^\alpha\text{(overlap)} \quad . \tag{3-14}$$

The physical significance of Eq. (3-14) is the following: $\underset{\sim}{P}_x^\alpha$(charge) is the contribution to the dipole derivative due to motion of the fixed equilibrium charge, $\underset{\sim}{P}_x^\alpha$(charge flux) is due to the change in

charge on all atoms that occurs when atom α is displaced, and the term P_x^{α} (overlap) arises primarily from the change in the "atomic dipoles" from the electron lone pairs as the α atom moves, as well as from the changes in atomic dipole contributions from the bonding electrons. The "atomic dipole" was defined by Coulson (67) as the contribution to the total dipole moment due to the displacement of the centroid of charge due to the electrons from the centroid of positive charge due to the nucleus of atom α. By examining the elements of all these components in this charge-charge flux-overlap (CCFO) model (66) it is possible to interpret the APTs and further analyze the intensity parameters of a molecular system. Each of the three component tensors also has invariant properties. The mathematical expressions for these quantities were developed by Chin (28). For the effective charge of the charge tensor he obtained

$$\chi^{\alpha}(C) = (1/3)\sum_i \left\{P^{\alpha}(C)_{ii}\right\}^2 \qquad (3\text{-}15)$$

where $P^{\alpha}(C)_{ii}$ is a diagonal term of the charge tensor for atom α, given by (66)

$$P^{\alpha}(C)_{ii} = Q_{\alpha} = N_{\alpha} - Z_{\alpha} \quad . \qquad (3\text{-}16)$$

Here Q_{α} is the Mulliken net atomic charge, N_{α} is the Mulliken population (68), and Z_{α} is the number of electrons in the neutral atom.

The effective charge $\chi^{\alpha}(CF)$ for the charge flux tensor is given by

$$\chi^{\alpha}(CF)^2 = Tr\left\{P^{\alpha}(CF)\left[P^{\alpha}(CF)\right]^{+}\right\} \qquad (3\text{-}17)$$

where P(CF) is the charge flux for atom α.

We are interested in these two invariants because we want to obtain the charge undeformability values for the APTs of uracil. This parameter was defined by Chin (28) as

$$\text{charge undeformability} = \chi^{\alpha}(C)/\chi^{\alpha}(CF) \quad . \qquad (3\text{-}18)$$

It was suggested by Chin (28) that this ratio is a good parameter to measure charge flows.

For the rest of the invariant properties of the component tensors the reader should consult Ref. 28.

Atomic Polar Tensors for Uracil

The equilibrium geometry of uracil used throughout all this study was a slightly modified version of that calculated for the optimized geometry by Nishimura, Tsuboi, Kato, and Morokuma (14) using the STO-3G basis set. The C-H and N-H bond lengths were decreased slightly from their predicted values to bring them into better agreement with experimental values. That geometry and the numbering of the atoms used in these calculations are given in Fig. 3-1. In addition, Fig. 3-1 indicates the orientation of the principal Cartesian axes. In terms of these axes, the principal Cartesian coordinates for the atomic positions are listed in Table 3-1. The calculated values for the principal moments of inertia I_{xx}, I_{yy}, and I_{zz} are also given in this table. The molecule is planar, in agreement with the experimental structure found for uracil (69). Therefore, this molecule belongs to the C_s symmetry point group.

With the 4-31G basis set (70) and the GAUSSIAN 76 system of computer programs (71), the total energy calculated for uracil with this geometry was -411.85092268 Hartrees, and the total dipole moment value was calculated to be 5.487 Debye, with components: p_x^o = 5.289 D, p_y^o = -1.460 D, and p_z^o = 0.000 D. Experimentally, Kulakowska, Geller, Lesyng, and Wierzchowski (72) determined that the total dipole moment for uracil in dioxane is 4.160 D, within experimental uncertainty.

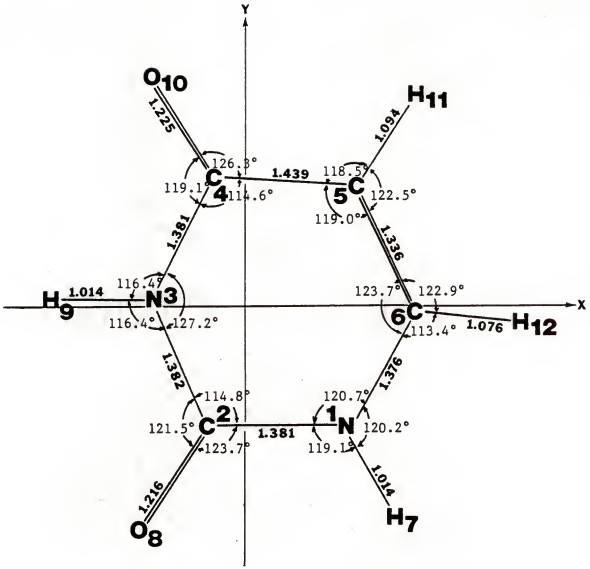

Figure 3-1. Uracil geometry and atom numbering as used in the present study. The molecule is oriented in its principal Cartesian coordinate system.

TABLE 3-1
PRINCIPAL CARTESIAN COORDINATES, MOMENTS OF INERTIA AND DIPOLE MOMENT COMPONENTS FOR THE ASSUMED EQUILIBRIUM GEOMETRY OF URACIL

	Principal Cartesian Coordinates (Å)		
Atom	X	Y	Z
N_1[a]	1.022080	-1.201760	0.000000
C_2	-0.358920	-1.203150	0.000000
N_3	-0.939870	0.050810	0.000000
C_4	-0.292760	1.270810	0.000000
C_5	1.144910	1.186370	0.000000
C_6	1.723390	-0.017890	0.000000
H_7	1.516120	-2.087260	0.000000
O_8	-1.032580	-2.215490	0.000000
H_9	-1.953500	0.078090	0.000000
O_{10}	-0.959190	2.298670	0.000000
H_{11}	1.722080	2.115730	0.000000
H_{12}	2.790810	-0.153530	0.000000

Principal Moments of Inertia ($uÅ^2$)

I_{xx} = 245.860840
I_{yy} = 129.714401
I_{zz} = 375.575195

Dipole Moment Components[b]

p_x = 5.289 D = 1.233 eÅ
p_y = -1.460 D = -0.304 eÅ
p_z = 0.000 D = 0.000 eÅ

---

[a] Atom numbering as given in Fig. 3-1.

[b] Experimental dipole moment value is 4.160 D; Ref. 72.

The APTs for uracil were calculated by Chin according to procedures described in Chapter 2, and published in Ref. 17. However, a sign mistake was made while writing-up one of the dipole derivatives in the computer, resulting in small changes in some of the APTs reported (17). The implications of this sign change will be discussed in Chapter 4, when we present the predicted intensities for uracil. The calculated values of the dipole moment derivatives P_S are displayed in Table 3-2. The problem just mentioned with the sign was in the $\underline{x}$ component of the S_{20} coordinate. Its value should be -0.0834 e. Also, the values of the $\underset{\sim}{P}_\rho$ tensor (Eq. (2-37)) are given in this table.

The corrected APTs for all 12 atoms of uracil are given in Table 3-3 for the coordinate system shown in Fig. 3-1. Note that the units of the dipole derivatives in the APTs are in multiples of the charge of the electron e, on atomic units. Conversions from other units are 4.8 D A^{-1} = 1 e = 1.602 x 10^{-19} C. The APT invariants χ_α, $\bar{P}_\alpha$, and $\beta_\alpha{}^2$ were calculated using Eqs. (3-6), (3-7) and (3-8), and are also included in Table 3-3. The χ_α values have been partitioned into $\chi_\alpha^{a'}$ (for in-plane) and $\chi_\alpha^{a''}$ (for out-of-plane). The importance of these χ_α values will be made clear when we use them in the next section with the total absolute intensity sum for uracil.

TABLE 3-2
CALCULATED DIPOLE MOMENT DERIVATIVES FOR URACIL

	ρ_1[a]	ρ_2	ρ_3	ρ_4	ρ_5	ρ_6	S_7[b]	S_8	S_9	S_{10}	S_{11}	S_{12}
x	0.0000	0.0000	0.0000	0.0000	0.0000	0.0157	-.2861	0.0286	0.4662	0.0772	-.1462	-.0045
y	0.0000	0.0000	0.0000	0.0000	0.0000	0.0569	-.2145	-.3104	0.0655	0.5828	-.0513	-.3338
z	0.0000	0.0000	0.0000	-.0194	-.0968	0.0000	0.0000	0.0000	0.0000	0.0000	0.0000	0.0000

	S_{13}	S_{14}	S_{15}	S_{16}	S_{17}	S_{18}	S_{19}	S_{20}	S_{21}	S_{22}	S_{23}	S_{24}
x	0.4620	0.0265	-.0711	0.0528	0.2255	-.0558	0.2292	-.0834	-.1584	-.1153	0.2947	-.0185
y	-.2147	0.4782	0.1431	-.1033	0.0722	0.4601	-.0195	0.3111	-.1517	-.0602	-.1265	0.2522
z	0.0000	0.0000	0.0000	0.0000	0.0000	0.0000	0.0000	0.0000	0.0000	0.0000	0.0000	0.0000

	S_{25}	S_{26}	S_{27}	S_{28}	S_{29}	S_{30}	S_{31}	S_{32}	S_{33}	S_{34}	S_{35}	S_{36}
x	-.0726	-.0197	0.0495	0.0000	0.0000	0.0000	0.0000	0.0000	0.0000	0.0000	0.0000	0.0000
y	0.1097	-.0966	-.0374	0.0000	0.0000	0.0000	0.0000	0.0000	0.0000	0.0000	0.0000	0.0000
z	0.0000	0.0000	0.0000	-.2823	0.2244	-.1318	0.2231	-.2019	-.2416	0.3209	-.4292	0.2989

[a] Columns ρ_1 to ρ_6 contain the elements of $\underline{P}_\rho$ (see Eq. (2-37)) in e $u^{-\frac{1}{2}}$ units.

[b] Columns S_7 to S_{27} have the elements of $\underline{P}_S$ (see Eq. (2-38)) in e units for the 21 A' (in-plane) modes, and columns S_{28} to S_{36} contain the elements of $\underline{P}_S$ for the 9 A'' (out-of-plane) modes.

TABLE 3-3
CORRECTED ATOMIC POLAR TENSORS FOR URACIL

N_1[b]

$$\begin{pmatrix} -.957^{a} & 0.163 & 0 \\ -.678 & -.978 & 0 \\ 0 & 0 & -.729 \end{pmatrix}$$

$\chi_\alpha^{c} = 0.9815$
$\chi_\alpha^{a'} = 0.8867$
$\chi_\alpha^{a''} = 0.4209$
$\bar{p}_\alpha = -.8880$
$\beta_\alpha^{2} = 0.7866$

C_2

$$\begin{pmatrix} 1.641 & 0.238 & 0 \\ 0.443 & 1.988 & 0 \\ 0 & 0 & 0.850 \end{pmatrix}$$

$\chi_\alpha = 1.5938$
$\chi_\alpha^{a'} = 1.5164$
$\chi_\alpha^{a''} = 0.4907$
$\bar{p}_\alpha = 1.4930$
$\beta_\alpha^{2} = 1.3999$

N_3

$$\begin{pmatrix} -.623 & -.054 & 0 \\ -.094 & -1.403 & 0 \\ 0 & 0 & -.660 \end{pmatrix}$$

$\chi_\alpha = 0.9668$
$\chi_\alpha^{a'} = 0.8885$
$\chi_\alpha^{a''} = 0.3810$
$\bar{p}_\alpha = -.8953$
$\beta_\alpha^{2} = 0.5985$

C_4

$$\begin{pmatrix} 1.449 & 0.014 & 0 \\ -.677 & 1.557 & 0 \\ 0 & 0 & 0.680 \end{pmatrix}$$

$\chi_\alpha = 1.3472$
$\chi_\alpha^{a'} = 1.2887$
$\chi_\alpha^{a''} = 0.3926$
$\bar{p}_\alpha = 1.2286$
$\beta_\alpha^{2} = 1.3738$

C_5

$$\begin{pmatrix} -.549 & 0.110 & 0 \\ 0.565 & -.444 & 0 \\ 0 & 0 & -.428 \end{pmatrix}$$

$\chi_\alpha = 0.5811$
$\chi_\alpha^{a'} = 0.5260$
$\chi_\alpha^{a''} = 0.2471$
$\bar{p}_\alpha = -.4737$
$\beta_\alpha^{2} = 0.5099$

C_6

$$\begin{pmatrix} 0.437 & -.243 & 0 \\ 0.331 & 1.254 & 0 \\ 0 & 0 & 0.268 \end{pmatrix}$$

$\chi_\alpha = 0.8173$
$\chi_\alpha^{a'} = 0.8025$
$\chi_\alpha^{a''} = 0.1547$
$\bar{p}_\alpha = 0.6530$
$\beta_\alpha^{2} = 1.0870$

H_7

$$\begin{pmatrix} 0.191 & -.087 & 0 \\ -.028 & 0.236 & 0 \\ 0 & 0 & 0.437 \end{pmatrix}$$

$\chi_\alpha = 0.3117$
$\chi_\alpha^{a'} = 0.1831$
$\chi_\alpha^{a''} = 0.2523$
$\bar{p}_\alpha = 0.2880$
$\beta_\alpha^{2} = 0.0640$

O_8

$$\begin{pmatrix} -.867 & -.482 & 0 \\ -.463 & -1.233 & 0 \\ 0 & 0 & -.620 \end{pmatrix}$$

$\chi_\alpha = 1.0170$
$\chi_\alpha^{a'} = 0.9520$
$\chi_\alpha^{a''} = 0.3580$
$\bar{p}_\alpha = -.9067$
$\beta_\alpha^{2} = 0.9554$

---

continued

TABLE 3-3 continued

H_9	O_{10}	H_{11}	H_{12}
$\begin{pmatrix} 0.275 & -.002 & 0 \\ -.057 & 0.158 & 0 \\ 0 & 0 & 0.446 \end{pmatrix}$	$\begin{pmatrix} -.979 & 0.320 & 0 \\ 0.638 & -1.309 & 0 \\ 0 & 0 & -.592 \end{pmatrix}$	$\begin{pmatrix} 0.023 & -.012 & 0 \\ 0.006 & 0.114 & 0 \\ 0 & 0 & 0.197 \end{pmatrix}$	$\begin{pmatrix} -.041 & 0.035 & 0 \\ 0.014 & 0.060 & 0 \\ 0 & 0 & 0.151 \end{pmatrix}$
$\chi_\alpha = 0.3177$	$\chi_\alpha = 1.0850$	$\chi_\alpha = 0.1323$	$\chi_\alpha = 0.0991$
$\chi_\alpha^{a'} = 0.1860$	$\chi_\alpha^{a'} = 1.0298$	$\chi_\alpha^{a'} = 0.0676$	$\chi_\alpha^{a'} = 0.0472$
$\chi_\alpha^{a''} = 0.2575$	$\chi_\alpha^{a''} = 0.3418$	$\chi_\alpha^{a''} = 0.1138$	$\chi_\alpha^{a''} = 0.0872$
$\bar{P}_\alpha = 0.2930$	$\bar{P}_\alpha = -.9600$	$\bar{P}_\alpha = 0.1113$	$\bar{P}_\alpha = 0.0567$
$\beta_\alpha^2 = 0.0678$	$\beta_\alpha^2 = 1.1506$	$\beta_\alpha^2 = 0.0230$	$\beta_\alpha^2 = 0.0298$

[a]Units are electrons (e).

[b]The atomic numbering scheme and coordinate system orientation are defined in Fig. 3-1 and Table 3-1.

[c]The APT invariants are defined in Eqs. (3-6), (3-7), and (3-8).

Total Absolute Infrared Intensity Prediction for Uracil

Since now the APTs and dipole moment components (p_x^o, p_y^o, and p_z^o) are given in Table 3-3, and the principal moments of inertia in Table 3-1, the intensity sum rule (Eq. (3-13)) can be applied to see what is predicted for the ratio of the total intensity sum of all the in-plane vibrations (A') to the total sum for the out-of-plane vibrations (A") of uracil. This will be some measure of the accuracy of the prediction, particularly for the out-of-plane modes. For A' vibrations (active in the xy plane, according to Fig. 3-1) the square of the effective charge $(\chi^{a'})^2$ for atom α will be given by (64)

$$(\chi_\alpha^{a'})^2 = (1/3)[(\partial p_x/\partial X_\alpha)^2 + (\partial p_x/\partial Y_\alpha)^2 + (\partial p_y/\partial X_\alpha)^2 + (\partial p_y/\partial Y_\alpha)^2] \quad . \tag{3-19}$$

Also, for the A" vibrations (active in the xz or yz planes of Fig. 3-1) the square of the effective charge $(\chi^{a''})$ for each α atom is

$$(\chi_\alpha^{a''})^2 = (1/3)(\partial p_z/\partial Z_\alpha)^2 \quad . \tag{3-20}$$

The results of the calculated values for χ_α^2, $(\chi_\alpha^{a'})^2$, and $(\chi_\alpha^{a''})^2$ are displayed in Table 3-4.

The rotational correction expressions $\Omega^{a'}$ and $\Omega^{a''}$ for A' and A" vibrations, respectively, are obtained by partitioning the result of the solution of Eq. (3-13) with respect to the xy (for A'), and yz or xz (for A") planes. This was purposely done in Eq. (3-12) where the first bracket corresponds to $\Omega^{a'}$

$$\Omega^{a'} = (p_z^o)^2/I_{xx} + (p_z^o)^2/I_{yy} + [(p_x^o)^2 + (p_y^o)^2]/I_{zz} \tag{3-21}$$

and the second bracket gives $\Omega^{a''}$

$$\Omega^{a''} = (p_y^o)^2/I_{xx} + (p_x^o)^2/I_{yy} \quad . \tag{3-22}$$

These rotational correction expressions were calculated for uracil, and the values are $\Omega^{a'} = 3.39$ km mol^{-1} and $\Omega^{a''} = 9.49$ km mol^{-1}.

TABLE 3-4
INTENSITY SUM RULE APPLIED TO URACIL

Atom	m_α (u)	$1/m_\alpha$ (u^{-1})	$(\chi_\alpha{}^{a'})^2$ (in-plane)	$(\chi_\alpha{}^{a''})^2$ (out-of-plane)	$\chi_\alpha{}^2$ (total)	$(3/m_\alpha)(\chi_\alpha{}^{a'})^2$ (in-plane)	$(3/m_\alpha)(\chi_\alpha{}^{a''})^2$ (out-of-plane)	$(3/m_\alpha)(\chi_\alpha)^2$ (total)
N	14.0031	0.071413	0.78620	0.17714	0.96334	0.16843	0.03795	0.20638
C	12.0000	0.083333	2.29931	0.24083	2.54014	0.57483	0.06021	0.63504
N	14.0031	0.071413	0.78943	0.14520	0.93463	0.16912	0.03111	0.20023
C	12.0000	0.083333	1.66079	0.15413	1.81493	0.41520	0.03853	0.45373
C	12.0000	0.083333	0.27662	0.06106	0.33768	0.06915	0.01526	0.08441
C	12.0000	0.083333	0.64403	0.02394	0.66797	0.16101	0.00598	0.16699
H	1.0078	0.992260	0.03351	0.06366	0.09717	0.09975	0.18949	0.28924
O	15.9949	0.062520	0.90622	0.12813	1.03436	0.16997	0.02403	0.19400
H	1.0078	0.992260	0.03461	0.06631	0.10092	0.10304	0.19738	0.30042
O	15.9949	0.062520	1.06046	0.11682	1.17728	0.19890	0.02191	0.22081
H	1.0078	0.992260	0.00457	0.01294	0.01750	0.01360	0.03851	0.05211
H	1.0078	0.992260	0.00223	0.00760	0.00983	0.00665	0.02262	0.02927
				Total sum :		2.14965	0.68298	2.83263
				km mol^{-1} :		2095.69	665.84	2761.53
				$-\Omega$ (km mol^{-1}) :		-3.39	-9.49	-12.88
				Predicted intensity : (km mol^{-1})		2092.30	656.35	2748.65

Accordingly, the sum in the right-hand-side of Eq. (3-13) predicts for A' vibrational modes a total intensity of 2092.30 km mol^{-1} , while a total sum of 656.35 km mol^{-1} is predicted for A" vibrational modes. Consequently, the ratio between the predicted total intensity sums for in-plane modes to out-of-planes is: $\sum_{a'} A_s / \sum_{a''} A_s = 3.19$. The experimental value for this ratio was found to be about 3.70, from measurement of intensities of uracil in an argon matrix (16,17).

CHAPTER 4
RESULTS OF EXPERIMENTAL AND CALCULATED SPECTRA FOR URACIL

The principal considerations in this chapter are the normal coordinate analysis and the prediction of frequencies, as well as absolute infrared intensities, for uracil. We shall also review the assignment of the infrared spectrum of isolated uracil and contrast it with the spectrum in the solid phase, in solution, etc. In order to carry out these objectives, comparisons are made between our force constants and assignments for uracil with those reported in the literature. The importance of these comparisons is to illustrate and establish the basis for future studies of larger molecules.

Normal Coordinate Analysis for Uracil

To carry out the normal coordinate analysis (NCA) of uracil we used the procedure described in Chapter 2. Since uracil has 12 atoms and is planar, it belongs to the C_s symmetry group; there will be 21 in-plane vibrations of A' species, and 9 out-of-plane vibrations of A" species, for a total of 30 vibrational fundamentals.

In the present study our efforts have been directed to the 21 in-plane vibrations of uracil, for the following reasons. First, over the past few years NCAs and assignments of the infrared spectrum of uracil have been carried out mainly for these vibrations (12-15), using force constants obtained employing semiempirical methods (as will be discussed in more detail in the next chapter). Therefore, we can

make comparisons of our results using ab initio force constants with those obtained in the past, and evaluate the reliability of these force constants. Second, understanding uracil in-plane vibrations should help us to the proper interpretation of its complex spectrum, as well as of the spectra of related molecules, such as the methylated uracils. Of course, the out-of-plane vibrations are of interest also, but more difficult to study because coordinates for the out-of-plane and torsional modes have to be defined, and the corresponding force constants are less well known. Besides, the quantum mechanical calculations have not yet been made to obtain the ab initio force field for these vibrations.

In this study the force field given by Nishimura, Tsuboi, Kato, and Morokuma (14) was used. In their ab initio calculation they employed the STO-3G basis set to obtain energy gradients in the Cartesian coordinate system which were then numerically differentiated in order to produce the force constants (73). It is well known that the force constants calculated using a 4-31G basis set will give a better reproduction of the observed vibrational frequencies than will those calculated with the STO-3G set. Therefore, Nishimura et al. (14) proposed that the "STO-3G force constants" be multiplied by scaling factors chosen on the basis of their experience with other molecules to change these values to values for the force constants that would have been calculated using a 4-31G basis. In mathematical terms this would be equivalent to

$$F_{ij}(4\text{-}31G) = c_{ii}c_{jj}F_{ij}(STO\text{-}3G) \qquad (4\text{-}1)$$

where $F_{ij}(4\text{-}31G)$ is a 4-31G force constant, $F_{ij}(STO\text{-}3G)$ the same element obtained using the ab initio STO-3G basis set, and c_{ii} and c_{jj} are the scaling factors corresponding to the i and j diagonal force constants.

If the element is diagonal then

$$F_{ii}(4\text{-}31G) = c_{ii}F_{ii}(STO\text{-}3G) \quad . \qquad (4\text{-}2)$$

For example, they proposed for either a C=O or C=C stretch that the scaling factor is 0.82; for either a C=O or C=C bend the scaling factor is 1.08, etc. (see Table I in Ref. 14).

The internal coordinates for uracil are defined in Fig. 4-1 and the in-plane symmetry coordinates are given in Table 4-1. Here, the redundancies of the angular internal coordinates of the ring system have been removed. As seen in Fig. 4-1, there are 30 internal coordinates defined to describe the 21 in-plane degrees of freedom. Hence, the number of redundancies is 9. They may be classified as follows: six associated with the angles common to each ring atom, for example $\Delta\beta_{13} + \Delta\beta_{19} + \Delta\beta_{25} = 0$ (see Fig. 4-1); one cyclic redundancy corresponding to the constraint that all internal angles of the ring cannot be increased simultaneously, $\Delta\beta_{13} + \Delta\beta_{14} + \Delta\beta_{15} + \Delta\beta_{16} + \Delta\beta_{17} + \Delta\beta_{18} = 0$; and two other cyclic constraints which express the condition that the ring is closed so that linear combinations of the stretching and bending internal coordinates are constrained to zero (6,21). The removal of these nine redundancies makes the calculation easier, since they can just be eliminated after constructing the remaining coordinates to be orthogonal to the redundancy condition. For this reason the bending coordinates in Table 4-1 appear as linear combinations (73). Based on the symmetry coordinates of Table 4-1, the in-plane ab initio force constants for uracil, scaled to give "4-31G" values, are given in Table 4-2. Using these force constant values we carried out the NCA, setting up the $\underline{B}$ and $\underline{G}$ matrices (see Chapter 2). The eigenvalues were obtained and the frequencies calculated by solving Eq. (2-21). We found that the calculated

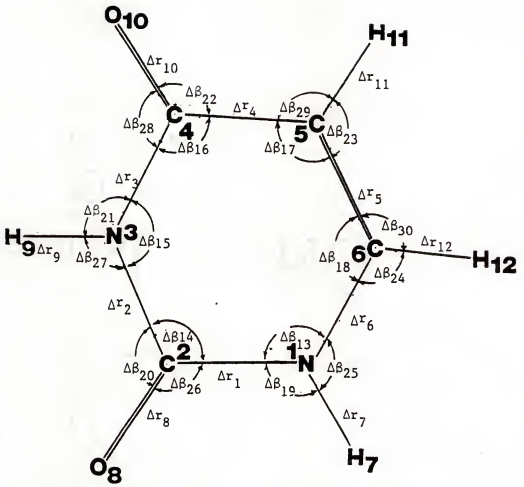

Figure 4-1. In-plane internal coordinates of uracil.

TABLE 4-1
IN-PLANE SYMMETRY COORDINATES FOR URACIL

$S_1 = \Delta r_1$	νN_1C_2 stretching
$S_2 = \Delta r_2$	νC_2N_3 stretching
$S_3 = \Delta r_3$	νN_3C_4 stretching
$S_4 = \Delta r_4$	νC_4C_5 stretching
$S_5 = \Delta r_5$	νC_5C_6 stretching
$S_6 = \Delta r_6$	νC_6N_1 stretching
$S_7 = \Delta r_7$	νN_1H_7 stretching
$S_8 = \Delta r_8$	νC_2O_8 stretching
$S_9 = \Delta r_9$	νN_3H_9 stretching
$S_{10} = \Delta r_{10}$	νC_4O_{10} stretching
$S_{11} = \Delta r_{11}$	νC_5H_{11} stretching
$S_{12} = \Delta r_{12}$	νC_6H_{12} stretching
$S_{13} = (\Delta\beta_{13}-\Delta\beta_{14}+\Delta\beta_{15}-\Delta\beta_{16}+\Delta\beta_{17}-\Delta\beta_{18})/\sqrt{6}$	δRing deformation I
$S_{14} = (\Delta\beta_{13}-\Delta\beta_{14}-\Delta\beta_{15}+\Delta\beta_{16}-\Delta\beta_{17}-\Delta\beta_{18})/\sqrt{12}$	δRing deformation II
$S_{15} = (\Delta\beta_{14}-\Delta\beta_{15}+\Delta\beta_{17}-\Delta\beta_{18})/2$	δRing deformation III
$S_{16} = (\Delta\beta_{19}-\Delta\beta_{25})/\sqrt{2}$	δN_1H bending
$S_{17} = (\Delta\beta_{20}-\Delta\beta_{26})/\sqrt{2}$	δC_2O bending
$S_{18} = (\Delta\beta_{21}-\Delta\beta_{27})/\sqrt{2}$	δN_3H bending
$S_{19} = (\Delta\beta_{22}-\Delta\beta_{28})/\sqrt{2}$	δC_4O bending
$S_{20} = (\Delta\beta_{23}-\Delta\beta_{29})/\sqrt{2}$	δC_5H bending
$S_{21} = (\Delta\beta_{24}-\Delta\beta_{30})/\sqrt{2}$	δC_6H bending

Note: The atomic numbering is shown in Fig. 4-1, which also gives the internal coordinate definitions. Since the only element of symmetry (besides E) is σ_h, each internal stretching coordinate is a symmetry coordinate. But to represent bending motions, with internal coordinates, appropriate linear combinations must be made.

TABLE 4-2

IN-PLANE AB INITIO FORCE CONSTANTS FOR URACIL OBTAINED BY SCALING STO-3G VALUES TO GIVE 4-31G VALUES

	S_1	S_2	S_3	S_4	S_5	S_6	S_7	S_8	S_9	S_{10}	S_{11}	S_{12}	S_{13}	S_{14}	S_{15}	S_{16}	S_{17}	S_{18}	S_{19}	S_{20}	S_{21}
S_1[a]	7.356[b]	0.468	-.268	0.112	-.204	0.461	0.000	0.908	0.000	-.070	0.000	0.000	0.082	0.181	0.147	0.070	-.420	0.000	-.037	-.068	0.000
S_2		7.497	0.455	-.172	0.076	-.233	0.000	0.888	0.000	-.084	0.000	0.000	0.000	-.146	-.081	0.000	0.409	-.100	0.083	0.036	0.000
S_3			7.003	0.327	-.192	0.171	0.000	-.083	0.000	1.036	0.000	0.000	0.043	0.000	-.145	-.036	-.118	0.049	-.682	0.000	0.000
S_4				6.042	0.464	-.363	0.000	-.090	0.000	0.686	0.000	0.000	0.038	0.000	0.244	0.045	0.032	0.000	0.245	-.125	0.000
S_5					10.728	0.554	0.000	0.099	0.000	-.128	0.000	0.000	-.066	-.243	0.068	0.000	-.030	-.035	-.056	0.193	-.135
S_6						8.079	0.000	-.053	0.000	-.073	-.100	0.000	-.137	0.059	-.288	-.185	0.112	0.060	0.100	0.000	0.226
S_7							8.256	-.036	0.000	0.000	0.000	0.000	-.074	-.066	0.000	0.000	0.000	0.000	0.000	0.000	0.000
S_8								13.298	0.000	0.000	0.000	0.000	0.276	0.169	-.313	0.000	0.000	0.000	0.000	0.000	0.000
S_9									8.150	0.000	0.000	0.000	-.093	0.047	0.067	0.000	-.031	0.000	0.032	0.000	0.000
S_{10}										13.500	0.000	0.000	0.290	-.356	0.000	0.000	0.045	0.000	-.071	0.000	0.000
S_{11}											6.330	0.000	-.081	0.040	-.068	0.000	0.000	0.000	0.000	0.000	0.000
S_{12}												6.181	0.070	0.029	0.062	0.000	0.000	0.000	0.000	0.000	0.000
S_{13}													1.898	0.000	-.046	-.010	0.000	0.011	-.060	0.011	0.029
S_{14}				Symmetric										1.710	-.098	0.000	-.146	0.131	0.091	-.104	0.096
S_{15}				$F_{ij} = F_{ji}$											1.663	0.134	-.058	-.088	0.177	-.057	-.013
S_{16}																0.619	0.056	-.017	-.009	-.014	0.007
S_{17}																	1.256	0.053	-.063	-.010	-.025
S_{18}																		0.599	0.065	-.015	0.000
S_{19}																			1.258	0.039	-.024
S_{20}																				0.579	0.008
S_{21}																					0.649

[a]The S symmetry coordinates correspond to those given in Table 4-1.

[b]Units: md A^{-1} for stretch-stretch elements, md Å for bend-bend elements, and md for bend-stretch elements.

These force constant values are obtained using the scaling factors given by Nishimura, Tsuboi, Kato, and Morokuma (14) to the STO-3G force field that they obtained.

frequencies should be further scaled by 0.90 to bring them into better agreement with experimental data. This scaling is necessary for frequencies calculated using the 4-31G force field. For example, a similar conclusion was reached by Wiberg, Walters, Wong, and Colson (74), in their study of frequencies and intensities of pyridine. The resulting adjusted frequencies for the in-plane normal modes of uracil are given and compared with the observed values in Table 4-3, which also includes contributions greater than 5 % to the potential energy distributions (PEDs, see Eq. (2-29)) for each normal mode. The frequencies that we calculated agreed with predictions by Nishimura, Tsuboi, Kato, and Morokuma (14) for uracil within 3 %. This slight discrepancy is due to the small differences in the G matrix, arising from the slight differences in our assumed geometry as compared to theirs. The results of our study have been reported and discussed by Chin, Scott, Szczepaniak, and Person (17). Our assignments of the uracil spectrum will be discussed in the next sections.

Comparison of Results

In this section we want to establish a comparison between the ab initio force constants for uracil and the semiempirical force constants reported in the literature. We are also interested in comparing the calculated frequencies using both ab initio and semiempirical constants, as well as the assignment descriptions or PEDs. Our motive for these comparisons is twofold: first, this will give us some insight into the reliability of ab initio force constants, and second we will verify that our calculation and assignment of spectra gives expected results. This understanding should prove of some value when we study larger molecules.

TABLE 4-3
RESULTS FOR URACIL IN-PLANE VIBRATIONS

mode	ν(Expl.)[a]	R.I.[b]	ν(Calc.)[c]	A_g[d]	Potential Energy Distribution (%)[e]
ν_1	3482	166	3479	108	νN_1H
ν_2	3433	100	3454	97	νN_3H
ν_3	3130	4	3070	11	νC_5H
ν_4	2970	8	3031	9	νC_6H
ν_5	1774 1762 1758 1733	680	1775	993	$\nu C_2O(58)$, $\nu C_2N_3(10)$, $\nu N_1C_2(8)$, $\delta N_3H(8)$
ν_6	1720 1707 1699	291	1760	458	$\nu C_4O(56)$, $\nu C_5C_6(12)$, $\nu C_4C_5(10)$, $\nu C_2O(8)$
ν_7	1644	33	1671	2	$\nu C_5C_6(54)$, $\nu C_4O(18)$, $\nu C_6N_1(14)$, $\delta C_6H(14)$
ν_8	1473	83	1483	69	$\delta N_1H(31)$, $\nu C_6N_1(25)$, $\nu C_2O(12)$, $\nu C_4C_5(8)$
ν_9	1461	7	1406	10	$\delta N_3H(35)$, $\nu C_2N_3(21)$, $\nu N_1C_2(12)$, $\nu C_4C_5(12)$
ν_{10}	1401	56	1390	167	$\delta N_1H(17)$, $\nu C_2N_3(16)$, $\nu N_1C_2(15)$, $\delta C_2O(15)$, $\nu N_3C_4(13)$, $\delta C_4O(8)$
ν_{11}	1389	21	1382	4	$\delta C_6H(29)$, $\delta C_5H(15)$, $\delta N_1H(14)$, $\delta N_3H(14)$, $\nu C_4O(8)$, $\nu C_2O(7)$
ν_{12}	1219	4	1254	18	$\nu N_3C_4(27)$, $\delta N_3H(22)$, $\delta C_5H(14)$, $\nu C_2N_3(13)$, $\nu C_4C_5(11)$, $\nu N_1C_2(10)$, $\delta C_4O(10)$
ν_{13}	1186	109	1175	44	$\delta C_6H(40)$, $\delta C_5H(22)$, $\delta N_1H(15)$, $\nu C_6N_1(9)$

---

continued

TABLE 4-3 continued

ν_{14}	1076	14	1066	18	$\nu C_6N_1(34)$, $\delta C_5H(22)$, $\nu C_5C_6(14)$, $\delta N_1H(8)$
ν_{15}	963	2	995	8	δ Ring I(72), $\nu N_3C_4(7)$
ν_{16}	958	7	933	1	$\nu N_1C_2(24)$, $\nu C_4C_5(18)$, $\nu C_2N_3(10)$, $\delta N_3H(10)$, $\nu N_3C_4(9)$
ν_{17}	719	12	739	5	$\nu C_4C_5(29)$, $\nu N_1C_2(15)$, $\nu N_3C_4(8)$, $\nu C_2N_3(7)$
ν_{18}	557	17	564	8	δ Ring II(56), $\nu N_3C_4(8)$
ν_{19}	537	7	535	8	$\delta C_2O(27)$, $\delta C_4O(27)$, δ Ring II(20)
ν_{20}	516	23	512	31	δ Ring II(55), $\delta C_4O(17)$, δ Ring III(14), $\delta C_2O(14)$
ν_{21}	393	33	374	26	$\delta C_2O(35)$, $\delta C_4O(34)$, δ Ring III(8), δ Ring II(7)

[a]Matrix isolation infrared spectral data (in Ar matrix) taken from Ref. 16.

[b]These intensities are the values of the integrated absorbances relative to ν_2 having an intensity of 100 units.

[c]Calculated frequencies using the force field given in Table 4-2, after scaling by 0.90.

[d]Predicted intensities using the APTs of Table 3-3, in km mol^{-1}.

[e]PED calculated using Eq. 2-29.

Force constants in uracil studies compared

In general, force constants obtained by ab initio quantum mechanical methods show systematic deviations from those considered the most reliable ones determined semiempirically from a large number of independent experimental data by spectral fit refinements, as will be discussed in the next chapter. We are mainly concerned with the patterns followed by the force constants with the use of each approach (ab initio and semiempirical). Some illustrative comparisons of force constants for uracil are given in Table 4-4. The first column shows values for some of the diagonal force constants obtained by Nishimura, Hirakawa and Tsuboi (6, to which we will refer as NHT). The treatment they followed involved a spectral fit refinement using the experimental frequencies obtained for uracil and three deutero-derivatives. They attempted to reproduce the observed frequencies for these molecules carrying out a NCA with force constants obtained by means of an iterative procedure. Column 2 refers to force constants from a simple valence force field calculated by Susi and Ard (12, SA). They used frequencies from four isotopic uracil species, for a total of 83 experimental frequencies, in their refinement to obtain 23 force constants. Column 3 corresponds to the study by Bandekar and Zundel (3, BZ) on crystalline uracil. Initially, they constructed a force field for uracil transferring force constants from small model compounds, such as N-methylacetamide and acetone. The final set of force constants involved the frequencies of all four uracil molecules for the complete unit cell (48 atoms). Force constants of the study by Bowman and Spiro (15, BS) are given in column 4. They calculated a force field for uracil using the semiempirical molecular orbital calculation, MNDO, and a method of molecular orbital

TABLE 4-4
COMPARISON OF DIAGONAL FORCE CONSTANTS FOR URACIL REPORTED IN THE LITERATURE

		NHT[a]	SA[b]	BZ[c]	BS[d]	HC[e]	NTKM[f]	Scaled Values[g]
1.	N_1C_2 str.[h]	6.380[i]	6.380	6.960	7.057	5.694	7.356	5.958
2.	C_2N_3 str.	6.380	6.380	7.030	8.356	5.780	7.497	6.072
3.	N_3C_4 str.	6.380	6.380	6.320	7.499	5.609	7.003	5.672
4.	C_4C_5 str.	6.202	6.202	6.120	6.830	5.168	6.042	4.894
5.	C_5C_6 str.	8.700	8.702	8.510	8.909	8.459	10.728	8.690
6.	C_6N_1 str.	6.380	6.380	6.820	7.520	5.810	8.079	6.544
7.	N_1H str.	5.397	5.397	5.520	5.465	6.671	8.256	6.687
8.	C_2O str.	11.000	11.000	9.620	9.601	10.131	13.298	10.771
9.	N_3H str.	5.397	5.397	5.390	5.412	6.590	8.150	6.602
10.	C_4O str.	10.500	10.500	9.620	10.771	10.452	13.500	10.935
11.	C_5H str.	5.204	5.204	5.250	5.247	5.341	6.330	5.127
12.	C_6H str.	5.204	5.204	5.250	5.246	5.204	6.181	5.007
13.	N_1H bend.	0.510	0.417	0.510	---	0.641	0.619	0.501

---

continued

TABLE 4-4 continued

14.	C_2O bend.	1.034	1.034	1.240	---	1.012	1.215	0.984
15.	N_3H bend.	0.510	0.417	0.510	---	0.640	0.599	0.485
16.	C_4O bend.	1.034	1.034	1.220	---	1.022	1.258	1.019
17.	C_5H bend.	0.302	0.403	0.600	---	0.447	0.579	0.469
18.	C_6H bend.	0.302	0.403	0.600	---	0.380	0.649	0.526
19.	C_4O/C_5C_6[j]	0.225	-0.225	---	0.872	-0.090	-0.128	-0.104

[a]Data from the study by Nishimura, Hirakawa, and Tsuboi (6).

[b]Data from the study by Susi and Ard (12).

[c]Data from the study by Bandekar and Zundel (3).

[d]Data from the study by Bowman and Spiro (15).

[e]Data from the study by Harsanyi and Csaszar (75).

[f]Data from the study by Nishimura, Tsuboi, Kato, and Morokuma (14).

[g]Data from the study by Nishimura et al. (14) scaled by 0.81.

[h]Numbering of atoms is defined in Fig. 4-1, and symmetry coordinates in Table 4-1.

[i]Units are mdyne Å^{-1} for stretching constants, and mdyne Å for bending constants.

[j]Stretching/stretching interaction force constant.

constraint on the interaction coordinates. Then, they evaluated a final set of force constants, starting from their initial MNDO values, via a nonlinear least-squares fit of the diagonal elements to observed frequencies. Also in Table 4-4, column 5 presents some force constants obtained using the semi-empirical CNDO/2 method by Harsanyi and Czaszar (75, HC). They made use of correcting factors (obtained from their studies of maleimide) for these CNDO/2 values to reproduce the gas phase infrared spectrum. In column 6 we show some values obtained at the STO-3G level and corrected to "4-31G level", in the calculation by Nishimura, Tsuboi, Kato, and Morokuma (14, NTKM). These are the same force constants that we are using, and described previously, in the present study.

An inspection of Table 4-4 shows that the empirically obtained force constant values (NHT, SA, and BZ) are very similar. The same does not hold true for those found using different theoretical methods (BS, CH, and NTKM). Nevertheless, the pattern followed by ab initio force constants compares very well with that followed by the empirical ones.

Let us examine some particular cases in the comparison of force constants given in Table 4-4. The C_2=O stretching force constant values are: 11.0 (NHT), 11.0 (SA), and 9.62 (BZ) mdyn Å^{-1} for the empirical cases, and 9.601 (BS), 10.131 (HC), and 13.298 (NTKM) mdyn Å^{-1} for the calculated values. The NTKM value of 13.298 mdyn Å^{-1} is much higher than for all other instances. Since we must scale the calculated frequencies by a factor of 0.90 to get agreement with observed data, all 4-31G force constants (NTKM) must be scaled by 0.81; the results of this scaling are presented in column 7 of Table 4-4. After scaling,

the value of 13.298 mdyn Å^{-1} for the C_2=O stretching force constant by NTKM is reduced to 10.771 mdyn Å^{-1}, which agrees very well with the other ones listed above.

For the N_1H bend, the force constant values in Table 4-4 are: empirically, 0.510 (NHT), 0.417 (SA), and 0.510 (BZ); calculated, 0.641 (HC) and 0.619 (NTKM). Again, those values calculated quantum mechanically are higher than the empirical ones. The value from NTKM after scaling by 0.81 of 0.501 mdyn Å is similar to those obtained empirically.

It is not possible to make similar comparisons for many interaction constants because what was determined in the past empirically for a molecule were simple valence force fields containing only diagonal terms. Nearly all other interaction constants had to be assumed to be zero. The interaction force constants for the C_4=O stretch/C_5=C_6 stretch were however obtained in previous studies and are given in the last line of Table 4-4. All we can say is that its value was expected to be small, and probably negative, as given by SA (-0.225 mdyn Å^{-1}), HC (-0.090 mdyn Å^{-1}), and NTKM (-0.128 or -0.104 mdyn Å^{-1} when scaled by 0.81).

The evidence presented in Table 4-4 supports the idea that ab initio force constants are reliable enough to be used in NCA calculations. We strongly recommend their use when proper scaling factors are applied to them, since our results (17-19) clearly show that these force constants reproduce the experimental spectrum, within $\pm$ 20 cm^{-1} in the frequencies. This value was obtained through a least squares procedure of the experimental and calculated frequency data for uracil (17) and methylated uracils (18,19).

Comparison of Infrared Spectral Assignments for Uracil

Now we may compare the sets of frequencies calculated by NCA calculations by the different workers mentioned above. These sets of values are shown in Table 4-5. First, it is worth noting just what experimental data were used in the fitting of frequencies in each study. It is briefly summarized in the following: NHT (6), resonance Raman spectra of neutral aqueous solutions of uracil plus results from SA; SA (12), ordinary laser Raman and infrared spectra for polycrystalline uracil; BZ (3), also infrared and Raman spectra for solid uracil; BS (15) used the experimental frequencies of SA; and HC (75) tried to fit data from the gas phase infrared spectrum of uracil. Actually, NTKM (14) did not try to fit the calculated frequencies to the observed values, but instead to see how close the predicted frequencies using ab initio force constants are to the observed ones. In the present study we used predicted frequencies and infrared intensities, as well as PEDs, to decide which experimental band in the matrix-isolated spectrum of uracil was to be assigned to which calculated mode.

A close examination to Tables 4-3 and 4-5 shows a surprising similarity in the frequency assignment descriptions in terms of the PEDs. For example, except for the BZ assignment of the two N-H stretches, in which they calculated about half-and-half mixing of these modes, the rest of the workers agree that the two N-H stretches are local modes. The spectral region in which the C=O stretches and $C_5=C_6$ stretch are assigned is rather interesting. Here, the general consensus is that the C_2=O stretching frequency is higher than the corresponding value for the C_4=O stretch. The calculated listed values in Table 4-5 going from left to right are for C_2O : 1697, 1684, 1721, 1725, 1765

TABLE 4-5

COMPARISON OF FREQUENCIES FOR URACIL FROM DIFFERENT STUDIES

NRT[a]		Sa[b]		Sz[c]		BS[d]		CH[e]		NTEN[f]	
	3134[g]	νNH in-phase (99)	3164	νN_1H(53), νN_3H(43)	3144	νN_1H[h]	3460	νN_1H	3478	νN_1H(99)
------	3131	νNH out-of-phase(99)	3162	νN_3H(54), νN_1H(44)	3127	νN_3H	3438	νN_3H	3453	νN_3H(99)
------	3100	νCH in-phase(98)	3099	νC_6H(71), νC_5H(27)	3102	νC_5H(47), νC_6H(53)	3112	νC_5H	3068	νC_5H(95)
------	3092	νCH out-of-phase(99)	3090	νC_5H(72), νC_6H(27)	3092	νC_5H(53), νC_6H(47)	3067	νC_6H	3031	νC_6H(95)
1697	νC_4O(76), νN_1C_2(11)	1684	νC_4O(74)	1721	νC_4O(35), νC_2O(23)	1725	νC_4O(32), νC_2O(10)	1765	νC_2O	1775	νC_2O(53)
1648	νC_2O(68), νC_6C_5(18)	1653	νC_2O + νC_5C_6 in-ph.(68)	1673	νC_4O(40), νC_2O(34)	1669	νC_4O(42), νC_2O(26)	1739	νC_4O	1748	νC_4O(56)
1610	νC_5C_6(71)	1605	νC_4O + νC_5C_6 noph.(75)	1635	νC_5C_6(47), νC_2O(12)	1619	νC_5H(65), νC_6N_1(14)	1614	νC_5C_6	1664	νC_5C_6(57)
1494	δN_1H(65)	1504	δN_1H(63)	1520	δN_1H(55)	1507	νC_2O(30), νC_6N_1(19)	1503	δN_1H + δC_2O + νCH	1483	ν-Ring(50), δN_1H(26)
1464	δN_3H(36), νN_1C_2(16)	1465	ν-Ring(61)	1456	νC_6N_1(22), δN_1H(22)	1473	δC_2O(20), νC_6N_1(17)	1446	δN_3H + νCH + νC_2O	1397	ν-Ring(55), δN_3H(32)
1445	δN_3H(35), νC_5C_6(11)	1424	δN_3H(66)	1401	δC_5H(53), νC_4C_5(17)	1429	νN_1C_2(27), νC_2O(25)	1392	νCH + δN_1H	1378	δN_3H(20), δCH(35)
1373	νC_4C_5(26), νC_2N_3(30)	1397	δC H in-phase(62)	1396	((not assigned))	1390	δC_6H(20), δN_1H(19)	1340	νC_5C_6 + νCH + N_3H	1372	ν-Ring(39), δN_1H(30)
1248	νC_6N_1(37), δC_6H(13)	1248	ν-Ring(86)	1241	δC_6H(35)	1266	δC_5O(22), δC_6H(19)	1225	δCH	1247	ν-Ring(63); Kekule
------		1211	δCH out-of-phase(77)	1201	δN_3H(61)	1227	νN_3C_4(59), νC_2N_3(41)	1104	δCH + νCH	1171	δCH out-of-ph.(64)
------		1125	ν-Ring(83)	1118	νN_1C_6(21), νC_5C_6(31)	1117	νC_6N_1(42), νC_5C_6(14)	1040	δCH + δ-Ring + νCH	1069	ν-Ring(55)
------		1028	ν-Ring(57)	1009	ν-Ring(46)	1005	νN_1C_2(26), νC_4C_5(33)	996	δCH	978	δ Ring I(75)
------		980	ν, δ-Ring(77)	981	δ-Ring(58)	975	νN_1C_2(37), νC_2N_3(28)	923	νC_5C_6 + νCH	932	ν-Ring(61)
793	δCH_1C(7)	801	ν, δ-Ring(58)	788	δ-Ring(22)	796	$\delta C_6C_6N_1$(11)	773	νC_5C_6 + δ-Ring	740	δ-Ring(67); breathing
------		576	δ-Ring(63)	571	δC_5O(74)	569	δC_5H(10), δC_6H(10)	597	δ-Ring	551	δ-Ring III(57)
------		564	δCO in-phase(77)	547	δC_2O(48), δC_4O(18)	547	δC_5H(13), δC_2O(10)	548	δ-Ring	532	δCO in-phase(60)
		536	δ-Ring(63)	539	δC_2O(41)	527	δC_2O(16), δC_4O(15)	525	δCO	502	δ Ring II(67)
		384	CO out-of-ph.(72)	356	C_2O( ), C_4O	390	C_2O(16), C_4O(12)	365	δCO	374	δCO out-of-pb.(69)

[a]Data from the study by Nishimura, Hirakawa and Tsuboi (6)

[b]Data from the study by Susi and Ard (12).

[c]Data from the study by Randekar and Zundel (3).

[d]Data from the study by Bowman and Spiro (15).

[e]Data from the study by Czaszar and Harasnyi (75).

[f]Data from the study by Nishimura, Tsuboi, Kato, and Morokuma (14), after scaling by 0.90.

[g]Frequencies are in cm^{-1}.

[h]The numbering of atoms follows Fig. 3-1. The PEDe in the parentheses are in %.

and 1775 cm^{-1}; and for C_4O are : 1648, 1653, 1673, 1669, 1739, and 1748 cm^{-1}. It should be remembered that the differences in these calculated values are mainly due to attempts to fit spectral data obtained in different phases (aqueous, solid, etc.), where hydrogen bonding lowers this mode. Anyway, the PEDs reported by NHT, SA, and HC compare very well for these modes with those of our study (Table 4-3). The value predicted for the C_5=C_6 frequency and PEDs are almost the same in all the studies, except BS, who do not predict it to be important in any mode.

The remaining assignments for the uracil spectrum are similar in all the seven studies, as shown in Tables 4-3 and 4-5. However, many of the modes show extensive mixing which is sensitive to the values of the force constants. Everything considered, the agreement between these different treatments is remarkable, but the differences are important.

Predicted Absolute Infrared Intensities for Uracils

The predicted infrared intensities for uracil and seven of its deuterated derivatives were reported by Chin, Scott, Szczepaniak, and Person (17). Since we had to correct the APTs for uracil (as explained in Chapter 3) it is now appropriate to describe the effect of such correction on the predicted intensities. First, the only change occurs in the intensities of the following modes (see Table I of Ref. 17): ν_1(N_1H stretch), ν_2(N_3H stretch), ν_5(mainly C_2=O stretch), and ν_6 (mainly C_4=O stretch). For the PED description of these modes see Table 4-3.

In Table 4-6 are given the wavenumbers and calculated intensities for the four vibrational modes just mentioned. Interestingly, the ν_1

TABLE 4-6

CORRECTED INTENSITIES FOR MODES ν_1, ν_2, ν_5, AND ν_6 OF URACILS

	ν_1	A_s	ν_2	A_s	ν_5	A_s	ν_6	A_s
Uracil	3479	108	3454	97	1775	993	1760	458
1-D Uracil	2558	83	3454	98	1767	1081	1757	336
3-D Uracil	3479	107	2535	70	1766	622	1752	821
1,3-di-D Uracil	2556	81	2535	73	1756	479	1750	930
5-D Uracil	3479	108	3454	97	1774	942	1753	503
6-D Uracil	3479	108	3454	97	1774	974	1757	469
5,6-di-D Uracil	3479	108	3454	97	1774	935	1751	499
Perdeutero Uracil	2557	80	2535	72	1755	609	1742	799

Note: Units are for frequencies cm^{-1} and for intensities km mol^{-1}.

mode for uracil now has an intensity of 108 km mol^{-1}, and ν_2 a value of 97 km mol^{-1}. These results now agree better with the experimentally observed intensities. It should be mentioned that previously (17) one of the dramatic differences between our calculated spectrum and the experimental matrix spectrum was the predicted "reversal" in this pattern of intensities. Another important result is evident from Table 4-6 concerning the predicted intensities of ν_5 and ν_6. For uracil these values are respectively 993 and 458 km mol^{-1}, so that the calculated ratio of the intensities A_5/A_6 is 2.17, while previously it was 1.64 (17). The experimental intensity ratio for the same modes is about 2.34, taking the ratio of the values of the relative integrated absorbances for these modes, 680/291 respectively, reported by Chin et al. (17) for uracil.

The right pattern is also predicted for the intensities of the N-D and C=O stretching modes of N_1,N_3-dideuterouracil, as shown in Table 4-6 (compare with Table II of Ref. 17). The N_1D stretching mode has an experimental relative intensity of 112, and the corresponding value for the N_3D stretch is 73. The predicted respective values given in Table 4-6 are 81 and 73 km mol^{-1}. The ratio of the experimental relative integrated absorbance of the C_2=O stretching mode to that of the C_2=O stretching mode is 391/612, or 0.64, while the calculated corresponding value from Table 4-6 is 479/930, or 0.52.

Our assignment (17) of the vibrational spectrum of uracil does not need to be changed on the basis of the new values of predicted intensities. The new corrected results for the predicted intensities give us more confidence in the validity of the calculated APTs for uracil.

However, it seems that one must be extremely careful in carrying out calculations of intensities because the simplest mistake can have important implications.

Simulation of Infrared Spectra

In order to have a visual comparison between the observed spectrum and the calculated frequencies and absolute intensities for uracil, the calculated spectrum was simulated and compared with a corresponding simulation of the matrix spectrum. For the simulation of the calculated spectrum, all bands were assumed to have the same constant half-width (5 cm^{-1}, estimated from the experimental matrix spectrum) and a peak height chosen to give an area proportional to the calculated intensity for each band from each normal mode at the calculated frequency. The intensity proportionality factor was chosen empirically so that the sum of all the intensities for the in-plane modes in the experimental spectrum is equal to the sum of intensities from the ab initio calculation of APTs, using the intensity sum rule to obtain the total predicted absolute intensity, as described in the last section of Chapter 2. There we found that the total intensity predicted for the entire spectrum of uracil is 2749 km mol^{-1} (Table 3-4).

The simulation for the ab initio predicted spectrum for the 21 in-plane normal modes of uracil is shown at the top part of Fig. 4-2, along with the simulated experimental spectrum of matrix-isolated uracil (in argon) shown at the bottom part of the figure, which includes out-of-plane vibrations. These simulations, and a comparison with the spectrum predicted by Harsanyi and Czaszar (75) for uracil using the CNDO/2 method have been discussed by Szczepaniak, Szczesniak, Nowak, Scott, Chin, and Person (18).

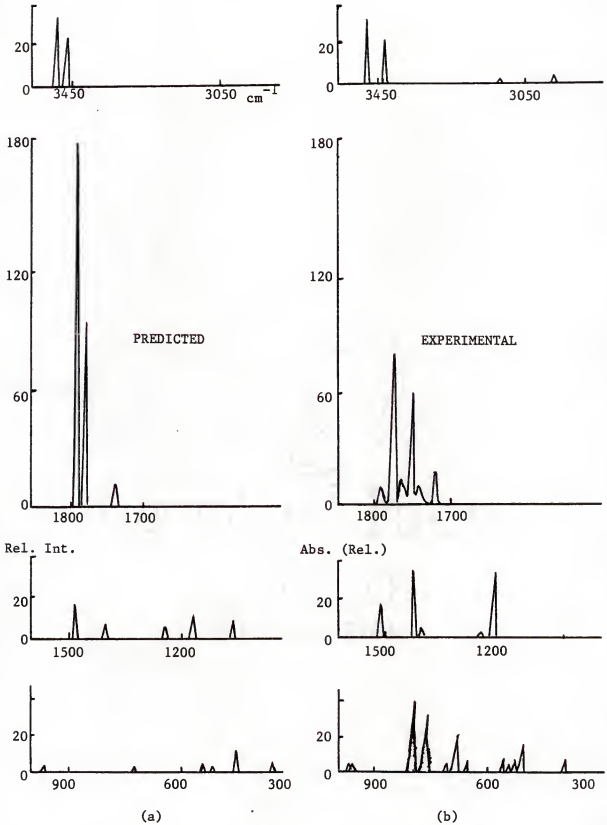

Figure 4-2. Simulated infrared spectra for uracil. a) ab initio predicted spectrum; b) Matrix isolation infrared spectrum in argon matrix. (Redrawn and corrected from Refs. 17 and 18).

Discussion of Results

Examining Table 4-3 and Fig. 4-2 we can see that the predicted frequency and absolute intensity pattern agrees closely with the experimental matrix spectrum for uracil, within the typical "factor-of-two". This excellent agreement leads us to believe that the ab initio force field at the "4-31G level" that was used in the NCA is a good approximation for the in-plane modes of uracil.

As it was mentioned in the previous section, Harsanyi and Czaszar (75) studied both the in-plane and out-of-plane vibrations of uracil by carrying out a NCA with a force field obtained at the CNDO/2 level. This force field was then scaled by correcting factors in order to yield calculated frequencies in good agreement with the experimental gas phase infrared spectrum. These scaling factors were taken from studies of maleimide (a five atom molecule with some similarity to uracil), and then used with the rough CNDO/2 force field calculated for uracil. Some of the force constant values so obtained were given in column 5 of Table 4-4. The frequencies calculated with this force field are shown in column 5 of Table 4-5.

We have compared Harsanyi and Czaszar (75) results with our calculation and with the experimental spectrum (18). We found that the most drastic discrepancy between their prediction and the experimental spectrum exists in the NH and CH stretching regions (see Fig. 1A of Ref. 18). The CNDO/2 calculation predicts much stronger intensities for the CH stretches than for the NH stretches. This result contrasts dramatically with the experimental spectrum, where the NH stretches are quite intense but the CH stretches are hardly visible. Other than

that, the scaled CNDO/2 prediction of the spectrum agrees surprisingly well with the experimental spectrum and with the more complicated STO-3G (and 4-31G) ab initio calculation.

For our assignment of the uracil infrared spectrum we have relied heavily on the experimental spectrum of the matrix isolated sample obtained by Szczesniak, Nowak, Rostkowska, Szczepaniak, Person, and Shugar (16) (see Chapter 2). Very recently, Maltese, Passerini, Nunziante-Cesaro, Dobos, and Harsanyi (2) and Barnes, Stuckey, and Le Gall (5) have also reported spectral data for matrix isolated uracils from studies in argon matrices. All three sets of data for uracil from studies in Ar matrices have been collected in Table 4-7, together with the proposed assignment of the infrared spectrum from each study.

In order to discuss and compare the assignment for the uracil infrared spectrum we have partitioned the spectrum in three regions: the 4000 - 2000 cm^{-1} region, the 2000 - 1600 cm^{-1} region, and the 1600 - 400 cm^{-1} region.

Spectral Region Between 4000 - 2000 cm^{-1}

The highest absorptions in this region are assigned to the two NH stretches. All three studies presented in Table 4-7 agree in the assignment of the 3485 cm^{-1} to N_1H and 3435 cm^{-1} to N_3H. Slight discrepancies in frequency suggests some calibration errors. Therefore, there is consensus for the NH stretching region assignment by the three works.

The predicted C_5H and C_6H stretching frequencies of 3070 cm^{-1} (11 km mol^{-1}) and 3031 cm^{-1} (9 km mol^{-1}) for uracil (see Tables 4-3 and 4-7) were assigned without much basis (16) to very weak absorption bands observed at 3130 cm^{-1} (Rel. Int. of 4) and 2970 cm^{-1} (Rel. Int.

TABLE 4-7
COMPARISON OF MATRIX-ISOLATION SPECTRAL DATA
AND ASSIGNMENTS FOR URACIL FROM DIFFERENT STUDIES

Barnes et al.[a]			Maltese et al.[b]		Szczesniak et al.[c]			
Ar-matrix	solid		Ar-matrix		Ar-matrix	R. I.[d]	A[e]	Approx. PEDs (%)[f]
3485 s	3210 sh	νN_1H	3490 m 3484 vw	νN_1H	3482	166	108	$\nu N_1H(100)$
3435 s	3110 s	νN_3H	3440 m	νN_3H	3433	100	97	$\nu N_3H(100)$
(3084)[g]	(3080)[g]	νC_5H			3130	4	11	$\nu C_5H(95)$
----		νC_6H			2970	8	9	$\nu C_6H(96)$
1764 vs 1761 vs	1718 vs	νC_2O	1763 vs 1761 vs	νC_2O	1774;1762 1758;1733	680	993	νC_2O
1706 vs	1675 s	νC_4O	1706 s 1703 s	νC_4O	1720;1707	291	458	$\nu C_4O(56)$
1643 m	1640 s	$\nu C_5C_6+\delta CH$	1643 m,b	νC_5C_6	1644	33	2	$\nu C_5C(54),\nu C_4O(18),\delta C_6H(14),\nu C_6N_1(14)$
1472 ms	1455 m	ν-Ring + δNH	1471 m	Ring in-plane	1473	83	69	$\delta N_1H(31),\nu$-Ring(33),$\nu C_2O(12)$
					1461	7	10	$\delta N_3H(35),\nu$-Ring(45)
1399 vs	1424 s	ν-Ring + δNH	1400 m	δNH	1401	56	167	ν-Ring(44),$\delta N_1H(17)$
1389 m 1386 mw	1395 mw	$\delta CH + \delta NH$	1388 mw	δCH	1389	21	4	$\delta CH(44),\delta NH(28),\nu CO(15)$
1360 vw	1344 vw	ν-Ring	1360 vw	(not assigned)				
1217 w	1220 sh	CH	1216 vw	Ring in-plane	1219	4	18	$\nu N_3C_4(27),\delta N_3H(22),\delta C_5H(14)$
1184 vs	1240 s	ν-Ring + δNH	1185 m	δNH	1186	109	44	$\delta CH(62),\delta NH(15)$
1073 w 1066 w	1095 w	$\delta NH + \delta CH$	1073 w 1070 w	δCH	1076	14	18	ν-Ring(48),$\delta CH(22),\delta NH(8)$
(1001)[g]	1005 w	δ-Ring			963	2	8	δ-Ring(72)
958 w	994 m	ν-Ring + δNH	970 vw	Ring in-plane	958	7	1	ν-Ring(61),$\delta NH(10)$

---

continued

TABLE 4-7 continued

(761)[g]	776 w	Ring breath.	759 m	γCH(out-of-pl.)	719	12	5	ν-Ring breath.(59)
559 w 555 w	588 w	δ-Ring	587 vw	δ-Ring	557	17	8	δ-Ring(56)
536 w	564 m	δCO	558 w	δCO	537	7	8	δCO(54),δ-Ring(20)
516 w	544 s	δ-Ring	539 mw	δCO	516	23	31	δ-Ring(69),δCO(31)
391 m	435 s	δCO	520 m	δ-Ring	393	33	26	δCO(69),δ-Ring(15)

[a]Data from the study by Barnes, Stuckey, and Le Gall (5), the second column refers to data for a solid.

[b]Data from the study by Maltese, Passerini, Nunziante-Cesaro, Dobos, and Harsanyi (2).

[c]Data from the study by Szczesniak, Nowak, Rostkowska, Szczepaniak, Person, and Shugar (16).

[d]R. I. stands for relative intensity. The values shown here are the integrated absorbances relative to ν_2 having an intensity of 100 units. Since the calculated intensity for ν_2 is 97 km/mol, the relative intensities compare directly with the calculated values.

[e]A_s is the predicted absolute intensity using the APTs (see Eq. (2-35)), in km mol^{-1}.

[f]The PEDs are calculated using Eq. (2-29). See Table 4-3 for the results of uracil.

[g]Frequency observed in the Raman spectrum only.

of 8). Barnes, Stuckey, and Le Gall (5) observed a medium Raman band at 3084 cm^{-1}, which they assign to the C_5H stretching. We believe this assignment is probably correct. The C_6H stretch was not observed by Barnes et al. (5) for uracil in the argon matrix, but for deuterated uracils (C_5,C_6-D and N_1,N_3-D) in the solid phase at 20 K they observed respectively a "shoulder" at 2295 cm^{-1} and a weak band at 3000 cm^{-1}, which they assign to this mode. Neither one of the CH stretching frequencies were observed in the infrared studies.

Spectral Region Between 2000 - 1600 cm^{-1}

According to the prediction (see Tables 4-3 and 4-7) we expect to find three more fundamental modes of vibration for uracil in this region, namely the C_2O and C_4O carbonyl stretches and the $C_5{=}C_6$ ring stretch. We predicted the C_2O stretching mode at 1775 cm^{-1} (993 km mol^{-1}), the C_4O stretch at 1760 cm^{-1} (458 km mol^{-1}) and the $C_5{=}C_6$ stretch at 1671 cm^{-1} (2 km mol^{-1}). The experimental spectrum shows that this is a very complex region. It has been suggested by Szczesniak, Nowak, Rostkowska, Szczepaniak, Person, and Shugar (16) that the most likely explanation for such complexity is that Fermi resonance occurs between the strong carbonyl fundamentals and overtone or combination bands from the lower frequency modes.

The assignments by the three studies in Table 4-7 assign the $C_2{=}O$ stretching mode at a higher frequency than the $C_4{=}O$ one. The following observed frequencies in cm^{-1} are assigned to the $C_2{=}O$ and $C_4{=}O$ stretches respectively: Barnes et al. (5), 1764 vs/1761 vs and 1706 vs; Maltese et al. (2), 1763 vs/1761 vs/1756 ms/1740 ms/1733 ms/1727 s and 1706 s/1703 s; and present study, 1774 m/1762 vs/1758 s/1733 s and 1720 w/1707 s/1699 mw. Our prediction of intensities indicates

that A_5 is about twice A_6; in fact this is the pattern observed in the matrix infrared spectrum. There is also quite general agreement in the studies concerning the assignment of the C_5=C_6 stretching mode, except that our calculation of PEDs shows strong mixing of this mode with other modes. However, the assignments by Barnes et al. (5) and Maltese et al. (2) consider this mode to have a more localized character. The observed frequencies in cm^{-1} assigned to this mode are: Barnes et al. (5), 1643 m; Maltese et al. (2), 1643 m; and the present study, 1644 mw. Our intensity calculation for this mode is 2 km mol^{-1}, while its relative experimental value is 33.

Spectral Region Between 1600 - 350 cm^{-1}

The remaining 14 in-plane fundamentals of uracil are located in this region (see Tables 4-3 and 4-7). An inspection of Table 4-7 shows that there is a close agreement between the observed frequencies of Barnes et al. (5) and those observed by Szczesniak et al. (16) for uracil in an Ar matrix. However, there are some discrepancies with the frequencies observed by Maltese et al. (2), especially the lower values. In particular, it looks as if the 587 cm^{-1} (vw) value of Maltese et al. (2) was caused by some impurity, because if this value were eliminated and the last three frequencies placed up by one step, then there would be a good agreement between all three studies.

CHAPTER 5
TRANSFER OF VIBRATIONAL PARAMETERS

In this chapter we want to discuss how feasible or realistic it is to predict frequencies and infrared intensities of different molecules making use of some a priori knowledge of the force field and APTs of structurally and chemically related molecules. First we shall consider the problem in general. Some examples will be given concerning the transfer of the vibrational parameters--force constants and APTs. For the particular case of uracil a detailed comparison will be made of these two sets of parameters with the values obtained for other molecules. Evidence supporting the hypothesis that the transfer of force constants and APTs is a valid procedure will lead us to apply it to the transfer from uracil to 1-methyluracil, 3-methyluracil, and 1,3-dimethyluracil.

Transfer of Force Constants

The term "force constant" is used specifically for the harmonic (quadratic) constants. Except for the simplest molecules, the task of determining force constants from experimental data is a difficult problem, due to the large number of unknown constants compared to the amount of available data. For a secular equation of order n, there are $(1/2)(n)(n + 1)$ independent force constants, but there are only n fundamental vibration frequencies (21,24-26,76). Therefore, it is in general impossible to calculate a unique set of values for those force constants from a set of frequencies alone. In the case of large

polyatomic molecules, Zerbi (77) has pointed out that since no unique choice of the vibrational potential can be indicated, only chemical and physical common sense as well as a critical examination of the results for derived physical quantities associated with vibrational motions may be suggested as general criteria for wise handling of the force constants.

In order to obtain a physically meaningful set of force constants, therefore, one should employ as many additional data for these physical quantities associated with the vibrational motions (such as isotope shifts of frequencies, values of Coriolis constants, mean amplitudes of vibration, etc.) as is possible. The small shift in vibrational frequencies caused by isotopic substitution are sensitive functions of the force field (78) since the potential remains the same from one isotopic species to another. For example, the study of Chalmers and McKean (79) on CF_4 and $^{13}CF_4$ demonstrates that quite accurate force and frequencies are obtained by the use of isotopic data.

Another valuable source of information in the force constants determination are the values of the Coriolis constants (80) which relate the mutual interactions of the normal vibrations through molecular rotation. Physically, these constants measure the vibrational angular momentum generated by the movement of the atoms in the vibrations. They are of particular value in determining the values of the interaction force constants connecting the symmetry coordinates used (42,43). However, precise evaluation of the Coriolis constants for a molecule is very difficult, particularly for a large molecule like uracil.

Additional data that may be used to evaluate force constants include mean-square amplitudes of vibration, which are determined experimentally as part of the structure determination by the gas-phase electron diffraction technique (81). Their relationship to the molecular force field arises because their magnitudes depend on the squares of the relative Cartesian displacement in the normal vibrations of different pairs of atoms (82).

Further experimental data such as the inertia defect parameters for planar molecules (83), the ℓ-type doubling constants for symmetric and spherical tops (84), etc., may be also employed when attempting to determine experimental molecular force fields.

The most used approach toward the evaluation of the force constants for large molecules involves some method of adjusting the force constants so that the calculation reproduces the values of the larger number of independent experimental parameters as closely as possible (26,85-95). Generally, the method of least-squares refinement is used for this purpose. In such an iterative refinement procedure one modifies a "guessed" force field (obtained by transferring force constants from similar fragments in smaller molecules) to fit a generally larger number of experimental frequencies and other parameters. Then the calculated eigenvalues (Eq. (2-1)) are compared with the experimental ones in the least-squares sense. If the differences in eigenvalues

$$\Delta\lambda_i = \lambda_i(\text{obsd.}) - \lambda_i(\text{calcd.})$$

are small, corrections of the order of Δf can be applied to the force constant matrix F to reduce the error vector $\Delta\lambda$ (85). Statistical methods are used to evaluate the results so obtained (26,85-87).

Unfortunately, for larger molecules even the frequency data are incomplete and the additional data are non-existent. As a consequence, it is necessary to impose constraints on the force field (12) which are often very difficult to justify physically. Even with these additional constraints, the iterative least-squares procedure often becomes unstable and the refinement fails to converge.

The principal problem with the least-squares method is the fact that it usually only fits the fundamental observed frequencies (3N - 6, where N is the number of atoms), which will be subject to experimental uncertainties. Moreover, for large molecules the additional experimental data (frequencies from isotopic molecules, Coriolis constants, etc.) are not available and it is not possible, at this stage, to do better.

Let us consider a second approach to the problem of force constant determination. This involves the theoretical evaluation of the molecular energy by quantum mechanical methods at the ab initio level (76). Recent progress in computational techniques and computers has made reliable ab initio force field calculations increasingly accesible to spectroscopists (14,40,73). This has significantly improved our knowledge of molecular force fields.

Both approaches for determining force constants will be examined in more detail in the following discussion. Some examples will be presented, but our principal concern will be to examine the validity of each of these approaches for treating moderate-to-large sized molecules.

Least-square Refinements Approach

In the past, the usual method of obtaining the force constants for a large molecule has been to transfer values from similar and usually simpler molecules, and then refine to fit the observed frequencies. A starting point would be, for example, to transfer force constants from small molecules with analogous fragments, since the experimental information available for a simpler molecule may be complete enough to determine accurately that molecule's force constants. These values then form the initial basis for a sequence of improvements or refinements generated by comparison with experimental data. There is a vast literature related to this approach (12-14,26,85,89-96). It was pointed out by Needham and Overend (92) that because the experimental information is usually incomplete for all but the simplest molecules, the result of a refinement of force constants contain a large measure of arbitrariness. In the particular case where the number of independent pieces of data greatly exceed the number of independent force constants (in simple molecular systems) this approach has met with considerable success (87,93).

Let us consider some of these cases where the application of such treatments has produced reliable force constants. For example, a refined force field for NF_3 was obtained by Allan, Duncan, Holloway, and McKean (94) using ^{15}N isotope shifts. They were able to rule out any ambiguous force constants by determining the centrifugal distortion constants of the molecule. Their force field reproduced quite well the experimental frequencies. Another good example is the study by Jones, Ryan, and Asprey (95) to determine the force constants of NOF, and NOBr. They used frequency data, centrifugal distortion constants, and ^{18}O, ^{15}N, and

halogen isotope shifts to fit the force constants to the spectral data. A third and final example is the force field determined for CO_2 by Machida and Overend (96). They were successful in obtaining force constants taking into consideration anharmonicity effects. A great many other refined and reliable force fields of small molecules (6 atoms or less) have been reported in the literature for the past forty years. For more examples see the reviews by Shimanouchi (86), Duncan (88), Shimanouchi and Nakagawa (89), and Overend (90).

Since the force constant refinement approach relies heavily upon the observed frequencies, the frequencies for a large number of similar molecules (including isotopic derivatives) must be measured and assigned in order to achieve a meaningful refinement. Such complete sets of data are not presently available for any but a very few small molecules, and biological molecules, in particular, have not been so thoroughly studied.

A number of least-square force constants refinements for the pyrimidine (12 atoms) and purine (13 - 16 atoms) bases have been made (1,12,13), with resulting fits that are not nearly so good as those for the simpler molecules given as examples above. For example, the refinement of Susi and Ard (12) for uracil gives a rather poor fit in the frequency region 900 cm^{-1} to 1400 cm^{-1}. Furthermore, they found it necessary to constrain many of the force constants to constant values during the refinement in order to prevent the refinement from diverging as the iteration proceeded.

Quantum Mechanical Approach

Force constants are determined by the electronic nature of the atoms forming the bonds in a molecule. There is some reason to believe

that chemically similar parts of molecules (for example a C-H bond in ethane and a C-H bond in methane) should have similar force constants. The ab initio quantum mechanical calculation of force constants in recent years has supported this idea (40,73,75,97). For the present work, it is of special significance that a force field obtained for a molecule in an ab initio calculation using the 4-31G basis set reproduces quite well the spectral frequencies, when multiplied by the proper scaling factors (14,98-100). Pulay, Fogarasi, Pongor, and Vargha (97) have recommended a uniform procedure to carry out such scaling procedure for results from a similar 4-21G basis set. Their determination of the scaling factors is based on a least-squares fitting of the calculated vibrational frequencies to the experimental ones. Empirically adjusted ab initio force constants are now available for a number of prototype organic molecules such as benzene (73), methanol (98), propene (99), ethane (100), cyclobutane (101), and cubane (102). It is concluded that a combination of theoretical calculations with experimentally assigned frequencies makes it possible to obtain significant values of adjusted force constants. For example, it is generally found that diagonal stretching force constants are overestimated in ab initio calculations by about 10 - 15 % and diagonal bending force constants are overestimated by about 20 - 30 %, but occassionally calculated interaction force constants agree very well with the experimental values. These adjusted ab initio force fields have proved to be very useful for predicting spectra of molecules (73,74,98).

It should be made clear that the scaling procedure for the ab initio results can be carried out either for force constants or for the frequencies. For various reasons, the former approach is commonly

preferred. First, frequencies can be determined from the force constants but not vice versa. Also, many different types of force constants simultaneously contribute to a specific frequency. Moreover, the "correction" of ab initio force constants with the accuracy given for the scaling factors in the preceding paragraph still leads to overestimation of the vibrational frequencies by roughly 10 %. Pople, Schlegel, Krishnan, De Frees, and Binkley (103) demonstrated this conclusion in a study of the calculated frequencies of 37 molecules. Other studies (40,74,104) have reached the same conclusion.

So far we have seen that the scaling factors must play a major role in any scheme involving the transfer of "adjusted force constants" of smaller molecules to predict vibrational frequencies of larger molecules. To illustrate further we present the following sample of studies which have adjusted force constants obtained from ab initio quantum mechanical methods by empirical scale factors.

Scaled ab initio force fields were systematically obtained by Blom and Altona for ethane, propane, cyclopropane (100), propene (99), methanol (98), and ethene (105). In all their calculations they used the 4-31G basis set to obtain the complete general valence force field of each molecule. This ab initio force field was later scaled with different scaling factors in order to reproduce the experimental frequencies. For the first three molecules (100) a total of 180 vibrational frequencies (including those for deuterated analogues) were used in a fitting; the mean deviation between observed and calculated frequencies amounted to 10.4 cm^{-1} or 0.74 %. Similar results were obtained for the other molecules.

For the benzene molecule, Pulay, Fogarasi, and Boggs (73) obtained ab initio force fields with different basis sets (STO-3G, 4-21G, and 4-31G), which were then scaled with scaling factors determined by least-squares fitting to the observed spectrum. They found that these empirical scale factors fall in the range 0.7 - 0.9. Another important conclusion from this study was the fact that the calculated STO-3G force constants are qualitatively correct, in that at least their signs agree with those from the better basis sets.

The scale factors obtained for benzene (73) were directly applied to the ab initio (4-21G basis set) force field constants for pyridine by Pongor, Pulay, Fogarasi, and Boggs (106). This scaled force field was then used to predict the vibrational spectrum of pyridine. Comparison of experimental and predicted spectra showed a mean deviation of 5.7 cm^{-1} for the non-CH frequencies. They suggested that this method of obtaining scale factors for a related reference molecule and applying them to another will permit the accurate prediction of a truly unknown vibrational spectrum.

Using an ab initio calculation with a 4-31G basis set, Wiberg, Walters, Wong, and Colson (74) also determined a force field for pyridine, which they adjusted with scaling factors (constant for each symmetry class, and ranging from 0.73 - 0.86) to fit the observed frequencies for pyridine-d_0 , pyridine-d_5, and partially deuterated pyridines. Their fit between the observed and calculated frequencies gave a standard deviation of 6.6 cm^{-1}.

Transfer of Atomic Polar Tensors

As it has been previously pointed out in Chapters 2 and 3, the APTs for the atoms in a molecule are a natural representation of intensity

results for comparison with ab initio quantum mechanical calculations for that particular molecule. Since we are concerned here with the possibility of successful transfer of vibrational parameters, we shall address the following question: should we expect that the APTs for the atoms in a molecule to be exactly transferable to the atoms in a chemically similar molecule? If the evidence demonstrates that the answer to this question is affirmative, then the transferability of APTs provides a powerful tool for the prediction of absolute infrared intensities of larger molecules, starting with APT values from smaller molecules. As we attempt to answer this question it should be remembered that the elements of the APTs are expected to reflect contributions from dipole-induced dipole terms, changes in hybridization, etc., which are not all expected necessarily to be the same from one molecule to another.

Transfer of APTs from reference molecules with the aim of calculating the gas phase infrared intensities for similar molecules has been discussed by Person (60). He pointed out that since general rules have not been established to decide which APTs are the most suitable to be transferred to the molecule whose intensities are to be determined, this question poses a real challenge. However, some attempts by person and coworkers (23,32,39,63,64,107), Bruns (108,109), and others (58) have provided promissing results which might well serve as guidelines when trying to transfer APTs of atoms in a molecule to the same atoms in another molecule.

The first suggestion that APTs may be transferable was the discovery by King, Mast, and Blanchette (62) that the effective charge, ξ_α, appeared to be the same for H atoms in a wide variety of molecules.

Since the ξ_α (later redefined in terms of χ_α as three times χ_α, (see Eq. (3-6) and discussion of APT invariants in Chapter 3)) is an invariant of the APT, Newton and Person (32) conducted a study to examine the possibility of transferring the APTs themselves for H and F atoms in different fluorinated methane molecules. Their results were very encouraging. They concluded that the APTs for H and for F atoms from CH_3F are reasonable choices for transfer to calculate the infrared intensities of other fluoromethane molecules. They calculated intensities for CH_2F_2, CHF_3, and CF_4 using the APTs from CH_3F. The results obtained were always within a "factor of two" (32,63) of the experimental values, and for strong bands the agreement is much better.

Additional studies by Person and Newton (64,110) showed that this F atom APT could be transferred to predict the infrared intensities for fundamental vibrations of the CF_2 and CF_3 radicals. It was not obvious that the use of the F atom APT in this calculation would be successful, since CF_3 has an odd electron, and CF_2 has two odd electrons. Nevertheless, the results obtained are in very good agreement with experimental data. It has been pointed out by Person (60) that this study illustrates the potential power of this technique for applications to infrared studies of free radical reactions. Furthermore, the F atom APT of CH_3F was transferred to predict the infrared intensities for SF_6 and UF_6 molecules, by Person and Overend (111). They found that their predicted intensities agreed with experimental values within the experimental uncertainty.

Now let us consider some examples where the F atom APT from CH F cannot be successfully transferred to make intensity predictions. This is the case for the CF_3Cl molecule, as has been demonstrated by Golden,

Horner, and Overend (112). This non-transferability has been discussed by Person (60) in terms of atomic polarizabilities. He points out that we should not expect success in the transfer of an F atom APT from CH_3F to CF_3Cl because Cl is more polarizable than H or F atoms, so this "polarizability effect" causes a big charge flux contribution to the F atom APTs in CF_3Cl but not in CH_3F or in CF_4. The same argument has been used to explain failures of transferability of APTs to other molecules; for example, in F_2CO and F_2CS (113).

It has been shown by Rogers (39) that H and O atom APTs are also transferable from CH_3F and H_2O to CH_3OH, C_2H_5OH, and CH_3OCH_3 molecules. The transfer was not successful from HCHO to CH_3COCH_3, probably because of the influence from the polarizable C=O bond on the C-H intensity parameters. It was also found by Herrera, Ramos, and Bruns (108) that the APTs from cis-difluoro- and cis-dichloroethylene are directly transferable to their respective trans isomers, resulting in predicted intensities that are in agreement with the experimental intensities. In another study, Kagel, Powell, Hopper, Overend, Ramos, Bassi, and Bruns (114) successfully transferred H, F, and O atom APTs to HFCO and DFCO molecules from cis-$C_2H_2F_2$, H_2CO and F_2CO molecules. They reported that the calculated values of the infrared intensities for the former molecules are in good agreement with the experimental values. Also, transferring the C and O atom APTs of $Cr(CO)_6$ for the prediction of the intensities of $Mo(CO)_6$ and $W(CO)_6$, Bruns, Hase, and Brin (109) reproduced the experimental intensities of these heavier group VIB metal carbonyls within the usual "factor of two". However, when they attempted a direct transfer of the APTs from $Ni(CO)_4$ to $Mo(CO)_6$ and $W(CO)_6$ the experimental intensities were not correctly reproduced.

They suggested first, that this failure could be attributed to the difference in electronic structure of the Ni carbonyl as compared to that of Cr, Mo, or W carbonyls; and second, that the different symmetries imply differences in hybridization of the metal orbitals, and therefore different behaviours with respect to variation of bond distances and angles.

All the evidence presented shows that a priori guidelines have not been established as yet for transferring the appropriate APTs for "perfect" intensity predictions. However, it is very encouraging to note that the evidence demonstrates succesful results within a "factor of two" in the prediction of infrared intensities when the APTs are transferred for atoms in chemically related molecular environments.

Comparison of ab initio Vibrational Parameters

An examination and comparison of the force constants and APTs obtained by ab initio quantum mechanical methods for uracil and other molecules (e.g., pyridine) is expected to provide interesting details about the similarity or difference in the electronic nature of these molecules. Perhaps we could also obtain information on the direct transfer of such vibrational parameters between related molecules. Of course, we are not looking for exact values of ab initio force constants or APTs in two molecules, but rather for possible trends in values of these parameters. Anyway, this type of comparison should give more confidence about the use of quantum mechanical procedures in solving vibrational spectroscopy problems.

Ab initio Force Constants

The first comparison of ab initio values that we want to make is for some "corrected to 4-31G" force constants (see Chapter 4) of uracil

with those obtained for other molecules at the same level of approximation. In Table 5-1 are presented and compared some of these force constants. The values that are given in each column were taken from the following studies, Column 1: STO-3G "converted to 4-31G" for uracil by Nishimura, Tsuboi, Kato, and Morokuma (14); Column 2: 4-31G force constants determined for formamide by Sugawara, Hamada, Hirakawa, Tsuboi, Kato, and Morokuma (46); Column 3: 4-31G values for N-methylformamide obtained by Sugawara, Hirakawa, Tsuboi, Kato, and Morokuma (40); Column 4: gives some force constants at the 4-31G level for pyridine by Wiberg, Walters, Wong, and Colson (74); Column 5: shows some values at the 4-31G level for acetaldehyde obtained by Wiberg, Walters, and Colson (104); and Column 6: gives some force constants obtained for pyridine at the 4-21G level by Pulay, Fogarasi, and Boggs (106).

A close look to Table 5-1 shows how similar the value of the ab initio force constants are in the different molecules presented. Take, for example, the C_2O stretching values of 13.298 md A^{-1} for uracil, 13.864 md A^{-1} for formamide, 13.4 md A^{-1} for N-methylformamide, and 14.749 md A^{-1} for acetaldehyde. It is evident that all these values for this constant fall in a very narrow range. The same similarity holds true for the force constants for the C_2N_1 stretch, N_1H deformation, and OC_2N deformation. It is also interesting to note that the "corrected to 4-31G" force constant value of 6.181 md A^{-1} for the C_6H stretch in uracil seems to be overestimated when compared to the rest of the values given in Table 5-1: 5.708, 5.77, 5.218, 5.198, and 5.658 md A^{-1}.

TABLE 5-1
COMPARISON OF AB INITIO FORCE CONSTANTS

	Uracil[a]	Formamide[b]	N-Me For.[c]	Pyridine[d]	Acetaldeh.[e]	Pyridine[f]
N_1H stretch.[g]	8.256[h]	7.970	8.350	---	---	---
C_2N_1 stretch.	7.356	8.236	8.480	7.110	---	7.989
C_2O stretch.	13.298	13.864	13.400	---	14.749	---
C_5C_6 stretch.	6.042	---	---	6.529	---	6.949
C_6H stretch.	6.181	5.708	5.770	5.198	5.658	5.218
C_2O bend.	1.256	2.290	1.390	---	---	---
C_6H bend.	6.181	---	5.770	---	---	---
N_1H bend.	0.619	1.170	0.680	---	---	---
C_2N_1 stretch./C_2O stretch.	0.908	1.375	1.500	---	---	---
C_2N_1 stretch./C_2O bend.	-0.420	0.539	0.390	---	---	---
C_2N_1 stretch./N_1H bend.	0.070	0.206	0.240	---	---	---
C_2O bend. /N_1H bend.	0.056	0.039	0.080	---	---	---
N_1H stretch./C_2O stretch.	-0.036	-0.006	-0.040	---	---	---

---

continued

TABLE 5-1 continued

N_1H stretch./C_2N_1 stretch.	0.000	0.069	0.010	---	---	---
N_1H stretch./C_6H stretch.	0.000	-0.022	0.020	---	---	---
N_1H stretch./C_6H bend.	0.000	0.038	0.010	---	---	---

[a]Force constants taken from the study of uracil by Nishimura, Tsuboi, Kato, and Morokuma (14).

[b]Force constants taken from the study of formamide by Sugawara, Hamada, Hirakawa, Tsuboi, Kato, and Morokuma (46).

[c]Force constants taken from the study of N-methylformamide by Sugawara, Hirakawa, Tsuboi, Kato, and Morokuma (40).

[d]Force constants taken from the study of pyridine by Wiberg, Walters, Wong, and Colson (74).

[e]Force constants taken from the study of acetaldehyde by Wiberg, Walters, and Colson (104).

[f]Force constants taken from the study of pyridine by Pongor, Pulay, Fogarasi, and Boggs (106).

[g]Atom numbering is with respect to uracil (Fig. 3-1).

[h]Units: stretching in mdyne/Å and bending in mdyne Å.

In general, the interaction force constants calculated for the various molecules presented in Table 5-1 also have comparable values within the same order of magnitude. Also, their signs are usually predicted the same in all cases. It is not clear whether or not the discrepancies are meaningful.

APTs for uracil and pyridine

Let us now compare the APTs for uracil (see Table 3-3) from our calculations (17) with those for pyridine obtained by Wiberg, Walters, Wong, and Colson (74). Both calculations were carried out using a 4-31G basis set. In table 5-2 the APTs for each atom in uracil and pyridine are shown. The atom numbering follows that given in Fig. 5-1(a). In order to facilitate their comparison, the APTs have been expressed in a bond coordinate system, as defined in Figs. 5-1(b-g). Also, the APTs for pyridine obtained by Wiberg et al. (74) have been converted from D $\mathring{A}^{-1}$ to e units (1e = 4.803 D $\mathring{A}^{-1}$).

We see in Table 5-2 that the values for the APTs are very different for almost all atoms. It seems that the aromaticity of pyridine and non-aromaticity of uracil causes the atoms in the ring (N_1, C_2, C_4, C_5, and C_6) to be different chemically in the two rings and thus to have different effective charges χ. Basically the only similarities between these molecules lie in the APTs and the χ values of atoms H_{11} and H_{12}. This could well be expected given that the C_5=C_6 double bond in uracil could resemble the analogous bond in pyridine in its electronic nature and polarizability character. Hence, the terminal hydrogen atoms attached to these carbon atoms should be very similar.

It is interesting to notice that the N_1 atom is so different in pyridine than in uracil, due partly to attached H_7 atom in the latter.

TABLE 5-2
COMPARISON OF APTs FOR URACIL
WITH THOSE FOR PYRIDINE.
(units are electrons (e))

	Uracil[a]			Pyridine[b]		
C_2[c]	2.196	-.074	0	0.498	-.005	0
	0.131	1.433	0	0.168	0.104	0
	0	0	0.850	0	0	0.048
	χ = 1.594			χ = 0.310		
O_8[c]	-1.556	0.004	0	-.121	0.005	0
	0.023	-.543	0	0.018	0.075	0
	0	0	-.620	0	0	0.119
	χ = 1.017			χ = 0.108		
N_3[d]	-.620	-.033	0	0.102	0.015	0
	-.073	-1.406	0	-.146	-.382	0
	0	0	-.660	0	0	-.152
	χ = 0.967			χ = 0.259		
H_9[d]	0.276	-.002	0	-.104	-.010	0
	-.054	0.156	0	-.004	0.086	0
	0	0	0.446	0	0	0.152
	χ = 0.318			χ = 0.118		
C_4[e]	1.828	0.432	0	0.258	0	0
	-.259	1.178	0	0.002	0.167	0
	0	0	0.680	0	0	-.083
	χ = 1.347			χ = 0.184		
O_{10}[e]	-1.649	-.204	0	-.104	0	0
	0.114	-.639	0	0.002	0.085	0
	0	0	-.592	0	0	0.140
	χ = 1.085			χ = 0.117		

---

continued

TABLE 5-2 continued

C_5[f]

$$\begin{pmatrix} -.171 & -.330 & 0 \\ 0.125 & -.822 & 0 \\ 0 & 0 & -.428 \end{pmatrix} \qquad \begin{pmatrix} 0.102 & -.015 & 0 \\ 0.146 & -.382 & 0 \\ 0 & 0 & -.152 \end{pmatrix}$$

$\chi = 0.581$ $\qquad$ $\chi = 0.259$

H_{11}[f]

$$\begin{pmatrix} 0.086 & 0.033 & 0 \\ 0.051 & 0.051 & 0 \\ 0 & 0 & 0.197 \end{pmatrix} \qquad \begin{pmatrix} -.104 & 0.010 & 0 \\ 0.004 & 0.086 & 0 \\ 0 & 0 & 0.152 \end{pmatrix}$$

$\chi = 0.132$ $\qquad$ $\chi = 0.118$

C_6[g]

$$\begin{pmatrix} 0.439 & -.347 & 0 \\ 0.267 & 1.252 & 0 \\ 0 & 0 & 0.268 \end{pmatrix} \qquad \begin{pmatrix} 0.498 & 0.005 & 0 \\ -.168 & 0.104 & 0 \\ 0 & 0 & 0.048 \end{pmatrix}$$

$\chi = 0.817$ $\qquad$ $\chi = 0.310$

H_{12}[g]

$$\begin{pmatrix} -.046 & 0.022 & 0 \\ 0 & 0.064 & 0 \\ 0 & 0 & 0.151 \end{pmatrix} \qquad \begin{pmatrix} -.121 & -.005 & 0 \\ -.018 & 0.075 & 0 \\ 0 & 0 & 0.119 \end{pmatrix}$$

$\chi = 0.099$ $\qquad$ $\chi = 0.108$

N_1[h]

$$\begin{pmatrix} -.754 & 0.565 & 0 \\ -.276 & -1.181 & 0 \\ 0 & 0 & -.729 \end{pmatrix} \qquad \begin{pmatrix} -.488 & 0 & 0 \\ 0.002 & -.481 & 0 \\ 0 & 0 & -.388 \end{pmatrix}$$

$\chi = 0.982$ $\qquad$ $\chi = 0.455$

H_7[h]

$$\begin{pmatrix} 0.274 & -.018 & 0 \\ 0.041 & 0.153 & 0 \\ 0 & 0 & 0.437 \end{pmatrix} \qquad \begin{pmatrix} -.480 & 0.547 & 0 \\ -.235 & -1.028 & 0 \\ 0 & 0 & -.292 \end{pmatrix}$$ [i]

$\chi = 0.312$ $\qquad$ $\chi = 0.759$

[a]The APTs for uracil are those given in Table 3-3

[b]The APTs for pyridine are taken from those obtained by Wiberg et al. (74).

[c]Orientation is in the bond coordinate system of Fig. 5-1(b).

[d]Orientation as given in Fig. 5-1(c).

[e]Orientation as given in Fig. 5-1(d).

[f]Orientation as given in Fig. 5-1(e).

[g]Orientation as given in Fig. 5-1(f).

[h]Orientation as given in Fig. 5-1(g).

[i]This APT is the sum of the elements of the APTs for atoms N_1 and H_7 of uracil, in the axes orientation of Fig. 5-1(g).

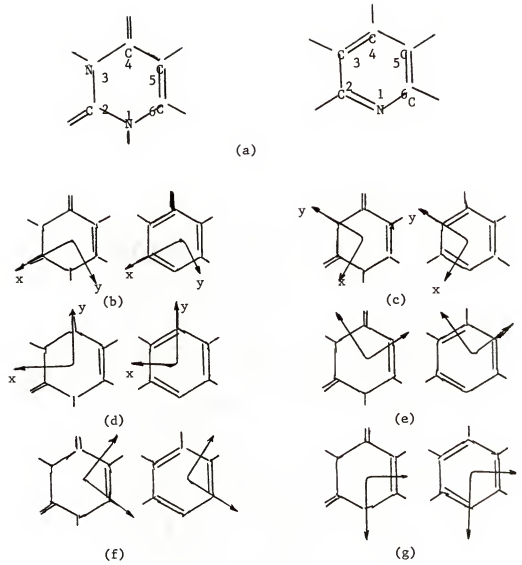

Figure 5-1. Coordinate bond axes representation. (a) Atom numbering for uracil and pyridine, (b) Bond coordinate system for atoms 2 and 8. Also, (c), (d), (e), (f), and (g) represent bond coordinate systems.

As shown in Table 5-2, a sum of the APT elements of atoms N_1 and H_7 of uracil gives some values similar to those of the APT for pyridine. In particular the $(\partial p_x/\partial x)$ and $(\partial p_z/\partial z)$ values of -0.488 and -0.388 e, respectively, for pyridine compare very well with the sum of the corresponding elements for atoms N_1 and H_7 in uracil (-0.480 and -0.292 e, respectively). Also note that the effective charge χ for atom N_1 in uracil is 2.16 times that of the N_1 atom of pyridine, while the ratio of $\chi(N_1 + H_7$ for uracil) to $\chi(N_1$ for pyridine) is just 1.66.

It is also evident from Table 5-2 that the APTs of the carbon atoms on the ring of both molecules show many fluctuations. The values for these atoms in uracil are always larger than those in pyridine.

In conclusion, from this comparison is obvious that the transfer of pyridine parameters to a pyrimidine ring would produce incorrect results.

Transfer of ab initio Vibrational Parameters to Methylated Uracils

Because of our interest in the methylated uracil molecules, we shall end this chapter discussing how force constants and APTs might be transferred to predict spectra of these particular molecules. This survey will serve as the basis for presentation of the actual results in Chapter 6.

As described in Chapter 2 we decided to carry out two types of calculations, namely: Calculation I where the methyl group is taken as a dynamic unit of mass 15 u, and Calculation II where the methyl group is properly treated as a four atom dynamic unit.

Transfer of ab initio Force Constants

The methylated uracils to be considered are the following: 1-methyluracil (1-Me U), 1-methyl-3-deuterouracil (1-Me-3-D U), 3-methyluracil (3-Me U), and 1,3-dimethyluracil (1,3-di Me U). Each one of these molecules will be discussed in more detail in Chapter 6. Here we just want to discuss which force constants can be used in each case.

For 1-Me U we can transfer the uracil "corrected to 4-31G" force constants directly to the ring system of the molecule, when carrying out both Calculation I and Calculation II. The same transfer should apply to the rings of 1-Me-3-D U, 3-Me U, and 1,3-di Me U. When treating any of these molecules in Calculation I, we can transfer the stretching, bending, and interaction ab initio force constants from N-methylformamide (40, see also Table 5-1) to the corresponding N-Me bond in the methylated uracils.

The values of the C-H stretching, bending, and interaction force constants to be used for the methyl group in Calculation II can be directly transferred from the CH_3 group attached to the nitrogen atom in N-methylformamide, from the ab initio calculation of the force constant values for this molecule (40), obtained using a 4-31G basis set. Also, the comparison of ab initio force constants in Table 5-1 shows some consistency between the values of force constants for uracil and for N-methylformamide. Another possibility is to make a direct transfer of the force constants for the methyl group obtained at the 4-31G level for N-methylacetamide by Sugawara, Hirakawa, Tsuboi, Kato, and Morokuma (115). We decided to use the force constant values from the N-methylacetamide study (115) because we had obtained the APTs for

N-methylacetamide, and we wanted to conduct a full study of frequencies and intensities for this molecule, which will be presented elsewhere (116).

Transfer of APTs

In order to decide on which APTs should be transferred to the atoms in 1-Me U, 1-Me-3-D U, 3-Me U, and 1,3-di Me U, the simplest approach would be just the direct transfer of APTs from each atom in uracil to the corresponding atoms in each particular molecule. For Calculation I this can be done exactly. The APT of the N_1H hydrogen atom in uracil is transferred to the Me dynamic unit in 1-Me U, or that for N_3H to 3-Me U, etc. This assumption is perhaps the most drastic in Calculation I.

For Calculation II there is a bigger challenge in deciding on the correct transfer of APTs for the $N\text{-}CH_3$ fragment in each one of the methylated uracils. The APTs for the CH_3 groups in acetone obtained by Rogers (39) from an *ab initio* calculation using a 4-31G basis set seem to reproduce well the intensity pattern of the methyl groups in the C-H stretching region of the methylated uracils. We can satisfy the null condition (Eq. (3-5)) by adjusting the APTs of the carbon and nitrogen atoms. In other words, we can transfer the APTs for all four atoms in the complete CH_3 group from acetone to the methylated uracils and use the null condition to determine the APT of the nitrogen atom to which the CH_3 is attached, or we might transfer those APTs for the hydrogen atoms from acetone to the methylated uracils, using the null condition to obtain the APT for the carbon atom of the CH_3 group. We have considered both alternatives in this study. Again we emphasize that the APTs for the rest of the atoms are transferred directly from uracil.

Inspired by the ab initio study of force constants for N-methylformamide (40) we decided to conduct an ab initio study of the APTs of a related molecule, N-methylacetamide (116). Since this molecule (N-methylacetamide) has two CH_3 groups, we propose to test the transfer of APTs from each one of them to the CH_3 group in the methylated uracils. Again, the null condition can be used to determine the nitrogen and carbon APTs in the $N-CH_3$ moieties of the methylated uracils. The APTs for N-methylacetamide are given in Table 5-3, from Ref. 116. The atom numbering and axes orientation for the APTs in Table 5-3 is according to Fig. 5-2.

TABLE 5-3
APTs FOR N-METHYLACETAMIDE

C_1

$$\begin{pmatrix} 0.012 & 0.050 & 0 \\ 0.208 & 0.618 & 0 \\ 0 & 0 & 0.382 \end{pmatrix}$$

$\chi = 0.437$

N_2

$$\begin{pmatrix} -.552 & 0.514 & 0 \\ 0.200 & -1.386 & 0 \\ 0 & 0 & -.815 \end{pmatrix}$$

$\chi = 1.032$

C_3

$$\begin{pmatrix} 1.328 & -.424 & 0 \\ -.454 & 1.665 & 0 \\ 0 & 0 & 0.511 \end{pmatrix}$$

$\chi = 1.314$

C_4

$$\begin{pmatrix} 0.167 & -.151 & 0 \\ -.116 & -.266 & 0 \\ 0 & 0 & -.010 \end{pmatrix}$$

$\chi = 0.212$

O_5

$$\begin{pmatrix} -1.252 & -.085 & 0 \\ 0.170 & -.826 & 0 \\ 0 & 0 & -.548 \end{pmatrix}$$

$\chi = 0.928$

H_6

$$\begin{pmatrix} 0.113 & -.038 & 0 \\ -.024 & 0.154 & 0 \\ 0 & 0 & 0.417 \end{pmatrix}$$

$\chi = 0.266$

H_7

$$\begin{pmatrix} 0.004 & 0.046 & 0 \\ -.042 & 0.103 & 0 \\ 0 & 0 & 0.126 \end{pmatrix}$$

$\chi = 0.101$

H_8

$$\begin{pmatrix} 0.084 & 0.015 & 0.070 \\ 0.015 & -.092 & -.120 \\ 0.067 & -.058 & -.080 \end{pmatrix}$$

$\chi = 0.128$

H_9

$$\begin{pmatrix} 0.084 & 0.015 & -.070 \\ 0.015 & -.092 & 0.120 \\ -.067 & 0.058 & -.080 \end{pmatrix}$$

$\chi = 0.128$

H_{10}

$$\begin{pmatrix} -.140 & 0.104 & 0 \\ 0 & 0.032 & 0 \\ 0 & 0 & 0.073 \end{pmatrix}$$

$\chi = 0.111$

H_{11}

$$\begin{pmatrix} 0.076 & -.023 & -.028 \\ 0.014 & 0.045 & 0.088 \\ -.042 & 0.046 & 0.012 \end{pmatrix}$$

$\chi = 0.084$

H_{12}

$$\begin{pmatrix} 0.076 & -.023 & 0.028 \\ 0.014 & 0.045 & -.088 \\ 0.042 & -.046 & 0.012 \end{pmatrix}$$

$\chi = 0.084$

Note: The atomic numbering scheme and coordinate system are shown in Fig. 5-2. Effective charges (χ) are calculated from Eq. (3-6). Units are electrons (e).

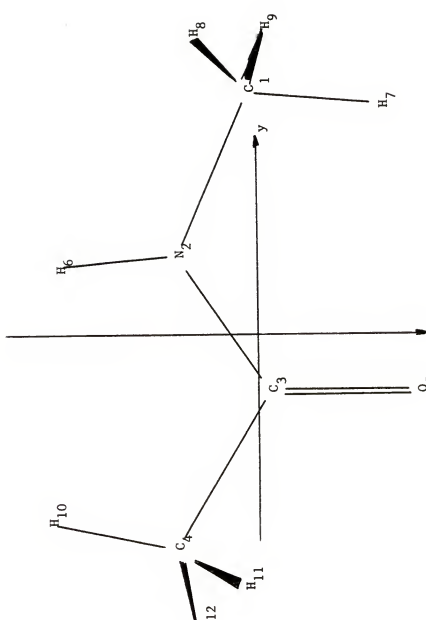

Figure 5-2. Atom numbering and orientation of the principal Cartesian coordinate axes of N-methylacetamide.

CHAPTER 6
PREDICTION OF INFRARED SPECTRA OF METHYLATED URACILS

This chapter deals with the details and results of the prediction of infrared spectra for the methylated uracils, using both Calculations I and II. We shall first consider the transfer of APTs and ab initio force constants from smaller molecules or molecular fragments to the following methylated uracils: 1-methyluracil (1-Me U), 1-methyl-3-deuterouracil (1-Me-3-D U), 3-methyluracil (3-Me U), and 1,3-dimethyluracil (1,3-di Me U). This is followed by a discussion and comparison of the results of the experimental matrix-isolated and predicted spectra for these molecules, in order to assign their observed frequencies and intensities.

Transfer of APTs

In our scheme for transferring vibrational parameters presented in Chapter 2 we explained that our predictions of frequencies and intensities were made on two levels: Calculation I and Calculation II. Let us now consider the transfer of APts to the methylated uracils using each one of these approaches.

Calculation I

In the first and simpler approach (Calculation I) the methyl group was treated as a single dynamical point mass of 15 u, so this calculation gives the effect of the heavy mass on the frequencies of the ring vibrations. Basically, the problem to solve is one similar to that of

determining frequencies and intensities for a deuterated uracil molecule, except that we use 15 u for the substituted atom instead of 2 u. In the experimental spectrum of the real molecule, of course, we see the characteristic absorptions by the vibrations within the methyl group, but we assume that this spectrum is known because it is characteristic. After making the changes in masses in uracil (Fig. 3-1), we place an atom of 15 u in the H_7 position for 1-Me U and 1-Me-3-D U (in this molecule 2 u is the mass for the replacement of H_9 by D_9), in the H_9 position for 3-Me U, and two 15 u atoms replace H_7 and H_9 for 1,3-di Me U. Basically, the force constants are assumed to be the same as uracil, and the frequencies are calculated for the "heavy mass uracils".

All the APTs used in Calculation I to predict intensities were transferred directly from uracil to the methylated uracils. These APTs are shown in Table 3-3 for uracil. No rotation of these APTs was necessary, because we made our calculation in the same Cartesian coordinate system which was used for uracil (Fig. 3-1).

Calculation II

The approach followed in Calculation II is much more elaborated because the methyl group was treated properly as a polyatomic substituent, so we have to carry out NCAs for 15-atom or 18-atom molecules instead of for 12-atom molecules. The APTs used for the CH_3 group in this calculation were transferred from acetone (39) or N-methylacetamide (116), and those for the ring atoms were transferred from uracil.

1-methyluracil

Let us consider first the case of Calculation II for 1-Me U, in which H_7 in uracil (Fig. 3-1) is replaced by the CH_3 group. The

equilibrium geometry and the numbering of atoms for this molecule are shown in Fig. 6-1, where the structural parameters given for the N-CH_3 fragment are derived from those reported for that fragment in N-methylformamide by Kitano and Kuchitsu (117) from an electron diffraction study. Khetrapal and Kunwar (118) found from NMR measurements that the 1-CH_3 group in 1,3-di Me U is oriented with one hydrogen in the plane pointing toward the 2-carbonyl group, and we have assumed this geometry for 1-Me U. Also included in Fig. 6-1 are the Cartesian coordinates for the CH_3 group; the coordinates for the remaining atoms are the same as for uracil (Fig. 3-1 and Table 3-1).

In order to test the transferability of APTs for the methyl in the methylated uracils in Calculation II, we tried several different sets of APTs, changing particularly those for the atoms in the CH_3 group from the values transferred from acetone, to those from the N-CH_3 and from the C-CH_3 groups of N-methylacetamide (Table 5-3). For 1-Me U the APTs transferred from acetone were those calculated by Rogers (39), but the coordinate system was rotated by +87.74° (Eq. (3-4)) in order to have them coincide with the coordinate axes for 1-Me U, as seen in Fig. 6-2. Since the APTs for N-methylacetamide (116) were calculated in the principal Cartesian system of Fig. 5-2 (Table 5-3), it was necessary to rotate this coordinate system for the APTs in the N-CH_3 group by +232.91° and for the APTs in the C-CH_3 group by +60.21° (Eq. (3-4)), as it is also shown in Fig. 6-2, in order to conform the coordinate axes orientation of 1-Me U (see Fig. 6-1). The resulting APTs after the rotations are given in Table 6-1, where Column 1 shows the APTs from acetone, and Columns 2 and 3 those from the N-CH_3 and C-CH_3 groups of N-methylacetamide, respectively. Also, the APT for the N_1

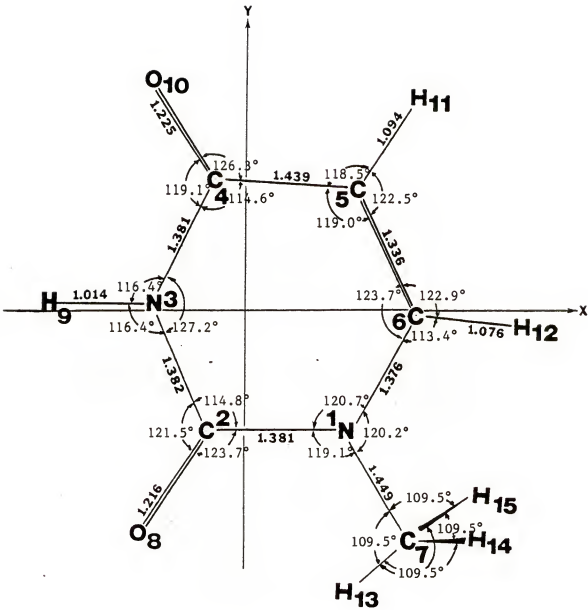

	x	y	z
C_7	1.732536	-2.476096	0.000000
H_{13}	1.012277	-3.294220	0.000000
H_{14}	2.365462	-2.565047	0.882945
H_{15}	2.365462	-2.565047	-0.882945

Figure 6-1. Geometrical parameters of 1-Me U and Cartesian coordinates for the CH_3 group in the Cartesian coordinate system of uracil. Coordinates for the ring atoms of uracil are given in Table 3-1. All C-H bond lenghts in the CH_3 group are taken as 1.092 Å.

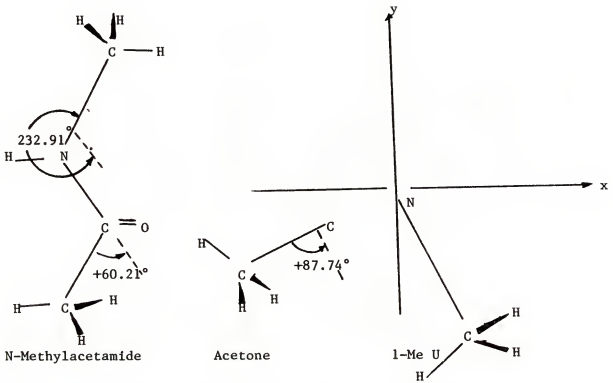

Figure 6-2. Rotation of coordinate system for N-Methylacetamide and acetone to conform the orientation of the APTs of 1-Me U.

TABLE 6-1
TRANSFERRED APTs (in e) FROM THE CH_3 GROUPS OF ACETONE, AND FROM THE N-CH_3 AND C-CH_3 GROUPS OF N-METHYLACETAMIDE, AND THAT FOR THE N_1 ATOM OF URACIL, USED FOR THE N-CH_3 GROUP OF 1-METHYLURACIL

	CH_3 of acetone[a,b]	N-CH_3 of N-Me A[a,c]	C-CH_3 of N-Me A[a,c]
$P_x(C_7)$	$\begin{pmatrix} -.062 & 0.106 & 0 \\ 0.068 & -.281 & 0 \\ 0 & 0 & 0.039 \end{pmatrix}$	$\begin{pmatrix} 0.274 & -.406 & 0 \\ -.248 & 0.356 & 0 \\ 0 & 0 & 0.382 \end{pmatrix}$	$\begin{pmatrix} -.044 & 0.237 & 0 \\ 0.271 & -.056 & 0 \\ 0 & 0 & -.010 \end{pmatrix}$
	$\chi = 0.183$	$\chi = 0.437$	$\chi = 0.212$
$P_x(H_{13})$	$\begin{pmatrix} 0.017 & -.059 & 0 \\ -.102 & -.044 & 0 \\ 0 & 0 & 0.101 \end{pmatrix}$	$\begin{pmatrix} 0.065 & -.004 & 0 \\ -.092 & 0.042 & 0 \\ 0 & 0 & 0.126 \end{pmatrix}$	$\begin{pmatrix} -.055 & -.049 & 0 \\ -.153 & -.052 & 0 \\ 0 & 0 & 0.073 \end{pmatrix}$
	$\chi = 0.094$	$\chi = 0.101$	$\chi = 0.111$
$P_x(H_{14}^d)$	$\begin{pmatrix} 0.013 & 0.004 & 0 \\ 0.016 & 0.081 & 0.013 \\ -.086 & -.038 & -.028 \end{pmatrix}$	$\begin{pmatrix} -.042 & 0.080 & 0 \\ 0.080 & 0.034 & 0.017 \\ -.086 & -.018 & -.080 \end{pmatrix}$	$\begin{pmatrix} 0.057 & -.003 & 0 \\ 0.033 & 0.064 & 0.019 \\ -.061 & -.013 & 0.012 \end{pmatrix}$
	$\chi = 0.102$	$\chi = 0.128$	$\chi = 0.083$
	N_1, uracil	N_1, N-Me A	C_1, N-Me A
$P_x(N_1,C_1)$	$\begin{pmatrix} -.957 & 0.163 & 0 \\ -.678 & -.978 & 0 \\ 0 & 0 & -.729 \end{pmatrix}$	$\begin{pmatrix} -1.426 & 0.461 & 0 \\ 0.146 & -.512 & 0 \\ 0 & 0 & -.085 \end{pmatrix}$	$\begin{pmatrix} 1.960 & 0.092 & 0 \\ 0.063 & 1.033 & 0 \\ 0 & 0 & 0.511 \end{pmatrix}$
	$\chi = 0.982$	$\chi = 1.032$	$\chi = 1.314$

[a] All APTs have been been rotated to coordinate axes of Fig. 6-1.

[b] APTs taken from the study of acetone by Rogers (39).

[c] APTs taken from the study of N-methylacetamide by Scott (116).

[d] $P_x(H_{15})$ is obtained by reversing the signs of the off-diagonal components of $P_x(H_{14})$ involving z.

atom of uracil (Fig. 3-1 and Table 3-3) is included in Table 6-1, and compared with those for the N_1 atom in the N-CH_3, and to the C_1 atom in the C-CH_3 fragments of N-methylacetamide. Note that these APTs depend also on the nature of the other groups attached to the N_1 (or C_1) atom, as well as in the CH_3 group. For all the APTs the effective charges (Eq. (3-6)) for each atom are also given in this table.

In our Calculation II we assumed that 1-Me-3-D U has the same geometry and vibrational parameters (force constants and APTs) as 1-Me U. Hence, the calculation of both molecules uses the same APTs and force constants.

Let us now compare the different sets of APTs given in Table 6-1. First, we note that there is some similarity in the diagonal elements of the APTs for the N_1 atoms in uracil and in N-methylacetamide: -0.957, -0.978, and -0.729 e in uracil compared with -1.426, -0.512, and -0.815 e respectively in N-methylacetamide, with χ values of 0.982 and 1.032 e, respectively. When we compare the APTs for C_7 in all three cases in Table 6-1, we see how different the χ values are: 0.183 e (acetone), 0.437 e (N-CH_3), and 0.212 e (C-CH_3). The elements of the APTs for this atom are different for each case. However, note that those for acetone, where the CH_3 group is attached to a -$COCH_3$ fragment, are more similar to those for C-CH_3 in N-methylacetamide (where the CH_3 is attached to the -$CONHCH_3$ fragment). The χ values are quite close, in fact. Finally, note how close the χ values are for all the H atoms, falling in a small range between 0.083 - 0.111. The elements of the H-atom APTs are quite different from each other, reflecting the different influence of the asymmetric attached groups. A more complete and in depth comparison could be carried out to analyze the APTs according to

contributions from charge, charge-flux and overlap (66). However, the values of the effective charge χ give some idea of how similar the behavior of one atom may be in different molecules.

Several sets of APTs for the atoms in 1-Me U are obtained depending on how we impose the null condition (Eq. (3-5)) to constrain to zero the sum of the APTs. We transferred directly APTs for all atoms of uracil (Table 3-3) except those for N_1 and H_7 atoms. For the N_1-CH_3 fragment we transferred APTs for each one of the sets in Table 6-1, satisfying the constraint from the null condition by choosing either the APT for N_1 or that for C_7. In the former case we transferred the APT for C_7 listed in Table 6-1; in the latter we transferred the APT for the N_1 atom from uracil. Therefore, six complete sets of APTs for 1-Me U were obtained following this procedure. Since the APTs for the atoms in the uracil ring system are given in Table 3-3, only the additional calculated APTs for the N-CH_3 group in 1-Me U are shown in Table 6-2.

Let us describe briefly each one of those sets in Table 6-2: set A uses the APTs from N_1 atom in uracil, the APTs of H atoms of the N-CH_3 group from N-methylacetamide, and the APT for C_7 atom was obtained by applying the null condition; set B uses the APTs transferred from the four atoms in the CH_3 group of N-CH_3 from N-methylacetamide, and the APT for N_1 was obtained from the null condition; set C uses the APTs transferred from N_1 in uracil and from the C-CH_3 group in N-methylacetamide for the H atoms, obtaining the APT of C from the null condition; set D makes use of the same APTs for the CH_3 atoms from the C-CH_3 group of N-methylacetamide, but the APT of N_1 is obtained from the null condition; set E makes use of the APTs from N_1

TABLE 6-2
SETS OF APTs FOR 1-METHYLURACIL (in e units)

Set[a]	N_1^{u}[b]			$C_7^{n.c.}$[c]			H_{13}^{am}(N-CH_3)[d]			H_{14}^{am}(N-CH_3)[f]		
A	-.957	0.163	0	0.210	-.243	0	0.065	-.004	0	-.042	0.080	-.138
	-.678	-.978	0	-.096	0.126	0	-.092	0.042	0	0.080	0.034	0.017
	0	0	-.729	0	0	0.471	0	0	0.126	-.086	-.018	-.080
	$N_1^{n.c.}$			$C_7^{am(N-CH_3)}$[d]								
B	-1.021	0.326	0	0.274	-.406	0						
	-.526	-1.208	0	-.248	0.356	0						
	0	0	-.640	0	0	0.382						
	N_1^{u}			$C_7^{n.c.}$								
C	-.957	0.163	0	0.132	-.032	0						
	-.678	-.978	0	0.059	0.160	0						
	0	0	-.729	0	0	0.340						
	$N_1^{n.c.}$			$C_7^{am(C-CH_3)}$			H_{13}^{am}(C-CH_3)			H_{14}^{am}(C-CH_3)[f]		
D	-.781	-.106	0	-.044	0.237	0	-.055	-.049	0	0.057	-.003	-.089
	-.890	-.762	0	0.271	-.056	0	-.153	-.052	0	0.033	0.064	0.019
	0	0	-.379	0	0	-.010	0	0	0.073	-.061	-.013	0.012

---

continued

TABLE 6-2 continued

$$
\begin{array}{l}
\\
\mathrm{E} \\
\\
\\
\mathrm{F} \\
\\
\end{array}
\left\{
\begin{array}{c}
\begin{array}{ccc} & N_1{}^{u} & \end{array} \quad \begin{array}{ccc} & C_7{}^{n.c.} & \end{array} \\
\begin{pmatrix} -.957 & 0.163 & 0 \\ -.678 & -.978 & 0 \\ 0 & 0 & -.729 \end{pmatrix} \begin{pmatrix} 0.148 & -.036 & 0 \\ 0.042 & 0.118 & 0 \\ 0 & 0 & 0.392 \end{pmatrix} \\
\\
\begin{array}{ccc} & N_1{}^{u} & \end{array} \quad \begin{array}{ccc} & C_7{}^{acetone\,e} & \end{array} \\
\begin{pmatrix} -.747 & 0.021 & 0 \\ -.704 & -.579 & 0 \\ 0 & 0 & -.376 \end{pmatrix} \begin{pmatrix} -.062 & 0.106 & 0 \\ 0.068 & -.281 & 0 \\ 0 & 0 & 0.039 \end{pmatrix}
\end{array}
\right\}
\begin{array}{ccc} & H_{13}{}^{acetone} & \end{array} \quad \begin{array}{ccc} & H_{14}{}^{acetone\,f} & \end{array}
$$

$$
\begin{pmatrix} 0.017 & -.059 & 0 \\ -.102 & -.044 & 0 \\ 0 & 0 & 0.101 \end{pmatrix} \quad \begin{pmatrix} 0.013 & 0.004 & -.120 \\ 0.016 & 0.081 & 0.013 \\ -.086 & -.038 & -.028 \end{pmatrix}
$$

[a]See text for complete description of each set of APTs. The numbering of atoms and orientation of all APTs corresponds to Fig. 6-1.

[b]The uracil (u) ring APTs are those given in Table 3-3.

[c]The n.c. abbreviation implies that this APT was obtained using the null condition (Eq. (3-5)).

[d]The am stands for N-methylacetamide, and am($N-CH_3$) and am($C-CH_3$) imply that these APTs are those of the $N-CH_3$ and $C-CH_3$ groups of N-methylacetamide.

[e]The acetone APT was taken from Ref. 39.

[f]$P_x(H_{15})$ is obtained by reversing the signs of the off-diagonal components of $P_x(H_{14})$ involving z.

in uracil and from the H atoms in CH_3 from acetone, with the APT of C_7 obtained from the null condition; set F uses all the APTs from the CH_3 group of acetone with the null condition determining the APT for the N_1 atom.

It should be noted that the pair of sets A and B, C and D, and E and F are the same except for the null condition assumption. Therefore, the chemical effect of replacing H_7 by CH_3 is assumed in sets A, C, and E to be concentrated on N_1; in B, D, and F it is assumed to be on C_7. The consequences of these assumptions will be seen when we discuss the predicted intensities for the vibrational modes of these methylated uracil molecules.

3-methyluracil

The procedure for obtaining the APTs for 3-Me U to be used in Calculation II follows the one just described for 1-Me U and 1-Me-3-D U. For the 3-Me U molecule, Fig. 6-3 shows the atom numbering and geometrical parameters used as well as the Cartesian coordinates for the CH_3 group in the Cartesian system of uracil (Fig. 3-1). The coordinate system for the APTs for the atoms from Table 6-1 was then rotated by +239.30° (Eq. (3-4)) to fit the orientation of the N-CH_3 group in 3-Me U, as shown in Fig. 6-4. The values of the APTs in this rotated coordinate system for 3-Me U are shown in Table 6-3. Again, we obtained six sets of APTs for the N-CH_3 fragment in 3-Me U depending on how the null condition is satisfied. These sets are given in Table 6-4. Their description is analogous to that given for the corresponding six sets of APTs for the N-CH_3 fragment of 1-Me U.

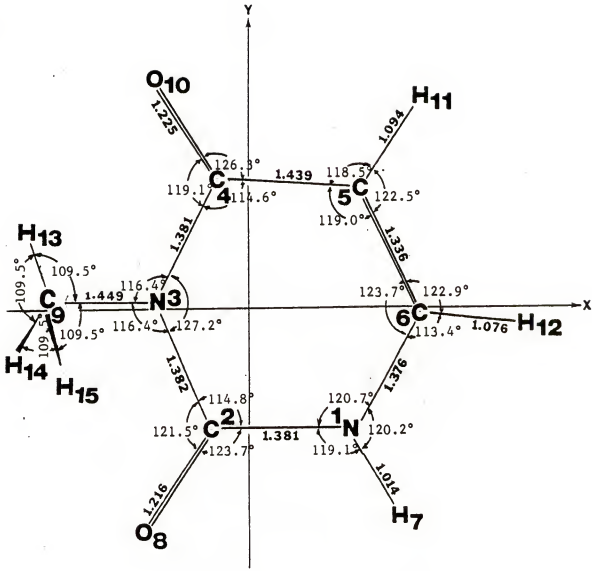

	x	y	z
C_7	-2.398326	0.090527	0.000000
H_{13}	-2.734069	1.127531	0.000000
H_{14}	-2.797948	-0.408282	0.882944
H_{15}	-2.797948	-0.408282	-0.882944

Figure 6-2. Geometrical parameters of 3-Me U and Cartesian coordinates for the CH_3 group in the Cartesian coordinate system of uracil. Coordinates for the ring atoms of uracil are given in Table 3-1. All C-H bond lenghts in the CH_3 group are taken as 1.092 Å.

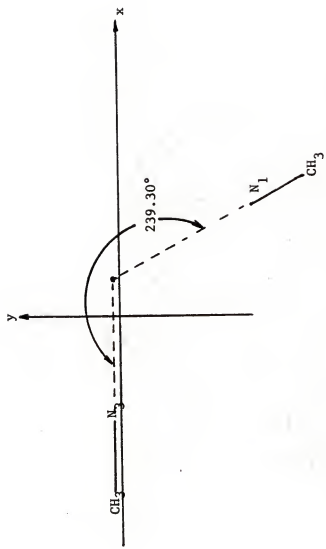

Figure 6-4. Rotation of axes of the APTs for 1-Me U to obtain the APTs of the N-CH_3 group of 3-Me U.

TABLE 6-3
TRANSFERRED APTs (in e) FROM THE CH_3 GROUPS OF ACETONE, AND FROM THE N-CH_3 AND C-CH_3 GROUPS OF N-METHYLACETAMIDE, AND THAT FOR THE N_3 ATOM OF URACIL, USED FOR THE N-CH_3 GROUP OF 3-METHYLURACIL

	CH_3 of acetone[a,b]	N-CH_3 of N-Me A[a,c]	C-CH_3 of N-Me A[a,c]
$P_x(C_9)$	$\begin{pmatrix} -.300 & 0.073 & 0 \\ 0.035 & -.043 & 0 \\ 0 & 0 & 0.039 \end{pmatrix}$	$\begin{pmatrix} 0.622 & 0.041 & 0 \\ 0.199 & 0.009 & 0 \\ 0 & 0 & 0.382 \end{pmatrix}$	$\begin{pmatrix} -.276 & -.134 & 0 \\ -.100 & 0.176 & 0 \\ 0 & 0 & -.010 \end{pmatrix}$
	$\chi = 0.183$	$\chi = 0.437$	$\chi = 0.212$
$P_x(H_{13})$	$\begin{pmatrix} 0.042 & 0.087 & 0 \\ 0.044 & -.070 & 0 \\ 0 & 0 & 0.101 \end{pmatrix}$	$\begin{pmatrix} 0.090 & 0.077 & 0 \\ -.011 & 0.017 & 0 \\ 0 & 0 & 0.126 \end{pmatrix}$	$\begin{pmatrix} 0.036 & 0.099 & 0 \\ -.005 & -.143 & 0 \\ 0 & 0 & 0.073 \end{pmatrix}$
	$\chi = 0.094$	$\chi = 0.101$	$\chi = 0.111$
$P_x(H_{14})$	$\begin{pmatrix} 0.054 & -.041 & 0.072 \\ -.029 & 0.040 & 0.096 \\ 0.011 & 0.093 & -.028 \end{pmatrix}$	$\begin{pmatrix} -.056 & -.072 & 0.085 \\ -.072 & 0.048 & 0.110 \\ 0.028 & 0.083 & -.080 \end{pmatrix}$	$\begin{pmatrix} 0.049 & -.028 & 0.062 \\ 0.008 & 0.072 & 0.067 \\ 0.019 & 0.060 & 0.012 \end{pmatrix}$
	$\chi = 0.102$	$\chi = 0.128$	$\chi = 0.083$
	N_3, uracil	N_3, N-Me A	C_3, N-Me A
$P_x(N_3,C_3)$	$\begin{pmatrix} -.623 & -.054 & 0 \\ -.094 & -1.403 & 0 \\ 0 & 0 & -.660 \end{pmatrix}$	$\begin{pmatrix} -1.016 & -.390 & 0 \\ -.704 & -.921 & 0 \\ 0 & 0 & -.815 \end{pmatrix}$	$\begin{pmatrix} 1.207 & 0.385 & 0 \\ 0.356 & 1.786 & 0 \\ 0 & 0 & 0.511 \end{pmatrix}$
	$\chi = 0.967$	$\chi = 1.032$	$\chi = 1.314$

[a]All APTs have been rotated to coordinate axes of Fig. 6-2.
[b,c,d]See footnotes b,c and d of Table 6-1.

TABLE 6-4
SETS OF APTs FOR 3-METHYLURACIL
(units are e)

Set	N_3^u	$C_9^{n.c.}$	$H_{13}^{am(N-CH_3)}$	$H_{14}^{am(N-CH_3)^c}$
G	$\begin{pmatrix} -.623 & -.054 & 0 \\ -.094 & -1.403 & 0 \\ 0 & 0 & -.660 \end{pmatrix}$	$\begin{pmatrix} 0.297 & 0.065 & 0 \\ 0.098 & 0.045 & 0 \\ 0 & 0 & 0.480 \end{pmatrix}$	$\begin{pmatrix} 0.090 & 0.077 & 0 \\ -.011 & 0.017 & 0 \\ 0 & 0 & 0.126 \end{pmatrix}$	$\begin{pmatrix} -.056 & -.072 & 0.085 \\ -.072 & 0.048 & 0.110 \\ 0.028 & 0.083 & -.080 \end{pmatrix}$
	$N_3^{n.c.}$	$C_9^{am(N-CH_3)}$		
H	$\begin{pmatrix} -.948 & -.030 & 0 \\ -.195 & -1.367 & 0 \\ 0 & 0 & -.562 \end{pmatrix}$	$\begin{pmatrix} 0.622 & 0.041 & 0 \\ 0.199 & 0.009 & 0 \\ 0 & 0 & 0.382 \end{pmatrix}$		
	N_3^u	$C_9^{n.c.}$	$H_{13}^{am(C-CH_3)}$	$H_{14}^{am(C-CH_3)^c}$
I	$\begin{pmatrix} -.623 & -.054 & 0 \\ -.094 & -1.403 & 0 \\ 0 & 0 & -.660 \end{pmatrix}$	$\begin{pmatrix} 0.141 & -.045 & 0 \\ -.068 & 0.157 & 0 \\ 0 & 0 & 0.349 \end{pmatrix}$	$\begin{pmatrix} 0.036 & 0.099 & 0 \\ -.005 & -.143 & 0 \\ 0 & 0 & 0.073 \end{pmatrix}$	$\begin{pmatrix} 0.049 & -.028 & 0.062 \\ 0.008 & 0.072 & 0.067 \\ 0.019 & 0.060 & 0.012 \end{pmatrix}$
	$N_3^{n.c.}$	$C_9^{am(C-CH_3)}$		
J	$\begin{pmatrix} -.206 & 0.035 & 0 \\ -.062 & -1.422 & 0 \\ 0 & 0 & -.301 \end{pmatrix}$	$\begin{pmatrix} -.276 & -.134 & 0 \\ -.100 & 0.176 & 0 \\ 0 & 0 & -.010 \end{pmatrix}$		

---

continued

TABLE 6-4 continued

$$
\begin{array}{l}
\\
K \\
\\
\\
L \\
\\
\end{array}
\left.
\begin{array}{c}
\begin{array}{cc} N_3{}^{u} & C_9{}^{n.c.} \end{array} \\
\begin{pmatrix} -.623 & -.054 & 0 \\ -.094 & -1.403 & 0 \\ 0 & 0 & -.660 \end{pmatrix}
\begin{pmatrix} 0.125 & -.007 & 0 \\ -.043 & 0.148 & 0 \\ 0 & 0 & 0.401 \end{pmatrix} \\
\\
\begin{array}{cc} N_3{}^{n.c.} & C_9{}^{acetone} \end{array} \\
\begin{pmatrix} -.198 & -.134 & 0 \\ -.172 & -1.212 & 0 \\ 0 & 0 & -.298 \end{pmatrix}
\begin{pmatrix} -.300 & 0.073 & 0 \\ 0.035 & -.043 & 0 \\ 0 & 0 & 0.039 \end{pmatrix}
\end{array}
\right\}
\begin{array}{c}
H_{13}{}^{acetone} \\
\begin{pmatrix} 0.042 & 0.087 & 0 \\ 0.044 & -.070 & 0 \\ 0 & 0 & 0.101 \end{pmatrix} \\
\\
\\
\\
\end{array}
\qquad
\begin{array}{c}
H_{14}{}^{acetone\,c} \\
\begin{pmatrix} 0.054 & -.041 & 0.072 \\ -.029 & 0.040 & 0.096 \\ 0.011 & 0.093 & -.028 \end{pmatrix} \\
\\
\\
\\
\end{array}
$$

[a]The numbering of atoms and orientation of APTs is according to Fig. 6-3.

[b]Notes b, c, d, and e of Table 6-2 apply to this table.

[c] To obtain the $P_x(H_{15})$ just reverse the $P_x(H_{14})$ elements involving z.

1,3-dimethyluracil

The case of 1,3-di Me U involves a combination of the APTs for 1-Me U and 3-Me U. First, Fig. 6-5 shows the geometry of 1,3-di Me U, where the only thing we have done is adding to the 1-Me U geometry (Fig. 6-1) the CH_3 group geometrical parameters taken from 3-Me U (Fig. 6-3).

In order to make the transfer of APTs in the methylated uracils a systematic and consistent procedure, we formed twelve sets of APTs for 1,3-di Me U combining sets A and B, C and D, and E and F for 1-Me U (Table 6-2) with sets G and H, I and J, and K and L for 3-Me U (Table 6-4), respectively. The resulting sets of APTs are shown in Table 6-5. This procedure guarantees that the sum of APTs closes to zero, and also that we are using the same APTs for these molecules. Therefore, we can test the transferability of APTs in this series of related compounds. Of course, we are expecting that the experimental and calculated intensities, as well as frequencies, of 1,3-di Me U to show similarities with those of other methylated uracils.

Transfer of ab initio Force Constants

In order to carry out Calculations I and II we used a combination of the "corrected to 4-31G" ab initio force constants for uracil (Table 4-2) with force constants obtained for N-methylformamide, using a 4-31G basis set, by Sugawara, Hirakawa, Tsuboi, Kato, and Morokuma (40). As stated earlier, the use of ab initio force constants from a 4-31G basis set calculation normally reproduces the experimental frequencies for a molecule after uniform scaling.

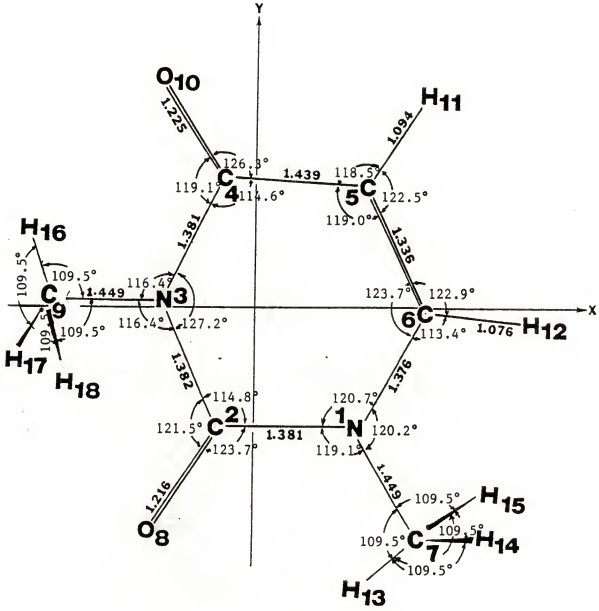

Figure 6-5. Geometry and atom numbering for 1,3-dimethyluracil in the Cartesian coordinate system of uracil. Coordinates for the ring atoms of uracil are given in Table 3-1, for the N_1-CH_3 methyl group in Fig. 6-1, and for the N_3-CH_3 methyl group in Fig. 6-2.

TABLE 6-5
SETS OF APTs FOR 1,3-DIMETHYLURACIL
(units are e)

$$
\begin{pmatrix} -.957 & 0.163 & 0 \\ -.678 & -.978 & 0 \\ 0 & 0 & -.729 \end{pmatrix}_{X_1}
\begin{pmatrix} 0.210 & -.243 & 0 \\ -.096 & 0.126 & 0 \\ 0 & 0 & 0.471 \end{pmatrix}_{C_7}
\begin{pmatrix} 0.065 & -.004 & 0 \\ -.092 & 0.042 & 0 \\ 0 & 0 & 0.126 \end{pmatrix}_{H_{13}}
\begin{pmatrix} -.042 & 0.080 & -.138 \\ 0.080 & 0.034 & 0.017 \\ -.086 & -.018 & -.080 \end{pmatrix}_{E_{14}}
$$

Set 1 → Set 2

$$
\left\{
\begin{pmatrix} -.623 & -.054 & 0 \\ -.094 & -1.403 & 0 \\ 0 & 0 & -.660 \end{pmatrix}_{X_3}
\begin{pmatrix} 0.297 & 0.065 & 0 \\ 0.098 & 0.045 & 0 \\ 0 & 0 & 0.480 \end{pmatrix}_{C_9}
\begin{pmatrix} 0.090 & 0.077 & 0 \\ -.011 & 0.017 & 0 \\ 0 & 0 & 0.126 \end{pmatrix}_{H_{16}}
\begin{pmatrix} -.056 & -.072 & 0.085 \\ -.072 & 0.048 & 0.110 \\ 0.028 & 0.083 & -.080 \end{pmatrix}_{H_{17}}
\right.
$$

$$
\left.
\begin{pmatrix} -.948 & -.030 & 0 \\ -.195 & -1.367 & 0 \\ 0 & 0 & -.562 \end{pmatrix}_{X_3}
\begin{pmatrix} 0.522 & 0.041 & 0 \\ 0.199 & 0.009 & 0 \\ 0 & 0 & 0.382 \end{pmatrix}_{C_9}
\begin{pmatrix} 0.090 & 0.077 & 0 \\ -.011 & 0.017 & 0 \\ 0 & 0 & 0.126 \end{pmatrix}_{H_{16}}
\begin{pmatrix} -.056 & -.072 & 0.085 \\ -.072 & 0.048 & 0.110 \\ 0.028 & 0.083 & -.080 \end{pmatrix}_{H_{17}}
\right\}
$$

$$
\begin{pmatrix} -1.021 & 0.326 & 0 \\ -.526 & -1.208 & 0 \\ 0 & 0 & -.640 \end{pmatrix}_{X_1}
\begin{pmatrix} 0.274 & -.406 & 0 \\ -.248 & 0.356 & 0 \\ 0 & 0 & 0.382 \end{pmatrix}_{C_7}
\begin{pmatrix} 0.065 & -.004 & 0 \\ -.092 & 0.042 & 0 \\ 0 & 0 & 0.126 \end{pmatrix}_{H_{13}}
\begin{pmatrix} -.042 & 0.080 & -.138 \\ 0.080 & 0.034 & 0.017 \\ -.086 & -.018 & -.080 \end{pmatrix}_{E_{14}}
$$

Set 3 → Set 4

$$
\left\{
\begin{pmatrix} -.623 & -.054 & 0 \\ -.094 & -1.403 & 0 \\ 0 & 0 & -.660 \end{pmatrix}_{X_3}
\begin{pmatrix} 0.297 & 0.065 & 0 \\ 0.098 & 0.045 & 0 \\ 0 & 0 & 0.480 \end{pmatrix}_{C_9}
\begin{pmatrix} 0.090 & 0.077 & 0 \\ -.011 & 0.017 & 0 \\ 0 & 0 & 0.126 \end{pmatrix}_{H_{16}}
\begin{pmatrix} -.056 & -.072 & 0.085 \\ -.072 & 0.048 & 0.110 \\ 0.028 & 0.083 & -.080 \end{pmatrix}_{H_{17}}
\right.
$$

$$
\left.
\begin{pmatrix} -.948 & -.030 & 0 \\ -.195 & -1.367 & 0 \\ 0 & 0 & -.562 \end{pmatrix}_{X_3}
\begin{pmatrix} 0.622 & 0.041 & 0 \\ 0.199 & 0.009 & 0 \\ 0 & 0 & 0.382 \end{pmatrix}_{C_9}
\begin{pmatrix} 0.090 & 0.077 & 0 \\ -.011 & 0.017 & 0 \\ 0 & 0 & 0.126 \end{pmatrix}_{H_{16}}
\begin{pmatrix} -.056 & -.072 & 0.085 \\ -.072 & 0.048 & 0.110 \\ 0.028 & 0.083 & -.080 \end{pmatrix}_{H_{17}}
\right\}
$$

continued

TABLE 6-5 continued

$$
\begin{pmatrix} -.957 & 0.163 & 0 \\ -.678 & -.978 & 0 \\ 0 & 0 & -.729 \end{pmatrix}
\begin{pmatrix} 0.132 & -.032 & 0 \\ 0.059 & 0.160 & 0 \\ 0 & 0 & 0.340 \end{pmatrix}
\begin{pmatrix} -.055 & -.049 & 0 \\ -.153 & -.052 & 0 \\ 0 & 0 & 0.073 \end{pmatrix}
\begin{pmatrix} 0.057 & -.003 & -.089 \\ 0.033 & 0.054 & 0.019 \\ -.061 & -.013 & 0.012 \end{pmatrix}
$$

Sec 5 → Sec 6

$$
\left\{
\begin{pmatrix} -.623 & -.034 & 0 \\ -.094 & -1.403 & 0 \\ 0 & 0 & -.660 \end{pmatrix}
\begin{pmatrix} 0.141 & -.045 & 0 \\ -.068 & 0.157 & 0 \\ 0 & 0 & 0.349 \end{pmatrix}
\begin{pmatrix} 0.036 & 0.099 & 0 \\ -.005 & -.143 & 0 \\ 0 & 0 & 0.073 \end{pmatrix}
\begin{pmatrix} 0.049 & -.028 & 0.062 \\ 0.008 & 0.072 & 0.067 \\ 0.019 & 0.060 & 0.012 \end{pmatrix}
\right.
$$

$$
\left.
\begin{pmatrix} -.206 & 0.035 & 0 \\ -.062 & -1.422 & 0 \\ 0 & 0 & -.301 \end{pmatrix}
\begin{pmatrix} -.276 & -.134 & 0 \\ -.100 & 0.176 & 0 \\ 0 & 0 & -.010 \end{pmatrix}
\begin{pmatrix} 0.036 & 0.099 & 0 \\ -.005 & -.143 & 0 \\ 0 & 0 & 0.073 \end{pmatrix}
\begin{pmatrix} 0.049 & -.028 & 0.062 \\ 0.008 & 0.072 & 0.067 \\ 0.019 & 0.060 & 0.012 \end{pmatrix}
\right\}
$$

$$
\begin{pmatrix} -.781 & -.106 & 0 \\ -.890 & -.762 & 0 \\ 0 & 0 & -.379 \end{pmatrix}
\begin{pmatrix} -.044 & 0.237 & 0 \\ 0.271 & -.056 & 0 \\ 0 & 0 & -.010 \end{pmatrix}
\begin{pmatrix} -.055 & -.049 & 0 \\ -.153 & -.052 & 0 \\ 0 & 0 & 0.073 \end{pmatrix}
\begin{pmatrix} 0.057 & -.003 & -.089 \\ 0.033 & 0.054 & 0.019 \\ -.061 & -.013 & 0.012 \end{pmatrix}
$$

Sec 7 → Sec 8

$$
\left\{
\begin{pmatrix} -.623 & -.034 & 0 \\ -.094 & -1.403 & 0 \\ 0 & 0 & -.660 \end{pmatrix}
\begin{pmatrix} 0.297 & 0.065 & 0 \\ 0.098 & 0.045 & 0 \\ 0 & 0 & 0.480 \end{pmatrix}
\begin{pmatrix} 0.036 & 0.099 & 0 \\ -.005 & -.143 & 0 \\ 0 & 0 & 0.073 \end{pmatrix}
\begin{pmatrix} 0.049 & -.028 & 0.062 \\ 0.008 & 0.072 & 0.067 \\ 0.019 & 0.060 & 0.012 \end{pmatrix}
\right.
$$

$$
\left.
\begin{pmatrix} -.206 & 0.035 & 0 \\ -.062 & -1.422 & 0 \\ 0 & 0 & -.301 \end{pmatrix}
\begin{pmatrix} -.276 & -.134 & 0 \\ -.100 & 0.176 & 0 \\ 0 & 0 & -.010 \end{pmatrix}
\begin{pmatrix} 0.036 & 0.099 & 0 \\ -.005 & -.143 & 0 \\ 0 & 0 & 0.073 \end{pmatrix}
\begin{pmatrix} 0.049 & -.028 & 0.062 \\ 0.008 & 0.072 & 0.067 \\ 0.019 & 0.060 & 0.012 \end{pmatrix}
\right\}
$$

---

continued

TABLE 6-5 continued

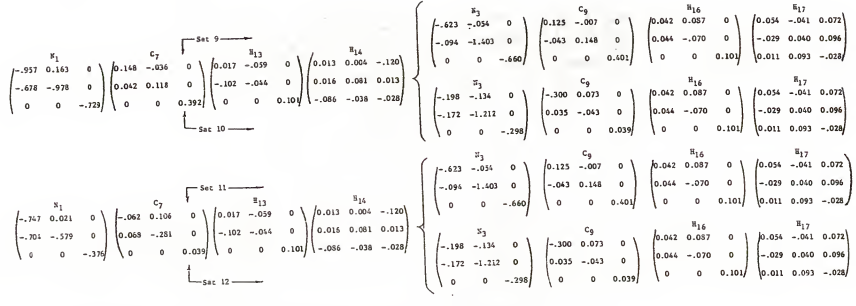

Note: Set 1 combines sets A and G of 1-Na U and 3-Na U, respectively, given in Tables 6-2 (for 1-Na U) and 6-4 (for 3-Na U).
Set 2 Combines sets A and H, set 3 E and G, set 4 B and H, set 5 C and I, set 6 C and J, set 7 D and I, set 8 D and J,
set 9 E and K, set 10 E and L, set 11 F and K, and set 12 F and L.

The internal and symmetry coordinates for all four methylated uracil molecules considered in this study are those listed for uracil in Fig. 4-1 and Table 4-1, respectively, for Calculation I (12 atoms).

1-Methyluracil

The replacement of H_7 atom position in uracil (Fig. 3-1) by CH_3 for Calculation II adds 9 more internal coordinates to 1-Me U, as shown in Fig. 6-6. The new set of in-plane symmetry coordinates for 1-Me U is displayed in Table 6-6.

The modification of the uracil force field (Table 4-2) to include the force constants transferred from N-methylformamide to 1 Me U has been underlined in Table 6-7. For example, the diagonal force constant for the S_7 symmetry coordinate (N_1-H_7 stretch) of 8.256 md $\AA^{-1}$ in uracil was changed to 5.960 md $\AA^{-1}$ (since it now corresponds to the N_1-C_7 stretch). Note that Calculation I is made using only the upper 21 x 21 submatrix of Table 6-7, while Calculation II uses the complete 26 x 26 matrix. Again, the same force constants were used for 1-Me-3-D U in Calculations I and II.

3-Methyluracil

Let us now consider the transfer of ab initio force constants for 3-Me U. The sets of in-plane internal and symmetry coordinates for this molecule are given in Fig. 6-7 and Table 6-8, respectively. The force field for this molecule is shown in Table 6-9, where the modifications of the uracil force field have again been underlined

1,3-Dimethyluracil

For 1,3-di Me U, Fig. 6-8 and Table 6-10 show the in-plane internal and symmetry coordinates, respectively. The force field which we used for this molecule was a combination of that obtained for 1-Me U

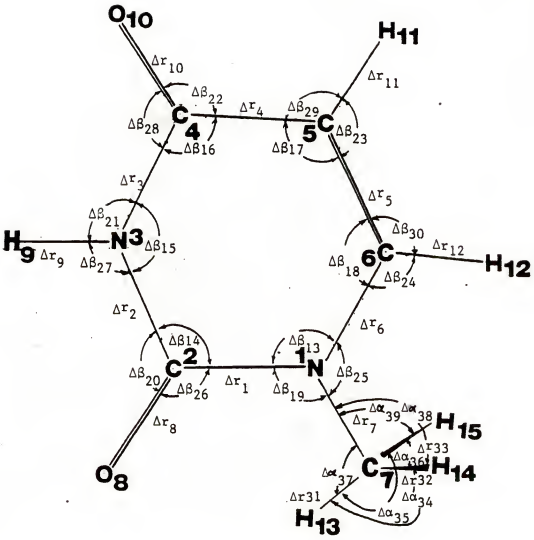

Figure 6-6. In-plane internal coordinates for 1-Me U.

TABLE 6-6
IN-PLANE SYMMETRY COORDINATES
FOR 1-Me U

$S_1 = \Delta r_1$	νN_1C_2 stretching
$S_2 = \Delta r_2$	νC_2N_3 stretching
$S_3 = \Delta r_3$	νN_3C_4 stretching
$S_4 = \Delta r_4$	νC_4C_5 stretching
$S_5 = \Delta r_5$	νC_5C_6 stretching
$S_6 = \Delta r_6$	νC_6N_1 stretching
$S_7 = \Delta r_7$	νN_1C_7 stretching
$S_8 = \Delta r_8$	νC_2O_8 stretching
$S_9 = \Delta r_9$	νN_3O_9 stretching
$S_{10} = \Delta r_{10}$	νC_4O_{10} stretching
$S_{11} = \Delta r_{11}$	νC_5H_{11} stretching
$S_{12} = \Delta r_{12}$	νC_6H_{12} stretching
$S_{13} = (\Delta\beta_{13}-\Delta\beta_{14}+\Delta\beta_{15}-\Delta\beta_{16}+\Delta\beta_{17}-\Delta\beta_{18})/\sqrt{6}$	δRing deformation I
$S_{14} = (\Delta\beta_{13}-\Delta\beta_{14}-\Delta\beta_{15}+\Delta\beta_{16}-\Delta\beta_{17}-\Delta\beta_{18})/\sqrt{12}$	δRing deformation II
$S_{15} = (\Delta\beta_{14}-\Delta\beta_{15}+\Delta\beta_{17}-\Delta\beta_{18})/2$	δRing deformation III
$S_{16} = (\Delta\beta_{19}-\Delta\beta_{25})/\sqrt{2}$	δN_1C bending
$S_{17} = (\Delta\beta_{20}-\Delta\beta_{26})/\sqrt{2}$	δC_2O bending
$S_{18} = (\Delta\beta_{21}-\Delta\beta_{27})/\sqrt{2}$	δN_3C bending
$S_{19} = (\Delta\beta_{22}-\Delta\beta_{28})/\sqrt{2}$	δC_4O bending
$S_{20} = (\Delta\beta_{23}-\Delta\beta_{29})/\sqrt{2}$	δC_5H bending
$S_{21} = (\Delta\beta_{24}-\Delta\beta_{30})/\sqrt{2}$	δC_6H bending
$S_{22} = (\Delta r_{31}+\Delta r_{32}+\Delta r_{33})/3$	νMe stretching
$S_{23} = (\Delta\alpha_{34}+\Delta\alpha_{35}+\Delta\alpha_{36}-\Delta\alpha_{37}-\Delta\alpha_{38}-\Delta\alpha_{39})/6$	δMe symm. def.
$S_{24} = (2\alpha r_{31}-\alpha r_{32}-\alpha r_{33})/6$	δMe deg. def.
$S_{25} = (2\Delta\alpha_{36}-\Delta\alpha_{34}-\Delta\alpha_{35})/6$	δMe deg. def.
$S_{26} = (2\Delta\alpha_{37}-\Delta\alpha_{38}-\Delta\alpha_{39})/6$	ρMe rocking

TABLE 6-7
FORCE CONSTANTS FOR 1-Me U

	S1	S2	S3	S4	S5	S6	S7	S8	S9	S10	S11	S12	S13
S1	7.356	0.468	-.268	0.112	-.204	0.461	0.230	0.908	0.000	-.070	0.000	0.000	0.082
S2		7.497	0.455	-.172	0.076	-.233	0.000	0.888	0.000	-.084	0.000	0.000	0.000
S3			7.003	0.327	-.192	0.171	0.000	-.083	0.000	1.036	0.000	0.000	0.043
S4				6.042	0.464	-.363	0.000	-.090	0.000	0.686	0.000	0.000	0.038
S5					10.728	0.554	0.000	0.099	0.000	-.127	0.000	0.000	-.066
S6						8.079	0.190	-.053	0.000	-.073	-.100	0.000	-.137
S7							5.960	-.020	0.000	0.000	0.000	0.010	-.074
S8								13.298	0.000	0.000	0.000	0.000	0.276
S9									8.150	0.000	0.000	0.000	-.093
S10										13.500	0.000	0.000	0.290
S11											6.330	0.000	-.081
S12												6.181	0.070
S13													1.898
S14													
S15													
S16													
S17													
S18													
S19													
S20													
S21													
S22													
S23													
S24													
S25													
S26													

Symmetric matrix

$F_{ij} = F_{ji}$

---

continued

TABLE 6-7 continued

	S14	S15	S16	S17	S18	S19	S20	S21	S22	S23	S24	S25	S26
S1	0.181	0.147	0.240	-.420	0.000	-.037	-.048	0.000	0.000	0.000	0.000	0.000	0.000
S2	-.146	-.081	0.000	0.409	-.100	0.083	0.036	0.000	0.000	0.000	0.000	0.000	0.000
S3	0.000	-.145	-.036	-.118	0.049	-.487	0.000	0.000	0.000	0.000	0.000	0.000	0.000
S4	0.000	0.244	0.045	0.032	0.000	0.245	-.125	0.000	0.000	0.000	0.000	0.000	0.000
S5	-.243	0.068	0.000	-.030	-.035	-.056	0.193	-.135	0.000	0.000	0.000	0.000	0.000
S6	0.059	-.288	-.185	0.112	0.060	0.100	0.000	0.226	0.000	0.000	0.000	0.000	0.000
S7	-.066	0.000	0.310	-.070	0.000	0.000	0.000	0.020	0.250	-.630	-.090	-.010	-.010
S8	0.169	-.313	0.020	0.000	0.000	0.000	0.000	0.000	0.030	-.070	0.010	0.010	0.010
S9	0.047	0.067	0.000	-.031	0.000	0.032	0.000	0.000	0.000	0.000	0.000	0.000	0.000
S10	-.356	0.000	0.000	0.045	0.000	-.071	0.000	0.000	0.000	0.000	0.000	0.000	0.000
S11	0.040	-.068	0.000	0.000	0.000	0.000	0.000	0.000	0.000	0.000	0.000	0.000	0.000
S12	0.029	0.062	-.060	0.000	0.000	0.000	0.000	0.000	0.000	0.000	0.000	0.000	0.000
S13	0.000	-.046	-.010	0.000	0.011	-.060	0.011	0.029	0.000	0.000	0.000	0.000	0.000
S14	1.710	-.098	0.000	-.146	0.131	0.091	-.104	0.096	0.000	0.000	0.000	0.000	0.000
S15		1.663	0.134	-.058	-.088	0.177	-.057	-.013	0.000	0.000	0.000	0.000	0.000
S16			1.040	-.010	-.017	-.009	-.014	-.010	-.040	-.020	-.090	-.030	-.060
S17				1.256	0.053	-.063	-.010	-.025	-.030	0.030	-.050	-.010	0.030
S18					0.599	0.065	-.015	0.000	0.000	0.000	0.000	0.000	0.000
S19						1.258	0.039	-.024	0.000	0.000	0.000	0.000	0.000
S20							0.579	0.008	0.000	0.000	0.000	0.000	0.000
S21								0.649	0.000	0.000	0.000	0.000	0.000
S22									5.980	0.130	0.120	0.030	0.020
S23										0.800	-.040	0.010	0.000
S24											5.950	-.190	0.150
S25												0.710	-.050
S26													1.000

Note: The symmetry coordinates are defined in Table 6-6. The units are md Å^{-1} for stretch-stretch, md Å for bend-bend, and md for bend-stretch elements.

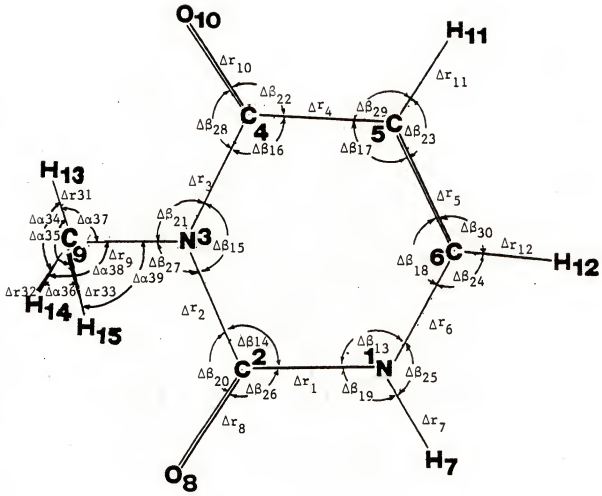

Figure 6-7, In-plane internal coordinates for 3-Me U.

TABLE 6-8
IN-PLANE SYMMETRY COORDINATES
FOR 3-Me U

$S_1 = \Delta r_1$	νN_1C_2 stretching
$S_2 = \Delta r_2$	νC_2N_3 stretching
$S_3 = \Delta r_3$	νN_3C_4 stretching
$S_4 = \Delta r_4$	νC_4C_5 stretching
$S_5 = \Delta r_5$	νC_5C_6 stretching
$S_6 = \Delta r_6$	νC_6N_1 stretching
$S_7 = \Delta r_7$	νN_1C_7 stretching
$S_8 = \Delta r_8$	νC_2O_8 stretching
$S_9 = \Delta r_9$	νN_3C_9 stretching
$S_{10} = \Delta r_{10}$	νC_4O_{10} stretching
$S_{11} = \Delta r_{11}$	νC_5H_{11} stretching
$S_{12} = \Delta r_{12}$	νC_6H_{12} stretching
$S_{13} = (\Delta\beta_{13}-\Delta\beta_{14}+\Delta\beta_{15}-\Delta\beta_{16}+\Delta\beta_{17}-\Delta\beta_{18})/\sqrt{6}$	δRing deformation I
$S_{14} = (\Delta\beta_{13}-\Delta\beta_{14}-\Delta\beta_{15}+\Delta\beta_{16}-\Delta\beta_{17}-\Delta\beta_{18})/\sqrt{12}$	δRing deformation II
$S_{15} = (\Delta\beta_{14}-\Delta\beta_{15}+\Delta\beta_{17}-\Delta\beta_{18})/2$	δRing deformation III
$S_{16} = (\Delta\beta_{19}-\Delta\beta_{25})/\sqrt{2}$	δN_1C bending
$S_{17} = (\Delta\beta_{20}-\Delta\beta_{26})/\sqrt{2}$	δC_2O bending
$S_{18} = (\Delta\beta_{21}-\Delta\beta_{27})/\sqrt{2}$	δN_3C bending
$S_{19} = (\Delta\beta_{22}-\Delta\beta_{28})/\sqrt{2}$	δC_4O bending
$S_{20} = (\Delta\beta_{23}-\Delta\beta_{29})/\sqrt{2}$	δC_5H bending
$S_{21} = (\Delta\beta_{24}-\Delta\beta_{30})/\sqrt{2}$	δC_6H bending
$S_{22} = (\Delta r_{31}+\Delta r_{32}+\Delta r_{33})/3$	νMe stretching
$S_{23} = (\Delta\alpha_{34}+\Delta\alpha_{35}+\Delta\alpha_{36}-\Delta\alpha_{37}-\Delta\alpha_{38}-\Delta\alpha_{39})/6$	δMe symm. def.
$S_{24} = (2\alpha r_{31}-\alpha r_{32}-\alpha r_{33})/6$	δMe deg. def.
$S_{25} = (2\Delta\alpha_{36}-\Delta\alpha_{34}-\Delta\alpha_{35})/6$	δMe deg. def.
$S_{26} = (2\Delta\alpha_{37}-\Delta\alpha_{38}-\Delta\alpha_{39})/6$	ρMe rocking

TABLE 6-9
FORCE CONSTANTS FOR 3-Me U

	S1	S2	S3	S4	S5	S6	S7	S8	S9	S10	S11	S12	S13
S1	7.356	0.468	-.268	0.112	-.204	0.461	0.000	0.908	0.000	-.070	0.000	0.000	0.082
S2		7.497	0.455	-.172	0.076	-.233	0.000	0.888	0.230	-.084	0.000	0.000	0.000
S3			7.003	0.327	-.192	0.171	0.000	-.083	0.230	1.036	0.000	0.000	0.043
S4				6.042	0.464	-.363	0.000	-.090	0.000	0.686	0.000	0.000	0.038
S5					10.728	0.554	0.000	0.099	0.000	-.128	0.000	0.000	-.066
S6						8.079	0.000	-.053	0.000	-.073	-.100	0.000	-.137
S7							8.256	-.036	0.000	0.000	0.000	0.000	-.074
S8								13.298	-.020	0.000	0.000	0.000	0.276
S9									5.960	-.020	0.000	0.000	-.093
S10										13.500	0.000	0.000	0.290
S11											6.330	0.000	-.081
S12												6.181	0.070
S13													1.898
S14													
S15													
S16													
S17													
S18													
S19													
S20													
S21													
S22													
S23													
S24													
S25													
S26													

Symmetric matrix

$F_{ij} = F_{ji}$

---

continued

TABLE 6-9 continued

	S14	S15	S16	S17	S18	S19	S20	S21	S22	S23	S24	S25	S26
S1	0.181	0.147	0.070	-.420	0.000	-.037	-.048	0.000	0.000	0.000	0.000	0.000	0.000
S2	-.146	-.081	0.000	0.409	0.240	0.083	0.036	0.000	0.000	0.000	0.000	0.000	0.000
S3	0.000	-.145	-.036	-.118	0.240	-.487	0.000	0.000	0.000	0.000	0.000	0.000	0.000
S4	0.000	0.244	0.045	0.032	0.000	0.245	-.125	0.000	0.000	0.000	0.000	0.000	0.000
S5	-.243	0.068	0.000	-.030	-.035	-.056	0.193	-.135	0.000	0.000	0.000	0.000	0.000
S6	0.059	-.288	-.185	0.112	0.060	0.100	0.000	0.226	0.000	0.000	0.000	0.000	0.000
S7	-.066	0.000	0.000	0.000	0.000	0.000	0.000	0.000	0.000	0.000	0.000	0.000	0.000
S8	0.169	-.313	0.000	0.000	0.020	0.000	0.000	0.000	0.030	-.070	0.010	0.010	0.010
S9	0.047	0.067	0.000	-.070	0.310	-.070	0.000	0.000	0.250	-.630	-.090	-.010	-.010
S10	-.356	0.000	0.000	0.045	0.020	-.071	0.000	0.000	0.030	-.070	0.010	0.010	0.010
S11	0.040	-.068	0.000	0.000	0.000	0.000	0.000	0.000	0.000	0.000	0.000	0.000	0.000
S12	0.029	0.062	0.000	0.000	0.000	0.000	0.000	0.000	0.000	0.000	0.000	0.000	0.000
S13	0.000	-.046	-.010	0.000	0.011	-.060	0.011	0.029	0.000	0.000	0.000	0.000	0.000
S14	1.710	-.098	0.000	-.146	0.131	0.091	-.104	0.096	0.000	0.000	0.000	0.000	0.000
S15		1.663	0.134	-.058	-.088	0.177	-.057	-.013	0.000	0.000	0.000	0.000	0.000
S16			0.619	0.056	-.017	-.009	-.014	0.007	0.000	0.000	0.000	0.000	0.000
S17				1.256	-.010	-.063	-.010	-.025	-.030	0.030	-.050	-.010	0.030
S18					1.040	-.010	-.015	0.000	-.040	-.020	-.090	-.030	-.060
S19						1.258	0.039	-.024	-.030	0.030	-.050	-.010	0.030
S20							0.579	0.008	0.000	0.000	0.000	0.000	0.000
S21								0.649	0.000	0.000	0.000	0.000	0.000
S22									5.980	0.130	0.120	0.030	0.020
S23										0.800	-.040	0.010	0.000
S24											5.950	-.190	0.150
S25												0.710	-.050
S26													1.000

Note: The symmetry coordinates are defined in Table 6-8. The units are md $Å^{-1}$ for stretch-stretch, md Å for bend-bend, and md for bend-stretch elements.

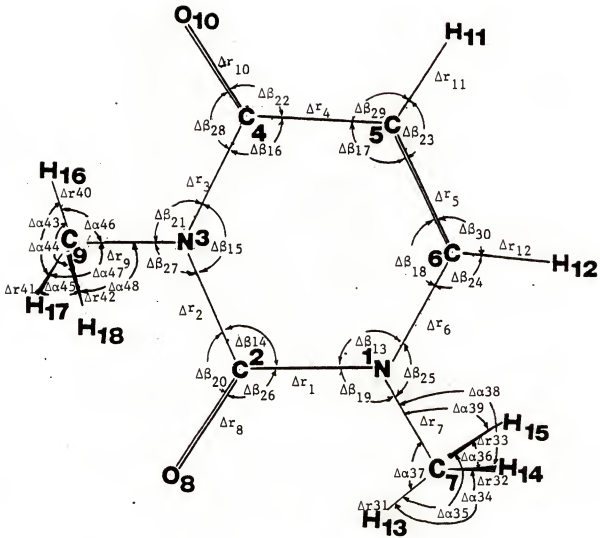

Fig. 6-8. In-plane internal coordinates for 1,3-di Me U.

TABLE 6-10
IN-PLANE SYMMETRY COORDINATES
FOR 1,3-di Me U

$S_1 = \Delta r_1$	νN_1C_2 stretching
$S_2 = \Delta r_2$	νC_2N_3 stretching
$S_3 = \Delta r_3$	νN_3C_4 stretching
$S_4 = \Delta r_4$	νC_4C_5 stretching
$S_5 = \Delta r_5$	νC_5C_6 stretching
$S_6 = \Delta r_6$	νC_6N_1 stretching
$S_7 = \Delta r_7$	νN_1C_7 stretching
$S_8 = \Delta r_8$	νC_2O_8 stretching
$S_9 = \Delta r_9$	νN_3C_9 stretching
$S_{10} = \Delta r_{10}$	νC_4O_{10} stretching
$S_{11} = \Delta r_{11}$	νC_5H_{11} stretching
$S_{12} = \Delta r_{12}$	νC_6H_{12} stretching
$S_{13} = (\Delta\beta_{13}-\Delta\beta_{14}+\Delta\beta_{15}-\Delta\beta_{16}+\Delta\beta_{17}-\Delta\beta_{18})/\sqrt{6}$	δRing deformation I
$S_{14} = (\Delta\beta_{13}-\Delta\beta_{14}-\Delta\beta_{15}+\Delta\beta_{16}-\Delta\beta_{17}-\Delta\beta_{18})/\sqrt{12}$	δRing deformation II
$S_{15} = (\Delta\beta_{14}-\Delta\beta_{15}+\Delta\beta_{17}-\Delta\beta_{18})/2$	δRing deformation III
$S_{16} = (\Delta\beta_{19}-\Delta\beta_{25})/\sqrt{2}$	δN_1C bending
$S_{17} = (\Delta\beta_{20}-\Delta\beta_{26})/\sqrt{2}$	δC_2O bending
$S_{18} = (\Delta\beta_{21}-\Delta\beta_{27})/\sqrt{2}$	δN_3C bending
$S_{19} = (\Delta\beta_{22}-\Delta\beta_{28})/\sqrt{2}$	δC_4O bending
$S_{20} = (\Delta\beta_{23}-\Delta\beta_{29})/\sqrt{2}$	δC_5H bending
$S_{21} = (\Delta\beta_{24}-\Delta\beta_{30})/\sqrt{2}$	δC_6H bending
$S_{22} = (\Delta r_{31}+\Delta r_{32}+\Delta r_{33})/\sqrt{3}$	νMe stretching
$S_{23} = (\Delta\alpha_{34}+\Delta\alpha_{35}+\Delta\alpha_{36}-\Delta\alpha_{37}-\Delta\alpha_{38}-\Delta\alpha_{39})/\sqrt{6}$	δMe symm. def.
$S_{24} = (2\alpha r_{31}-\alpha r_{32}-\alpha r_{33})/\sqrt{6}$	δMe deg. def.
$S_{25} = (2\Delta\alpha_{36}-\Delta\alpha_{34}-\Delta\alpha_{35})/\sqrt{6}$	δMe deg. def.
$S_{26} = (2\Delta\alpha_{37}-\Delta\alpha_{38}-\Delta\alpha_{39})/\sqrt{6}$	ρMe rocking
$S_{27} = (\Delta r_{40}+\Delta r_{41}+\Delta r_{42})/\sqrt{3}$	νMe symm. def.
$S_{28} = (\Delta\alpha_{43}+\Delta\alpha_{44}+\Delta\alpha_{45}-\Delta\alpha_{46}-\Delta\alpha_{47}-\Delta\alpha_{48})/\sqrt{6}$	δMe symm.
$S_{29} = (2\Delta r_{40}-\Delta r_{41}-\Delta r_{42})/\sqrt{6}$	νMe deg.
$S_{30} = (2\Delta\alpha_{45}-\Delta\alpha_{44}-\Delta\alpha_{43})/\sqrt{6}$	δMe deg.
$S_{31} = (2\Delta\alpha_{46}-\Delta\alpha_{47}-\Delta\alpha_{48})/\sqrt{6}$	ρMe rocking

TABLE 6-11
FORCE CONSTANTS FOR 1,3-di Me U

	S1	S2	S3	S4	S5	S6	S7	S8	S9	S10	S11	S12	S13	S14	S15
S1	7.356	0.468	-.268	0.112	-.204	0.461	0.230	0.908	0.000	-.070	0.000	0.000	0.082	0.181	0.147
S2		7.497	0.455	-.172	0.076	-.233	0.000	0.888	0.230	-.084	0.000	0.000	0.000	-.146	-.081
S3			7.003	0.327	-.192	0.171	0.000	-.083	0.230	1.036	0.000	0.000	0.043	0.000	-.145
S4				6.042	0.464	-.363	0.000	-.090	0.000	0.686	0.000	0.000	0.038	0.000	0.244
S5					10.728	0.554	0.000	0.099	0.000	-.127	0.000	0.000	-.066	-.243	0.068
S6						8.079	0.190	-.053	0.000	-.073	-.100	0.000	-.137	0.059	-.288
S7							5.960	-.020	0.000	0.000	0.000	0.000	-.074	-.066	0.000
S8								13.298	-.020	0.000	0.000	0.000	0.276	0.169	0.313
S9									5.960	-.020	0.000	0.000	-.093	0.047	0.067
S10										13.500	0.000	0.000	0.290	-.356	0.000
S11											6.330	0.000	-.081	0.040	-.068
S12												6.181	0.070	0.029	0.062
S13													1.898	0.000	-.046
S14														1.710	-.098
S15															1.663
S16															
S17															
S18															
S19															
S20															
S21															
S22															
S23															
S24															
S25															
S26															
S27															
S28															
S29															
S30															
S31															

Symmetric matrix

$F_{ij} - F_{ji}$

continued

TABLE 6-11 continued

	S16	S17	S18	S19	S20	S21	S22	S23	S24	S25	S26	S27	S28	S29	S30	S31
S1	0.240	-.420	0.000	0.037	-.048	0.000	0.000	0.000	0.000	0.000	0.000	0.00	0.00	0.00	0.00	0.00
S2	0.000	0.409	0.240	0.083	0.036	0.000	0.000	0.000	0.000	0.000	0.000	0.00	0.00	0.00	0.00	0.00
S3	-.036	-.118	0.240	-.487	0.000	0.000	0.000	0.000	0.000	0.000	0.000	0.00	0.00	0.00	0.00	0.00
S4	0.045	0.032	0.000	0.245	-.125	0.000	0.000	0.000	0.000	0.000	0.000	0.00	0.00	0.00	0.00	0.00
S5	0.000	-.030	-.035	-.056	0.193	-.135	0.000	0.000	0.000	0.000	0.000	0.00	0.00	0.00	0.00	0.00
S6	-.185	0.112	0.060	0.100	0.000	0.226	0.000	0.000	0.000	0.000	0.000	0.00	0.00	0.00	0.00	0.00
S7	0.310	-.070	0.000	0.000	0.000	0.020	0.250	-.630	-.090	-.010	-.010	0.00	0.00	0.00	0.00	0.00
S8	0.020	0.000	0.020	0.000	0.000	0.000	0.030	-.070	0.010	0.010	0.010	0.03	-.07	0.01	0.01	0.01
S9	0.000	-.070	0.310	-.070	0.000	0.000	0.000	0.000	0.000	0.000	0.000	0.25	-.63	-.09	-.01	-.01
S10	0.000	0.045	0.020	-.071	0.000	0.000	0.000	0.000	0.000	0.000	0.000	0.03	-.07	0.01	0.01	0.01
S11	0.000	0.000	0.000	0.000	0.000	0.000	0.000	0.000	0.000	0.000	0.000	0.00	0.00	0.00	0.00	0.00
S12	-.060	0.000	0.000	0.000	0.000	0.000	0.000	0.000	0.000	0.000	0.000	0.00	0.00	0.00	0.00	0.00
S13	-.010	0.000	0.011	-.060	0.011	0.029	0.000	0.000	0.000	0.000	0.000	0.00	0.00	0.00	0.00	0.00
S14	0.000	-.146	0.131	0.091	-.104	0.096	0.000	0.000	0.000	0.000	0.000	0.00	0.00	0.00	0.00	0.00
S15	0.134	-.058	-.088	0.177	-.057	-.013	0.000	0.000	0.000	0.000	0.000	0.00	0.00	0.00	0.00	0.00
S16	1.040	-.010	-.017	-.009	-.014	-.010	-.040	-.020	-.090	-.030	-.060	0.00	0.00	0.00	0.00	0.00
S17		1.256	-.010	-.063	-.010	-.025	-.030	0.030	-.050	-.010	0.030	-.03	0.03	-.05	-.01	0.03
S18			1.040	-.010	-.015	0.000	0.000	0.000	0.000	0.000	0.000	-.04	-.02	-.09	-.03	-.06
S19				1.258	0.039	-.024	0.000	0.000	0.000	0.000	0.000	-.03	0.03	-.05	-.01	0.03
S20					0.579	0.008	0.000	0.000	0.000	0.000	0.000	0.00	0.00	0.00	0.00	0.00
S21						0.649	0.000	0.000	0.000	0.000	0.000	0.00	0.00	0.00	0.00	0.00
S22							5.980	0.130	0.120	0.030	0.020	0.00	0.00	0.00	0.00	0.00
S23								0.800	-.040	0.010	0.000	0.00	0.00	0.00	0.00	0.00
S24									5.950	-.190	0.150	0.00	0.00	0.00	0.00	0.00
S25										0.710	-.050	0.00	0.00	0.00	0.00	0.00
S26											1.000	0.00	0.00	0.00	0.00	0.00
S27												5.98	0.13	0.12	0.03	0.02
S28													0.80	-.04	0.01	0.00
S29														5.95	-.19	0.15
S30															0.71	-.05
S31																1.00

Note: The symmetry coordinates are defined in Table 6-10. The units are md $\mathring{A}^{-1}$ for stretch-stretch, md $\mathring{A}$ for bend-bend, and md for bend-stretch elements.

(Table 6-7) and that for 3-Me U (Table 6-9). This force field is given in Table 6-11. Note also that Calculation I makes use of only the first 21 x 21 portion of this matrix, while Calculation II uses the complete 31 x 31 matrix.

Experimental and Predicted Spectra

For the matrix-isolated methylated uracil molecules (1-Me U, 1-Me-3-D U, 3-Me U, and 1,3-di Me U) the experimental infrared spectra have been reported by Szczesniak, Nowak, Szczepaniak, Chin, Scott, and Person (19). They interpreted such spectra making use of quantum mechanical predictions of frequencies and intensities of the normal vibrations, with a calculation that is basically the same as Calculation I in the present study, except that they used the APTs for uracil reported in Ref. 17, and here we are using the corrected APTs for uracil (Table 3-3). One interesting finding in the study by Szczesniak et al. (19) is the marked difference between spectral patterns, both observed and predicted in the carbonyl region for uracil and the methylated uracils.

The observed frequencies and relative intensities of the absorption bands given by Szczesniak et al. (19) have been collected and compared with our calculated frequencies (scaled by 0.90) and absolute intensities obtained with Calculations I and II, for all the in-plane normal modes of the methylated uracils, as shown in Tables 6-12 to 6-15. The PEDs are also given in these tables as part of the assignments for the in-plane fundamentals.

In order to compare the experimental matrix frequencies and intensities with the predicted results, we carried out simulations with the predicted results using Calculations I and II, to be compared with a similar simulation of the experimental spectra. The simulated spectra

TABLE 6-12
RESULTS FOR 1-METHYLURACIL IN-PLANE VIBRATIONS

Mode	Potential Energy Distribution (%)[a]	Calculation I ν(Cald.)[b]	0.9ν(Cald.)[c]	A_a[d]	ν(Expl.)[e]	R.I.[f]
1	νN_3H(100)	3838	3454	98	3430	123
2	νC_5H(95)	3411	3070	10	3092	g
3	νC_6H(95)	3370	3033	9		g
4	h					
5	h					
6	νC_2O(32), νC_4O(24), νC_2N_3(9), νC_4C_5(9), δ Ring II(9), δN_3H(9)	1966	1769	1110	1738 1734 1721	782
7	νC_2O(39), νC_4O(36), δ Ring I(10)	1948	1753	320	1704 1698	406
8	νC_5C_6(48), νC_4O(18), νC_6N_1(15), δC_6H(14)	1867	1680	6	1650	57
9	h				1482	67
10	νC_4C_5(19), νC_6N_1(18), νN_3C_4(13), νN_1C_2(11), δ Ring III(10)	1610	1449	137	1445	104
11	h				1432 1419 1415	101
12	νN_1C_2(29), νC_2N_3(23), νC_5C_6(14), δC_5H(11), νN_1Me(9), δC_2O(9)	1580	1422	113	1386	56
13	δN_3H(48), νC_4O(12), νN_3C_4(11)	1548	1394	10	1358	52

---

continued

TABLE 6-12 continued

14	νC_6N_1(27), νN_3C_4(18), δC_6H(14), νC_4C_5(12), δC_5H(10), δC_6H(9)	1410	1269	35	1320 1307	142
15	δC_6H(33), δN_3H(13), νN_3C_4(12), δN_1Me(9), δC_5H(8)	1386	1248	58	1224	52
16	νN_1Me(32), νC_2N_3(27), δ Ring I(21)	1347	1212	7	1188	17 or
17	h				1150	48
18	δC_5H(42), δC_6H(16), νC_5C_6(9)	1220	1098	0.1	1027	19
19	δ Ring I(27), νC_4C_5(18), νN_3C_4(13), νN_1C_2(8), δN_3H(7)	1058	953	4	963	13
20	δ Ring I(30), νN_1Me(23), νC_4C_5(12), δC_2O(10)	866	779	12	749	5
21	νN_1C_2(25), νC_4C_5(19), νC_6N_1(9), δ Ring II(9), νN_1Me(8)	808	727	11	712 or 749	5 5
22	δ Ring III(24), δN_1Me(13), νC_6N_1(12), δC_4O(11), δC_2O(10)	684	616	2	608	5
23	δ Ring III(37), δC_4O(21), δC_2O(20), νN_3C_4(8)	602	542	9	538	10
24	δ Ring II(52), δC_4O(15), νC_2N_3(9), νN_1Me(9), δ Ring III(8)	493	444	20	461	29
25	δC_4O(32), δC_2O(23), δ Ring II(18)	410	369	21	388	24
26	δN_1Me(69), δC_2O(19), δ Ring III(8)	352	316	4	below studied region	

Predicted Intensity Sum (km mol^{-1}) : 2002

---

continued

TABLE 6-12 continued

Calculation II

Mode	Potential Energy Distribution (%)[i]	ν(Calcd.)[j]	0.9ν(Calcd.)[k]	A_s[l] A	B	C	D	E	F
1	$\nu N_3H(100)$	3838	3454	98	98	98	98	98	98
2	$\nu C_6H(95)$	3411	3070	10	10	10	10	10	11
3	$\nu C_6H(95)$	3370	3033	10	10	10	10	10	10
4	νMe deg.(93), νMe sym.(7)	3331	2998	1	1	23	24	14	10
5	νMe sym.(93), νMe deg.(8)	3204	2884	52	58	8	5	16	11
6	$\nu C_2O(37)$, $\nu C_4O(20)$, $\nu C_2N_3(10)$, δ Ring II(9), $\delta N_3H(9)$, $\nu C_5C_6(8)$	1967	1770	1113	1132	1110	1097	1106	1062
7	$\nu C_4O(40)$, $\nu C_2O(33)$, δ Ring I(10), $\nu C_5C_6(7)$	1949	1754	323	322	331	328	330	326
8	$\nu C_5C_6(47)$, $\nu C_4O(19)$, $\nu C_6N_1(15)$, $\delta C_6H(14)$	1868	1681	5	8	6	3	6	4
9	δMe deg.(63), rock. Me(13), δMe sym. (7), $\nu N_1C_2(7)$	1668	1501	50	50	87	85	65	61
10	δMe sym.(74), $\nu C_5C_6(7)$	1631	1468	23	22	31	33	32	33
11	δMe deg.(27), $\nu N_1C_2(13)$, $\nu C_6S_1(13)$, $\nu C_4C_5(11)$, $\nu N_3C_4(8)$	1619	1457	87	88	78	72	88	74
12	δMe sym.(23), $\nu N_1C_2(19)$, $\nu C_2N_3(17)$, $\delta C_5H(10)$, $\nu C_6H(10)$, $\nu C_5C_6(9)$, $\nu N_1Me(9)$, $\delta N_3H(9)$	1569	1412	50	64	38	24	33	22
13	$\delta N_3H(43)$, $\nu N_3C_4(11)$, $\nu C_4O(11)$, $\nu C_2O(7)$, $\nu C_5H(7)$, $\nu C_6H(7)$	1548	1393	20	26	17	10	17	11
14	$\nu C_6N_1(17)$, $\delta C_6H(15)$, rock. Me(13), $\nu N_3C_4(12)$, $\nu C_4C_5(11)$	1450	1305	88	98	69	64	69	64
15	$\nu N_3C_4(20)$, $\delta N_3H(18)$, $\delta C_6H(18)$, $\delta C_5H(13)$, $\nu C_2N_3(10)$	1387	1248	34	45	33	27	32	20
16	$\nu N_1Me(40)$, $\nu C_2N_3(24)$, δ Ring I(21)	1344	1210	3	4	3	23	3	25
17	$\delta C_2H(29)$, $\delta C_6H(27)$, rock. Me(25)	1272	1144	20	22	16	13	22	25

---

continued

TABLE 6-12 continued

18	rock. Me(38), νC_6N_1(18), δC_3H(17), δ Ring I(8)	1150	1035	13	14	6	7	13	14
19	δ Ring I(23), νC_4C_5(19), νN_3C_4(12), νN_1C_2(11)	1053	948	4	3	6	9	7	9
20	δ Ring I(30), νN_1Me(24), νC_4C_5(12), δC_2O(10)	864	778	11	5	13	30	13	28
21	νN_1C_2(26), νC_6C_5(19), νC_6N_1(8)	807	726	11	8	11	16	11	18
22	δ Ring III(28), νC_6N_1(11), δN_1Me(10), δC_4O(10)	678	610	2	2	2	2	2	4
23	δ Ring III(33), δC_4O(23), δC_2O(22)	600	540	11	11	9	8	10	8
24	δ Ring II(51), δC_4O(15), νN_1Me(10), νC_2N_3(9), δ Ring III(8)	493	444	20	23	20	18	20	16
25	δC_4O(30), δC_2O(28), δ Ring II(19)	408	367	21	23	23	21	22	21
26	δN_1Me(74), δC_2O(13)	326	294	6	6	3	2	3	5
	Predicted Intensity Sum (km mol^{-1}) :	2088	2149	2062	2044	2056	1994		

[a] PED calculated using Eq. 2-29 (see Table 4-1 for the definition of the in-plane symmetry coordinates).

[b] Calculated frequencies using the first 21 x 21 sub-matrix of the force field given in Table 6-7, in cm^{-1}.

[c] Calculated frequencies in Calculation I scaled by 0.90.

[d] Predicted intensities in km mol^{-1} using the APTs of Table 3-3 for uracil.

[e] Matrix isolation infrared spectral data (in Ar matrix) taken from Refs. 19 and 20.

[f] Relative integrated intensity with respect to the intensity sum of all in-plane vibrations.

[g] Only a trace of absorbance is observed.

[h] Mode predicted in Calculation II only (involves methyl group vibration).

[i] PED obtained using Eq. 2-29 following the definition of the in-plane symmetry coordinates in Table 6-6.

[j] Calculated frequencies using the complete force field given in Table 6-7, in cm^{-1}.

[k] Calculated frequencies in Calculation II scaled by 0.90.

[l] Predicted intensities using the sets of APTs (A to F) given in Table 6-2.

TABLE 6-13
RESULTS FOR 1-METHYL-3-D-URACIL IN PLANE-VIBRATIONS

Calculation I

Mode	Potencial Energy Distribution (%)[a]	ν(Cald.)[b]	0.9ν(Cald.)[c]	A_s[d]	ν(Expl.)[e]	R.I.[f]
1	$\nu N_3D(99)$	2818	2536	70	2556	26
2	$\nu C_5H(95)$	3411	3070	10		g
3	$\nu C_6H(95)$	3370	3033	9		g
4	h					
5	h					
6	$\nu C_4O(40)$, $\nu C_5C_6(17)$, $\nu C_2O(14)$, δ Ring II(12)	1949	1754	1024	1739 1719	316 415
7	$\nu C_2O(60)$, $\nu C_4O(19)$, δ Ring I(10)	1947	1752	387	1704	583
8	$\nu C_5C_6(44)$, $\nu C_4O(23)$, $\nu C_6N_1(14)$, $\delta C_6H(13)$	1863	1677	16	1646	108
9	h				1490 1481	91
10	$\nu C_4C_5(19)$, $\nu C_6N_1(19)$, $\delta C_5H(12)$, $\nu N_3C_4(11)$, $\nu N_1C_2(10)$, δ Ring III(10)	1607	1446	123	1443	178
11	h				1425	91
12	$\nu N_1C_2(30)$, $\nu C_2N_3(20)$, $\nu C_5C_6(14)$, $\delta C_5H(12)$, $\nu N_1Me(10)$, $\delta C_2O(10)$	1576	1418	132	1378	137
13	$\nu N_3C_4(41)$, $\nu C_2N_3(23)$, $\delta N_3D(9)$, $\delta C_5H(8)$	1472	1325	15	1341	8

continued

TABLE 6-13 continued

14	$\delta C_6H(38)$, $\nu C_6N_1(30)$	1403	1262	73	1330	155
15	$\nu N_1Me(36)$, δ Ring I(16), $\delta C_5H(16)$, $\nu C_2N_3(11)$	1355	1220	2	1252 1211	11 8
16	h				1152 1149	50
17	$\delta C_6H(20)$, $\delta N_3D(17)$, $\nu N_1C_2(14)$, $\nu C_4C_5(13)$, $\delta C_5H(11)$, $\delta C_4O(10)$	1227	1104	3		g
18	$\delta C_5E(31)$, $\delta N_3D(16)$, δ Ring I(12), $\delta C_2O(9)$	1208	1087	2	1026	33
19	δ Ring I(34), $\delta N_3D(21)$, $\nu N_3C_4(9)$, $\nu N_1Me(9)$	979	880	10	876	11
20	$\nu C_4C_5(31)$, δ Ring I(14), $\delta N_3D(13)$, $\nu N_3C_4(12)$	831	748	6	733 or	3
21	$\nu N_1C_2(29)$, $\nu N_1Me(16)$, $\nu C_6N_1(10)$, $\delta N_3D(10)$, δ Ring II(9)	790	711	13	713	3
22	δ Ring III(27), $\delta N_1Me(12)$, $\delta C_4O(11)$, $\nu C_6N_1(10)$, $\delta C_2O(10)$	680	612	2	612	8
23	δ Ring III(33), $\delta C_2O(22)$, $\delta C_4O(20)$, δ Ring II(8)	593	534	8	505 or 533	37 or 5
24	δ Ring II(50), $\delta C_2O(17)$, δ Ring III(10), $\nu N_1Me(9)$, $\nu C_2N_3(8)$	490	441	20	460	40
25	$\delta C_4O(32)$, $\delta C_2O(23)$, δ Ring II(18), $\nu C_4C_5(7)$	408	368	21	387	30
26	$\delta N_1Me(69)$, $\delta C_2O(19)$, δ Ring III(9)	352	316	4	below studied region	

Predicted Intensity Sum (km mol^{-1}) : 1952

---

continued

TABLE 6-13 continued

Calculation II

Mode	Potential Energy Distribution (%)[i]	ν(Calcd.)[j]	0.9ν(Calcd.)[k]	A_g[l] A	B	C	D	E	F
1	νN_3D(99)	2818	2536	70	70	70	70	70	70
2	νC_3H(95)	3411	3070	10	10	10	10	10	10
3	νC_6H(95)	3370	3033	10	10	10	10	10	10
4	νMe deg.(93), νMe sym.(7)	3331	2998	1	1	23	24	14	10
5	νMe sym.(93), νMe deg.(8)	3204	2884	52	58	8	5	16	12
6	νC_2O(58), νC_2N_3(11), νC_5C_6(7)	1951	1756	1008	1026	1007	999	1003	956
7	νC_4O(53), νC_2O(14), νC_5C_6(12), νC_4C_5(10), δ Ring I(8)	1949	1754	468	414	415	405	416	408
8	νC_5C_6(43), νC_4O(24), νC_6N_1(14), δC_6H(13)	1864	1678	13	12	13	14	13	17
9	δMe deg.(65), rock. Me(13), δMe sym.(6), νN_1C_2(6)	1667	1500	46	45	80	79	60	56
10	δMe sym.(75), νC_5C_6(7)	1631	1468	26	24	34	37	36	37
11	δMe deg.(26), νC_6N_1(15), νN_1C_2(13), νC_4C_5(11), νN_3C_4(7), δ Ring III(7)	1616	1454	81	82	74	70	84	70
12	δMe sym.(22), νN_1C_2(20), δC_2H(14), δC_6H(14), νC_2N_3(13), νN_1C_7(11), νC_5C_6(10)	1565	1408	65	85	51	30	45	29
13	νN_3C_4(46), νC_2N_3(16), νC_4C_5(9), δN_3D(8), δC_3H(8)	1474	1327	30	32	27	24	28	31
14	δC_6H(27), νC_2N_3(13), νC_6N_1(12), rock. Me(12)	1442	1298	90	103	73	66	72	58
15	νN_1C_2(42), δ Ring I(16), δC_3H(14), νC_2N_3(10)	1351	1216	1	10	1	16	1	15
16	δC_6H(30), δC_5H(26), rock. Me(25)	1271	1144	22	25	18	15	25	28

---

continued

TABLE 6-13 continued

17	$\delta N_3 D(33)$, $\nu C_4 C_5(13)$, $\delta C_2 O(11)$, $\nu N_1 C_2(9)$, δ Ring I(9)	1217	1095	2	1	2	4	2	3
18	rock. Me(38), $\nu C_6 N_1(18)$, $\delta C_3 H(16)$, δ Ring I(7), $\nu N_1 C_2(6)$	1147	1032	13	13	7	8	13	15
19	δ Ring I(32), $\delta N_3 D(21)$, $\nu N_1 C_7(10)$, $\nu N_3 C_4(8)$	973	875	9	4	12	22	12	21
20	$\nu C_4 C_5(30)$, δ Ring I(15), $\delta N_3 D(13)$, $\nu N_3 C_4(12)$, $\nu N_1 C_7(8)$	830	747	5	4	6	10	6	9
21	$\nu N_1 C_2(30)$, $\nu N_1 C_7(16)$, $\delta N_3 D(10)$, δ Ring II(9), $\nu C_6 N_1(9)$	789	710	14	7	13	22	13	25
22	δ Ring III(30), $\delta N_1 D(10)$, $\delta C_4 O(10)$, $\nu C_6 N_1(9)$, $\delta C_2 O(9)$	674	607	2	2	2	2	2	3
23	δ Ring III(29), $\delta C_2 O(24)$, $\delta C_4 O(21)$, δ Ring II(9)	591	532	9	10	8	6	8	7
24	δ Ring II(50), $\delta C_4 O(17)$, $\nu N_1 C_7(9)$, δ Ring III(9), $\nu C_2 N_3(8)$	490	441	20	23	20	19	21	17
25	$\delta C_4 O(31)$, $\delta C_2 O(28)$, δ Ring II(19), $\nu N_3 C_4(7)$	407	366	21	23	23	21	22	21
26	$\delta N_1 C_7(74)$, $\delta C_2 O(13)$, δ Ring III(8)	326	294	6	6	3	2	3	5
	Predicted Intensity Sum (km mol^{-1}) :	2038	2099	2012	1993	2006	1944		

[a] to [1]All footnotes to Table 6-12 (a to l) apply to this table.

TABLE 6-14
RESULTS FOR 3-METHYLURACIL IN-PLANE VIBRATIONS

Mode	Potential Energy Distribution (%)[a]	Calculation I: ν(Cald.)[b]	0.9ν(Cald.)[c]	A[d]	ν(Expl.)[e]	R.I.[f]
1	νN_1H(100)	3866	3480	107	3480 3464	255
2	νC_5H(95)	3410	3070	11		g
3	νC_6H(96)	3368	3031	9		g
4	h					
5	h					
6	νC_2O(68), νN_1C_2(9), νC_2N_3(8), δ Ring I(7)	1968	1772	697	1744 1734	352
7	νC_4O(58), νC_5C_6(17), νC_4C_5(10), δ Ring II(10)	1948	1754	765	1697 1673	1020
8	νC_5C_6(51), νC_4O(24), δC_6H(13), νC_6N_1(12)	1854	1668	2	1648	30
9	h				1487	90
10	δN_1H(22), νC_6N_1(21), νN_1C_2(10), νC_2O(10), νC_4C_5(8)	1654	1489	116	1471	50
11	h				1431	35
12	νC_2N_3(23), δN_1H(18), νN_3Me(11), δC_2O(11), νN_1C_2(8)	1590	1430	120	1427	95
13	δC_6H(26), δN_1H(22), νC_4C_5(14), δC_5H(13), νN_3C_4(11), νC_5C_6(10), νN_1C_2(8)	1546	1391	0.03	1398	20

continued

TABLE 6-14 continued

14	νN_3C_4(37), νC_2N_3(22), δC_6H(13), δC_5H(11)	1473	1326	12	1274	34
15	δC_6H(22), δN_1H(19), νN_3Me(15), δ Ring I(11), νN_1C_2(10), δC_5H(9)	1323	1190	25	1212	39
16	δC_5H(27), νN_3Me(25), δ Ring I(15), δC_6H(11), νC_4C_5(9)	1290	1161	37	1124	80
17	h				1121	70
18	νC_6N_1(32), δC_5H(17), νC_5C_6(14), δ Ring I(10)	1179	1061	20	1070	12
19	νN_1C_2(26), νC_4C_5(18), δC_2O(13), δC_6H(10), δC_4O(8)	1149	1034	5		g
20	δ Ring I(42), νN_3Me(21), δ Ring III(12)	950	855	0.3		g
21	νN_3C_4(19), νC_4C_5(19), νN_1C_2(10), νC_2N_3(10), νN_3Me(10)	762	686	10	725	24
22	δC_2O(32), δC_4O(28), δN_3Me(10), δ Ring II(9)	634	570	10		g
23	δ Ring II(39), δ Ring III(20), δC_4O(6)	594	534	18	540	19
24	δ Ring III(29), δ Ring II(21), νN_3Me(9)	560	504	6	502	5
25	δC_4O(37), δC_2O(22), δ Ring III(21), δ Ring II(8), νN_3C_4(8)	388	349	25	400	5
26	δN_3Me(76), δC_2O(12), δ Ring II(10)	329	295	4	below studied region	

Predicted Intensity Sum (km mol^{-1}) : 1999

---

continued

TABLE 6-14 continued

Mode	Potential Energy Distribution (%)[1]	Calculation II (Calcd.)[1]	0.9 (Calcd.)[1]	A_g[1] G	H	I	J	K	L
1	$\nu N_1H(100)$	3866	3480	107	107	107	107	107	107
2	$\nu C_2H(95)$	3410	3070	11	11	11	11	11	11
3	$\nu C_6H(96)$	3368	3031	9	9	9	9	9	9
4	νMe deg.(93), νMe sym.(7)	3331	2998	1	1	24	25	11	15
5	νMe sym.(93), νMe deg.(8)	3204	2884	54	60	9	6	13	16
6	$\nu C_2O(67)$, $\nu C_2N_3(10)$, $\nu N_1C_2(9)$	1973	1776	670	672	672	669	637	668
7	$\nu C_2O(59)$, $\nu C_3C_6(16)$, $\nu C_4C_5(10)$, δ Ring II(9)	1951	1756	777	784	787	771	754	778
8	$\nu C_5C_6(51)$, $\nu C_4O(23)$, $\nu C_6N_1(13)$, $\delta C_6H(13)$	1854	1668	1	1	2	2	2	2
9	δMe deg.(25), δMe sym.(14), $\nu C_6N_1(9)$, $\delta N_1H(9)$, $\nu N_3C_4(8)$	1669	1502	80	90	132	117	119	133
10	δMe deg.(71), rock. Me(10)	1656	1491	57	64	30	26	22	28
11	δMe sym.(50), $\delta N_1H(18)$, $\nu C_6N_1(10)$	1618	1456	20	20	22	23	20	20
12	$\nu C_2N_3(31)$, δMe sym.(25), $\nu N_1C_2(17)$, $\nu N_3C_9(10)$	1582	1424	81	114	65	41	29	61
13	$\nu N_3C_4(26)$, $\delta N_1H(25)$, $\nu C_4C_5(15)$, $\delta C_6H(10)$	1555	1400	15	24	12	4	8	13
14	$\delta C_6H(28)$, $\delta C_5H(18)$, $\nu C_3C_4(15)$, rock. Me(7)	1512	1361	5	7	6	2	4	6
15	$\delta N_1H(19)$, $\delta C_6H(19)$, $\delta C_3H(16)$, $\nu N_1C_2(13)$, $\nu N_3C_9(10)$, $\nu C_6N_1(9)$	1327	1194	9	5	14	23	19	13
16	$\nu N_3C_9(33)$, $\delta C_5H(20)$, δ Ring I(19), $\nu C_4C_5(15)$	1291	1162	31	13	30	73	72	29
17	rock. Me(37), $\delta C_6H(19)$, $\nu N_1C_2(16)$	1246	1122	49	53	31	31	57	44

---

continued

TABLE 6-14 continued

18	νC_6N_1(34), δC_5H(18), νC_3C_5(14), δ Ring I(10)	1178	1061	24	23	24	25	27	24
19	rock. Me(28), νN_1C_2(15), νC_4C_5(11)	1085	977	7	7	1	0.4	2	2
20	δ Ring I(42), νN_3C_9(22), δ Ring III(12)	950	855	0.5	4	0.4	3	4	0.4
21	νN_3C_4(19), νC_4C_5(19), νC_2N_3(11), νN_3C_9(11), νN_1C_2(10)	762	686	10	6	10	18	17	11
22	δC_2O(33), δC_4O(29), δ Ring II(11)	628	565	9	9	10	10	12	9
23	δ Ring II(38), δ Ring III(19), δC_4O(7)	593	534	18	18	17	17	16	18
24	δ Ring III(29), δ Ring II(21), νN_3C_9(9)	559	503	6	7	6	6	5	6
25	δC_4O(35), δC_2O(24), δ Ring III(20), δ Ring II(9), νN_3C_4(7)	387	348	26	27	25	22	23	25
26	δN_3C_9(79), δC_2O(9), δ Ring II(8)	304	274	6	5	3	4	1	5
	Predicted Intensity Sum (km mol^{-1}) :		2084		2140	2060	2046	2000	2053

[e] PED calculated using Eq. 2-29 (see Table 4-1 for the definition of the in-plane symmetry coordinates).
[b] Calculated frequencies in cm^{-1} using the first 21 x 21 sub-matrix of the force field given in Table 6-9.
[c] Calculated frequencies in Calculation I scaled by 0.90.
[d] Predicted intensities in km mol^{-1} using the APTs of Table 3-3 for uracil.
[e] Matrix isolation infrared spectral data (in Ar matrix) taken from Refs. 19 and 20.
[f] Relative integrated intensity with respect to the intensity sum of all in-plane vibrations.
[g] Only a trace of absorbance is observed.
[h] Mode predicted in Calculation II only (involves methyl group vibration).
[i] PED obtained using Eq. 2-29 following the definition of the in-plane symmetry coordinates in Table 6-8.
[j] Calculated frequencies in cm^{-1} using the force field given in Table 6-9.
[k] Calculated frequencies in Calculation II scaled by 0.90.
[l] Predicted intensities using the sets of APTs (G to L) given in Table 6-4, in km mol^{-1}.

TABLE 6-15
RESULTS FOR 1,3-DIMETHYLURACIL IN-PLANE VIBRATIONS

Calculation I

Mode	Potential Energy Distribution (%)[a]	(Calc.)[b]	0.9 (Calc.)[c]	A_a[d]	(Expl.)[e]	R.I.[f]
1	$\nu C_5H(95)$	3411	3070	10		g
2	$\nu C_6H(95)$	3370	3033	9	3000	10
3	h					
4	h					
5	h					
6	h					
7	$\nu C_2O(62)$, $\nu C_2N_3(12)$, $\nu C_5C_6(6)$, δ Ring II(6)	1955	1760	466	1724	252
8	$\nu C_4O(54)$, $\nu C_5C_6(13)$, $\nu C_2O(11)$, $\nu C_4C_5(10)$ δ Ring I(8), δ Ring II(6)	1949	1754	965	1690 1686 1683 1680 1678	1102
9	$\nu C_5C_6(44)$, $\nu C_4O(25)$, $\nu C_6N_1(14)$, $\delta C_6H(13)$	1861	1675	15	1657	23
10	$\nu N_1C_2(18)$, $\nu C_2N_3(15)$, $\nu N_3C_4(14)$, δ Ring III(12), $\nu C_4C_5(11)$, $\nu C_6N_1(10)$, $\nu N_3C_9(9)$, $\delta C_4O(8)$	1634	1471	223	1488	117
11	h				1470	28
12	h				1446	75
13	$\delta C_5H(23)$, $\nu C_5C_6(17)$, $\delta C_6H(14)$, $\nu C_2N_3(13)$, $\nu N_1C_2(10)$	1588	1429	42	1436	87

---

continued

TABLE 6-15 continued

14	h				1404	49
15	h				1375	99
16	$\nu N_3C_4(42)$, $\nu C_2N_3(15)$, $\nu N_1C_2(12)$, $\nu C_6N_1(10)$, $\delta C_5H(10)$	1478	1330	4	1339	93
17	h				1271	10
18	$\nu C_2N_3(16)$, δ Ring I(16), $\delta C_6H(15)$, $\nu N_3C_9(12)$, $\nu N_1C_7(10)$, $\nu N_1C_2(8)$	1436	1292	35	1242	22
19	$\delta C_6H(29)$, $\nu N_1C_7(25)$, $\nu C_6N_1(21)$, δ Ring I(11)	1390	1251	46	1140	39
20	$\delta C_5H(48)$, $\nu N_3C_9(14)$, $\nu C_5C_6(8)$	1267	1140	7	1133	29
21	$\nu C_4C_5(26)$, $\delta C_6H(16)$, $\nu N_1C_2(11)$, $\delta C_4O(11)$	1184	1066	5		g
22	h				1003	35
23	$\nu N_3C_9(23)$, $\delta C_2O(16)$, $\nu N_1C_2(14)$, $\nu N_1C_7(13)$	1048	943	10		g
24	δ Ring I(40), $\nu N_1C_7(15)$, $\nu C_4C_5(9)$, δ Ring III(9)	885	796	7	712	10
25	$\nu N_3C_4(20)$, $\nu C_4C_5(13)$, $\nu C_6N_1(11)$, $\nu N_1C_2(9)$, $\nu N_3C_9(7)$	746	671	16	680	16
26	$\delta C_4O(29)$, $\delta C_2O(17)$, $\delta N_1C_7(15)$, $\nu C_4C_5(10)$, $\nu C_6N_1(9)$	672	605	3	613	8
27	δ Ring III(39), $\nu N_3C_9(11)$, $\delta C_2O(9)$, δ Ring I(7), δ Ring II(6)	563	507	2	512	13
28	δ Ring II(50), $\nu C_2N_3(13)$, $\nu N_1C_7(13)$, δ Ring III(6)	506	455	16	477	19
29	$\delta C_4O(42)$, δ Ring II(9), δ Ring III(9), $\delta N_1C_7(9)$, $\nu N_3C_4(8)$	390	351	18	404	36
30	$\delta N_1C_7(46)$, $\delta C_2O(33)$, $\delta N_3C_9(9)$, δ Ring II(9), δ Ring III(7)	356	321	9	below studied region	
31	$\delta N_3C_9(65)$, $\delta N_1C_7(18)$, $\nu C_2N_3(8)$, δ Ring III(6), δ Ring II(5)	317	285	2		

Predicted Intensity Sum (km mol^{-1}) : 1909

---

continued

TABLE 6-15 continued

Mode	Potential Energy Distribution (%)	Calculation II (Calcd.)	0.9 (Cd.)	A_s 1	2	3	4	5	6	7	8	9	10	11	12
1	$\nu C_3H(95)$	3411	3070	10	10	10	10	11	11	11	11	11	11	11	11
2	$\nu C_6H(95)$	3370	3033	10	10	10	10	10	10	10	10	10	10	10	10
3	νMe_3 deg.(79), νMe_1 deg.(14), νMe_3 sym.(6)	3331	2998	1	1	1	1	16	16	16	16	10	11	7	7
4	νMe_1 deg.(78), νMe_3 deg.(14), νMe_1 sym.(6)	3331	2998	1	1	1	1	32	33	32	34	20	15	19	14
5	νMe_3 sym.(89), νMe_3 deg.(8)	3204	2884	42	43	47	48	7	8	4	5	13	13	10	10
6	νMe_1 sym.(89), νMe_1 deg.(8)	3204	2884	64	69	65	70	10	7	10	6	19	15	19	15
7	$\nu C_4O(54)$, $\nu C_3C_6(13)$, $\nu C_4C_5(10)$, $\nu C_2O(10)$	1963	1767	463	470	472	480	467	454	455	442	466	457	420	432
8	$\nu C_2O(60)$, $\nu C_2N_3(12)$, $\nu N_1C_2(6)$, δ Ring II(6)	1951	1756	962	977	962	977	974	967	968	960	958	914	792	886
9	$\nu C_5C_6(44)$, $\nu C_4O(24)$, $\nu C_6N_1(14)$, $\delta C_6H(13)$	1863	1676	10	9	10	9	11	12	11	12	11	15	9	14
10	δMe_1 deg.(28), $\nu N_1C_2(11)$, δMe_3 sym.(11), rock. $Me_1(9)$, $\nu C_2N_3(7)$, $\nu C_6N_1(7)$	1677	1509	111	110	125	124	187	183	167	164	166	156	147	136
11	δMe_3 deg.(64), δMe_1 deg.(11), δMe_3 sym.(8)	1661	1495	5	5	5	5	11	11	11	11	5	5	1	5
12	δMe_1 deg.(43), δMe_3 deg.(17), δMe_3 sym.(16)	1646	1481	71	73	78	80	39	35	32	28	49	44	39	35
13	δMe_1 sym.(68), $\nu C_5C_6(7)$	1632	1469	16	15	15	14	22	23	22	24	26	27	14	23
14	δMe_3 sym.(65), $\nu C_6N_1(7)$	1603	1442	27	26	39	39	11	12	5	6	8	5	3	2
15	δMe_3 sym.(29), δMe_1 sym.(16), $\delta C_3H(12)$, $\nu N_1C_2(11)$, $\nu C_5C_6(8)$	1580	1422	34	42	42	51	21	14	18	11	16	13	28	11

continued

TABLE 6-15 continued

16	νN_3C_4(32), δC_5H(11), νC_6N_1(9), rock. Me_3(9)	1523	1371	21	25	30	35	17	13	5	3	18	16	55	10
17	δC_6H(19), δN_3C_9(11), rock. Me_1(11), νC_6N_1(9), νC_2N_3(8)	1478	1330	22	16	32	26	19	33	16	28	17	22	1	7
18	νN_3C_7(39), δ Ring I(20), δC_6H(13), νN_3C_9(10), νC_6N_1(7)	1391	1252	39	80	32	70	31	4	47	12	30	7	60	21
19	δC_5H(44), νN_3C_9(9), rock. Me_3(8), νC_4C_5(7), δC_6H(7)	1288	1159	2	1	0.4	0.1	4	6	13	15	2	4	8	10
20	δC_6H(23), rock. Me_3(19), rock. Me_1(15), νC_4C_5(13)	1261	1135	55	58	47	50	32	30	40	39	47	50	61	60
21	rock. Me_1(27), rock. Me_3(22), νN_3C_9(12), νN_1C_2(10), νC_6N_1(9)	1193	1074	15	9	10	5	8	15	18	28	13	21	29	42
22	rock. Me_1(19), rock. Me_3(15), νC_4C_5(13), νC_6R_1(7)	1113	1002	18	15	24	21	12	20	16	25	22	30	8	35
23	νN_3C_9(20), νN_1C_2(13), δC_2O(12), νN_3C_4(8), δC_5H(7)	1029	926	5	3	2	0.3	6	14	14	25	4	10	38	28
24	δ Ring I(38), νN_1C_7(17), νC_4C_5(10), δ Ring III(8)	880	792	6	2	8	3	8	20	6	17	7	17	12	15
25	νN_3C_4(19), νC_4C_5(13), νN_1C_2(10), νC_6N_1(10), νN_3C_9(7), δ Ring III(7)	744	669	14	12	11	9	15	16	20	20	14	18	16	21

continued

TABLE 6-15 continued

26	$\delta C_4O(31)$, $\delta C_2O(19)$, $\delta N_1C_7(12)$, $\nu C_4C_5(10)$, $\nu C_6N_1(8)$	660	594	3	2	2	2	2	3	4	5	3	4	7	4
27	δ Ring III(38), $\nu N_3C_9(11)$, $\delta C_2O(11)$, δ Ring I(7), δ Ring II(7)	562	506	3	2	4	4	2	2	1	1	2	3	0.3	1
28	δ Ring II(49), $\nu C_2N_3(13)$, $\nu N_1C_7(13)$	505	455	15	19	16	20	15	13	15	12	16	11	8	11
29	$\delta C_4O(39)$, $\delta C_2O(15)$, δ Ring II(12), δ Ring III(12), $\nu N_3C_4(8)$	387	348	20	21	22	23	21	20	19	18	20	21	19	19
30	$\delta N_1C_7(51)$, $\delta C_2O(24)$, $\delta N_3C_9(16)$	335	302	9	8	9	8	5	4	6	4	6	9	3	6
31	$\delta N_3C_9(63)$, $\delta N_1C_7(22)$, $\nu C_2N_3(7)$	290	261	4	4	3	3	1	2	1	2	3	1	2	1
	Predicted Intensity Sum (km mol^{-1}) :			2079	2140	2136	2197	2030	2011	2016	1997	2017	1955	1857	1902

[a] PED calculated using Eq. 2-29 (see Table 4-1 for the definition of the in-plane symmetry coordinates).

[b] Calculated frequencies in cm^{-1} using the first 21 x 21 sub-matrix of the force field given in Table 6-11.

[c] Calculated frequencies in Calculation I scaled by 0.90.

[d] Predicted intensities in km mol^{-1} using the APTs of Table 3-3 for uracil.

[e] Matrix isolation infrared spectral data (in Ar matrix) taken from Refs. 19 and 20.

[f] Relative integrated intensity with respect to the intensity sum of all in-plane vibrations.

[g] Only a trace of absorbance is observed.

[h] Mode predicted in Calculation II only (involves methyl group vibrations).

[i] PED obtained using Eq. 2-29 following the definition of the in-plane symmetry coordinates in Table 6-10.

[j] Calculated frequencies in cm^{-1} usiog the force field given in Table 6-11.

[k] Calculated frequencies in Calculation II scaled by 0.90.

[l] Predicted intensities using the sets of APTs (1 to 12) given in Table 6-5, in km mol^{-1}.

for all four methylated uracils are given in Figs. 6-9 to 6-12. All simulations were done as described in Chapter 4 for the simulated spectra of uracil.

We have also collected in Tables 6-12 to 6-15 all the predicted intensities for the methylated uracils using the different sets of APTs given in Tables 6-2, 6-4, and 6-5. A close look to these tables shows that it is difficult to decide which particular set of APTs better reproduces the experimental intensities. Some specific regions of the experimental spectra are very well reproduced with one set of APTs, while the same set of APTs does not reproduce other regions.

In order to facilitate the discussion of results, the spectra have been divided into three major regions: the N-H and C-H stretching region (3600 - 2000 cm^{-1}), the C=O and C=C stretching region (2000 - 1500 cm^{-1}), and the ring stretching and deformation region (1500 - 300 cm^{-1}). Let us now consider in detail each one of these spectral regions.

Spectral Region Between 3600 - 2000 cm^{-1}

From Tables 6-12 to 6-15 and Figs. 6-8 to 6-15 we can see that for the N_3H and N_1H stretching vibrations of 1-Me U and 3-Me U the observed frequencies in argon are somewhat lower than the predicted values, as was seen for uracil (Table 4-3). However, the observed wavenumber difference between these two N-H stretches, about 35 cm^{-1}, is close to the predicted value of 26 cm^{-1}, in contrast with uracil where the observed difference value was found to be around 50 cm^{-1} compared with the predicted value of 26 cm^{-1}. The experimental measured values (16) for the intensity of the N_1H stretching mode in 3-Me U vapor (75 km mol^{-1}) and that of the N_3H stretching

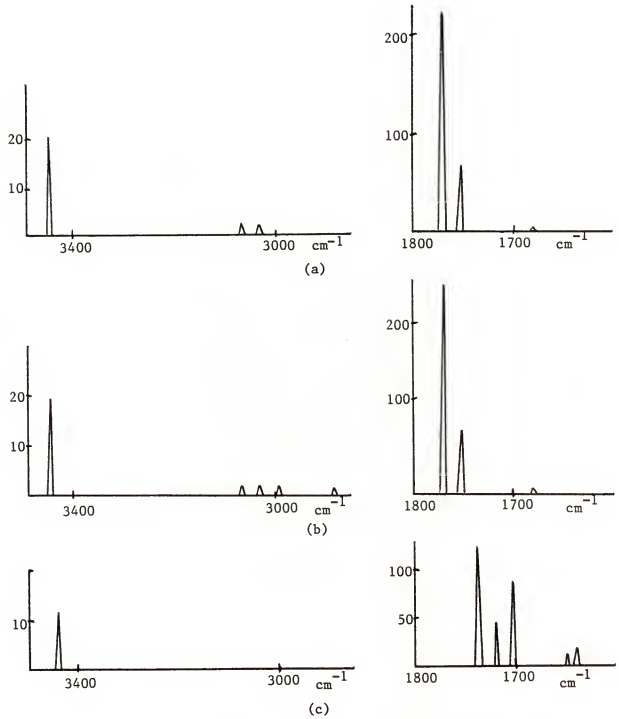

Figure 6-9. Simulated infrared spectra for 1-Me U. a) Predicted spectrum using Calculation I; b) Predicted spectrum using Calculation II with the set of APTs F for acetone given in Table 6-2; c) Experimental infrared spectrum in an argon matrix (see Ref. 19). The out-of-plane modes are indicated by "*".

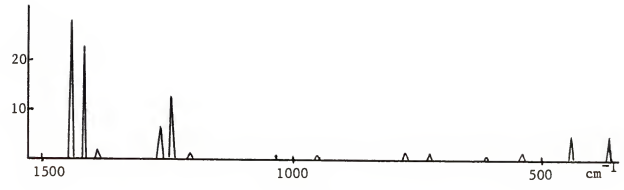

(a)

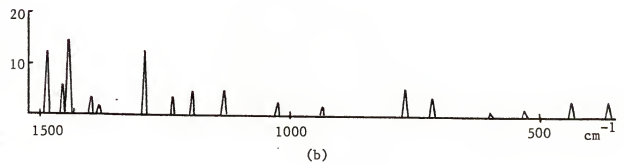

(b)

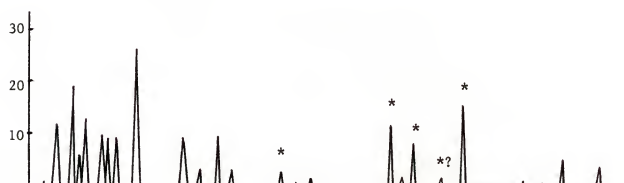

(c)

Figure 6-9 continued

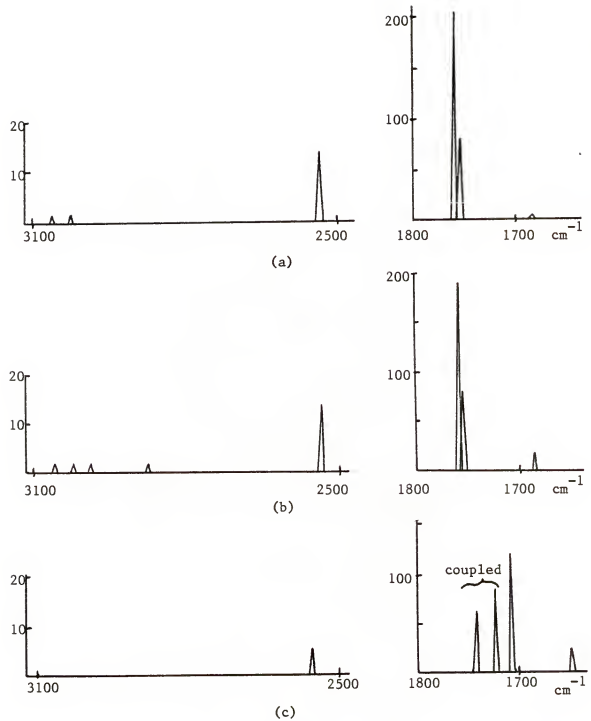

Figure 6-10. Simulated infrared spectra for 1-Me-3-D U. a) Predicted spectrum using Calculation I; b) Predicted spectrum using Calculation II with the set of APTs F for acetone given in Table 6-2; c) Experimental spectrum in an argon matrix (see Ref. 19). The out-of-plane modes are indicated by "*".

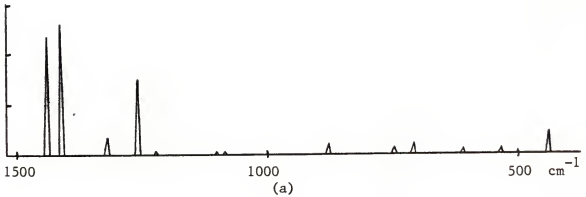

(a)

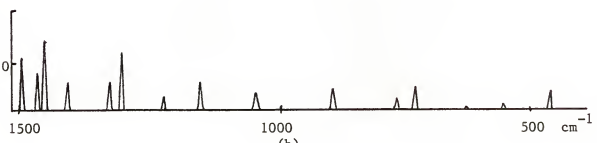

(b)

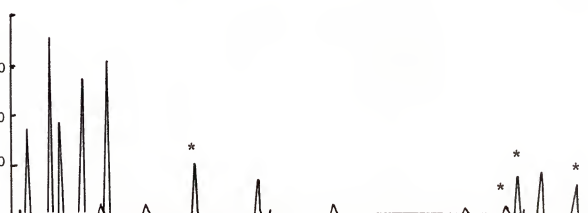

(c)

Figure 6-10 continued

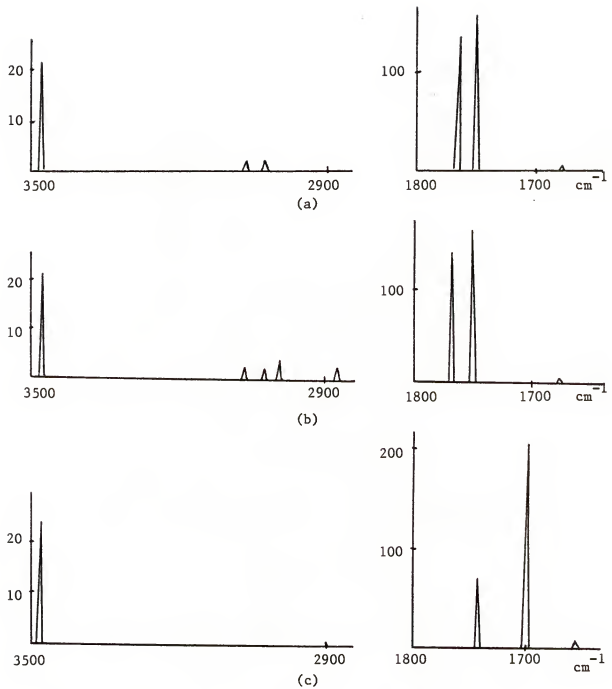

Figure 6-11. Simulated infrared spectra for 3-Me U. a) Predicted using Calculation I; b) Predicted using Calculation II with the set of APTs L for acetone given in Table 6-4; c) Experimental infrared spectrum in an argon matrix (see Ref. 19). The out-of-plane modes are indicated by "*".

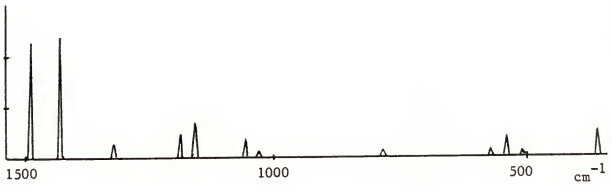

(a)

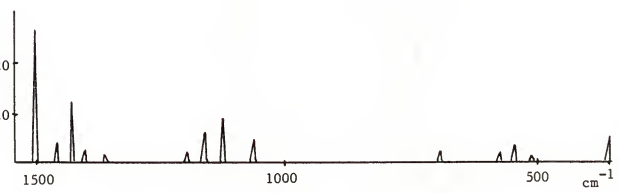

(b)

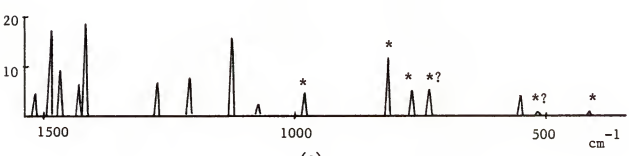

(c)

Figure 6-11 continued

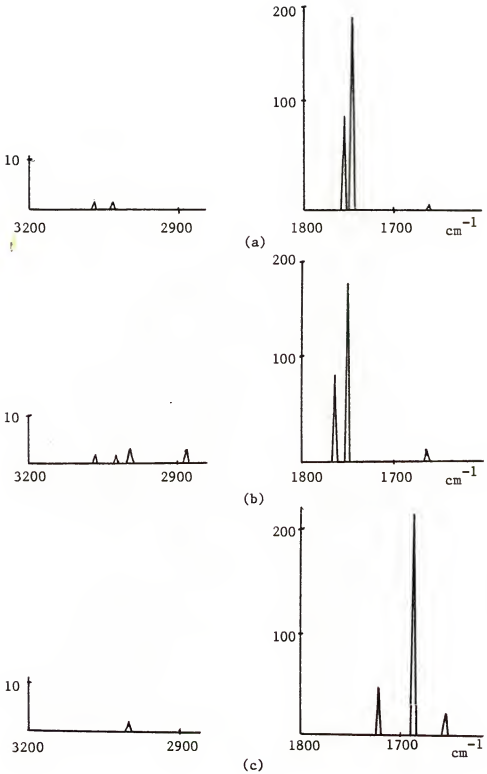

Figure 6-12. Simulated infrared spectra for 1,3-di Me U.
a) Predicted spectrum using Calculation I;
b) Predicted spectrum using Calculation II with the set of APTs 12 given in Table 6-5; c) Experimental infrared spectrum in an argon matrix (see Ref. 19).

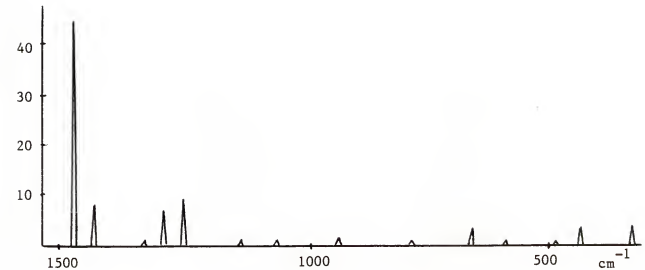

(a)

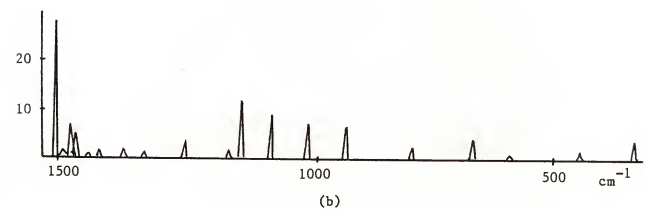

(b)

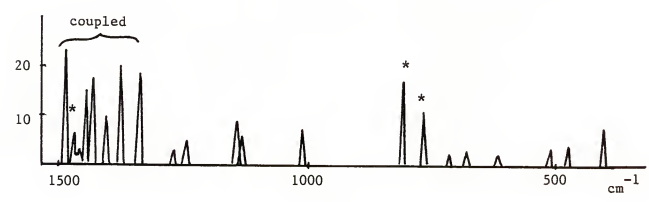

(c)

Figure 6-12 continued

mode of 1-Me U vapor (53 km mol^{-1}) are lower than the predicted values of 107 and 98 km mol^{-1}, respectively, but the discrepancy is still within the expected limit of a "factor of two". The experimental intensity ratio of the N_1H stretch in 3-Me U to that of the N_3H stretch in 1-Me U is 1.3, which is in good agreement with the value of 1.1 in this study. The predicted value of 0.7 in Ref. 17 for this ratio was also due to the use of the incorrect APTs for uracil.

It is also shown in Tables 6-12 to 6-15 and Figs. 6-9 to 6-12 that the C-H stretching modes of the uracil ring are always predicted with an intensity of about 10 km mol^{-1}, or 10 % that for N-H stretches, as it was for the uracil molecule (Table 4-3). Experimentally, only a trace of absorbance is observed for such C-H stretches in the matrix-isolated spectra. However, for the C-H stretches of the methyl groups on the methylated uracils, Calculation II predicts different intensities, which depend on the set of APTs used (Tables 6-12 to 6-15). The lowest predicted intensity values are for the case when the APTs of the H atoms of acetone are used, which is in better agreement with experimental data, because these absorptions are not observed in the matrix-isolated spectra. The APTs of the H atoms of N-methylacetamide do not predict good intensity values for these C-H stretches.

Spectral Region Between 2000 - 1500 cm^{-1}

The experimental spectra for the methylated uracils show a complex structure of the bands, because more than the expected bands are observed in the matrix (19). An inspection of Tables 6-12 to 6-15 and Figs. 6-9 to 6-17 shows that the frequencies of carbonyl (C_2O and C_4O) bands of methylated uracils are predicted to be slightly higher, and the separation between them predicted lower, than the

observed frequencies and separations of the bands. It will be interesting to compare the experimental and predicted sums and ratios for the intensities of modes 6 (C_2O stretching) and 7 (C_4O stretching) using Calculations I and II. This comparison is shown in Table 6-16 for 1-Me U, 1-Me-3-D U, 3-Me U, and for 1,3-di Me U. For 1-Me U the calculated ratio of the intensity of mode 6 to that of mode 7 in Calculation I (APTs of uracil) is 3.47, which is about 1.8 times the experimental value of 1.93. Also, we can see from Table 6-16 that the different sets of APTs used in Calculation II give, in general, lower ratios, but still larger than the experimental value. In uracil (Table 4-3) the ratio of the intensity for both stretches is 2.34 (experimentally) and 2.17 (predicted). The decrease of the experimental ratio going from uracil (2.34), to 1-Me U (1.93), to 1-Me-3-D U (1.25), to 3-Me U (0.34), to 1,3-di Me U (0.48) has been discussed by Szczesniak, Nowak, Szczepaniak, Chin, Scott, and Person (19).

For mode 8 (C=C stretching) the observed and scaled frequency values agree quite well in all the methylated uracils; however, the intensity prediction for this mode is always, using either Calculations I or II, much lower than the experimental values.

Spectral Region Between 1500 - 300 cm^{-1}

An examination of Tables 6-12 to 6-15 and Figs. 6-9 to 6-12 shows that there are only a few absorption bands which have similar frequencies and intensities in the experimental spectra of methylated uracils. For example, one of these is the band near 1490 cm^{-1}, which according to our PEDs calculation has predominant contribution from the CH_3 degenerate deformation vibration. In order to interpret

TABLE 6-16

COMPARISON OF RESULTS FOR MODES ν_6 AND ν_7 OF THE METHYLATED URACILS

mode	Expl.	Calcn. I	Calcn. II					
			1-Me U					
			A	B	C	D	E	F
ν_6	782	1110	1113	1132	1110	1097	1106	1062
ν_7	406	320	323	322	331	328	330	326
Sum (km mol^{-1})	1188	1430	1436	1454	1441	1425	1436	1388
A_6/A_7	1.93	3.47	3.44	3.52	3.53	3.34	3.35	3.26
			1-Me-3-D U					
			A	B	C	D	E	F
ν_6	731	1024	1008	1026	1007	999	1003	956
ν_7	583	387	408	414	415	405	416	408
Sum (km mol^{-1})	1314	1411	1416	1440	1422	1404	1419	1364
A_6/A_7	1.25	2.64	2.47	2.48	2.43	2.47	2.41	2.34
			3-Me U					
			G	H	I	J	K	L
ν_6	352	697	670	672	672	669	637	668
ν_7	1020	765	777	784	787	771	754	778
Sum (km mol^{-1})	1372	1462	1447	1456	1459	1440	1391	1446
A_6/A_7	0.34	0.91	0.86	0.86	0.85	0.87	0.84	0.86

---

continued

TABLE 6-16 continued

ν_6	252	466	463	470	472	480	467	454	455	442	466	457	420	432
ν_7	1102	965	962	977	962	977	974	967	968	960	958	914	792	886
Sum (km mol^{-1})	1352	1431	1425	1447	1434	1457	1441	1421	1423	1402	1424	1371	1212	1318
A_6/A_7	0.23	0.48	0.48	0.48	0.49	0.49	0.48	0.47	0.47	0.46	0.49	0.50	0.53	0.49

Note: The entries in this table are experimental (relative) and predicted absolute infrared intensities (km mol^{-1}). The calculated ratio A_6/A_7 using Calculation I or Calculation II is always greater than the experimental ratio by nearly a factor of two. However, the correct pattern is predicted for this ratio going from 1-Me U to 1,3-di Me U.

this region, it is very important to carry out Calculation II, since here is where we find all the in-plane deformation modes of the methyl groups. Moreover, because in Calculation II we are using different sets of APTs we can compare the predicted intensities obtained mainly because methyl group deformations. In the particular case of monomeric 1-Me U the assignment for most of the bands, based on our calculations given in Table 6-12 and Fig. 6-9, agrees quite well with previous assignments reported in the literature (1,4,13). However, the correspondence is not entirely straightforward because the previous spectra (1,4,13) are related to hydrogen bonded molecules in the crystal, while our spectrum corresponds to the monomeric molecules, only slightly perturbed by the interaction with the matrix. A close look to Table 6-12 and Fig. 6-9 shows that the results of Calculations I and II do not reproduce the experimental spectrum in this region as we expected, in particular the "rocking" deformation mode. The same pattern is observed for the other methylated uracil molecules (Tables 6-13 to 6-15 and Figs. 6-10 to 6-12). It is also interesting to note that in the methyl deformation region the experimental intensity is better reproduced when the APTs of the $N-CH_3$ group of N-methylacetamide are used.

The 1358 cm^{-1} band in the spectrum of 1-Me U is not present in the spectra of the other methylated uracils. It is predicted at 1394 cm^{-1} as having an intensity of 10 km mol^{-1} (Calculation I) and 1393 cm^{-1} with an intensity ranging from 10 to 26 km mol^{-1} (Calculation II). It is assigned to the NH_3 bending mode.

Summary

We have seen in this Chapter that vibrational parameters (force constants and atomic polar tensors) obtained at the ab initio level with a 4-31G basis set for uracil, acetone, N-methylformamide, and N-methylacetamide can be transferred to predict infrared frequency and intensity data of the methylated uracil molecules. These ab initio quantum mechanical calculations using a 4-31G basis set predict within a factor-of-two the experimental absolute intensities and within ± 20 cm^{-1} the experimental frequencies. These calculations, even in this limited form, are quantitative enough to be very useful to assign and to interpret the complex infrared spectra of these molecular systems. Furthermore, we can have considerable confidence in similar predictions for similar molecules.

We should certainly be able to use the ab initio force constants and APTs presented in this dissertation to predict intensities accurate to a factor-of-two for other pyrimidines, like cytosine. Therefore, the technique of transferring vibrational parameters to predict the infrared spectra of other molecules is a very promising one.

Since the calculated results presented in this dissertation are just a first step, future research in this theoretical and experimental area of biomolecules could be directed to the development of more refined schemes for transferring molecular parameters, with the aim of predicting more accurate intensity and frequency data which reproduces much more closer the experimental data. Perhaps, the next step to follow with this type of calculation could be the application of a perturbation theory refinement procedure to achieve this objective. Of course, more experimental work should

be done employing matrix-isolation techniques, including: infrared, Fourier transform infrared, Raman and resonance Raman, to get more data of biological molecules.

REFERENCES

1. M. Tsuboi, S. Takahashi, and I. Harada, in "Physicochemical Properties of Nucleic Acids," J. Duchesne, Ed. (Academic Press, New York, 1973), Vol. 2, Chap. 11.

2. M. Maltese, S. Passerini, S. Nunziante-Cesaro, S. Dobos, and L. Harsanyi, J. Mol. Struct. 116, 49 (1984).

3. J. Bandekar and G. Zundel, Spectrochim. Acta 39A, 343 (1983).

4. T. P. Lewis, H. T. Miles, and E. D. Becker, J. Phys. Chem. 88, 3253 (1984).

5. A. J. Barnes, M. A. Stuckey, and L. Le Gall, Spectrochim. Acta 40A, 419 (1984).

6. Y. Nishimura, A. Y. Hirakawa, and M. Tsuboi, in "Advances in Infrared and Raman Spectroscopy," R. J. H. Clark and R. E. Hester, Eds. (Heyden, London, 1978), Vol. 5, Chap. 4.

7. L. Stryer, "Biochemistry" (W. H. Freeman and Co., San Francisco, 1981).

8. D. Shugar and K. Szczepaniak, Int. J. Quantum Chem. 20, 573 (1981).

9. C. L. Angell, J. Chem. Soc. 504 (1961).

10. R. C. Lord and G. J. Thomas,Jr., Spectrochim. Acta 23A, 2551 (1967).

11. R. C. Lord and G. J. Thomas,Jr., Biochim. Biophys. Acta 142, 1 (1967).

12. H. Susi and J. S. Ard, Spectrochim. Acta 27A, 1549 (1971).

13. H. Susi and J. S. Ard, Spectrochim. Acta 30A, 1843 (1974).

14. Y. Nishimura, M. Tsuboi, S. Kato, and K. Morokuma, J. Am. Chem. Soc. 103, 1354 (1981).

15. W. D. Bowman and T. G. Spiro, J. Chem. Phys. 73, 5482 (1980).

16. M. Szczesniak, M. J. Nowak, H. Rostkowska, K. Szczepaniak, W. B. Person, and D. Shugar, J. Am. Chem. Soc. 105, 5969 (1983).

17. S. Chin, I. Scott, K. Szczepaniak, and W. B. Person, J. Am. Chem. Soc. 106, 3415 (1984).

18. K. Szczepaniak, M. Szczesniak, M. Nowak, I. Scott, S. Chin, and W. B. Person, Int. J. Quantum Chem.: Quantum Chem. Symp. 18, 547 (1984).

19. M. Szczesniak, M. J. Nowak, K. Szczepaniak, S. Chin, I. Scott, and W. B. Person, Spectrochim. Acta 41A, 223 (1985).

20. M. Szczesniak, M. J. Nowak, K. Szczepaniak, and W. B. Person, Spectrochim. Acta 41A, 237 (1985).

21. E. B. Wilson,Jr., J. C. Decius, and P. C. Cross, "Molecular Vibrations" (McGraw-Hill, New York, 1955).

22. T. Miyazawa, J. Chem. Phys. 29, 246 (1958).

23. W. B. Person and J. H. Newton, J. Chem. Phys. 61, 1040 (1974).

24. G. Herzberg, "Infrared and Raman Spectra of Polyatomic Molecules" (Van Nostrand Reinhold Co., New York, 1945).

25. S. Califano, "Vibrational States" (Wiley, New York, 1976).

26. I. W. Levin and R. A. R. Pearce, in "Vibrational Spectra and Structure," J. R. Durig, Ed. (Elsevier Scientific Publishing Co., Amsterdam, 1975), Vol. 4, Chap. 3.

27. F. A. Cotton, "Chemical Applications of Group Theory" (Wiley, New York, 1971).

28. S. Chin, Ph.D. Dissertation, University of Florida, 1984.

29. W. B. Person and B. Crawford,Jr., J. Chem. Phys. 26, 1295 (1957).

30. J. H. Wilkinson, "The Algebraic Eigenvalue Problem" (Oxford University Press, London, 1965).

31. Y. Morino and K. Kuchitsu, J. Chem. Phys. 20, 1809 (1952).

32. J. H. Newton, R. A. Levine, and W. B. Person, J. Chem. Phys. 67, 3282 (1977).

33. J. Overend, in "Infrared Spectroscopy and Molecular Structure," M. Davies, Ed. (Elsevier, Amsterdam, 1963), Chap. 10.

34. L. A. Curtiss and J. A. Pople, J. Mol. Spectrosc. 48, 413 (1973).

35. C. Eckart, Phys. Rev. 47, 552 (1935).

36. A. Sayvetz, J. Chem. Phys. 6, 383 (1939).

37. S. Chin and W. B. Person, J. Phys. Chem. 88, 553 (1984).

38. W. B. Person, in "Vibrational Intensities in Infrared and Raman Spectroscopy," W. B. Person and G. Zerbi, Eds. (Elsevier Scientific Publishing Co., Amsterdam, 1982), Chap. 4.

39. J. D. Rogers, Ph.D. Dissertation, University of Florida, 1980.

40. Y. Suagawara, A. Y. Hirakawa, M. Tsuboi, S. Kato, and K. Morokuma Chem. Phys. 62, 339 (1981).

41. A. Muller, in "Vibrational Spectroscopy: Modern Trends," A. J. Barnes and W. J. Orville-Thomas, Eds. (Elsevier, Amsterdam, 1977), Chap. 12.

42. I. M. Mills, in "Infrared Spectroscopy and Molecular Structure," M. Davies, Ed. (Elsevier, Amsterdam, 1963), Chap. 5.

43. S. Kondo, T. Nakanaga, and S. Saeki, Spectrochim. Acta 35A, 181 (1979).

44. K. B. Wiberg and J. J. Wendoloski, J. Am. Chem. Soc. 98, 5465 (1976).

45. M. Gussoni, in "Vibrational Intensities in Infrared and Raman Spectroscopy," W. B. Person and G. Zerbi, Eds. (Elsevier Scientific Publishing Co., Amsterdam, 1982), Chap. 5.

46. Y. Sugawara, Y. Hamada, A. Y. Hirakawa, M. Tsuboi, S. Kato, and K. Morokuma, Chem. Phys. 50, 105 (1980).

47. C. Castiglioni, M. Gussoni, and G. Zerbi, J. Chem. Phys. 82, 3534 (1985).

48. W. B. Person and D. Steele, in "Molecular Spectroscopy," R. F. Barrow, D. A. Long, and D. J. Millen, Eds. (The Chemical Society, London, 1974), Vol. 2, p. 357.

49. L. A. Gribov, "Intensity Theory for Infrared Spectra of Polyatomic Molecules," English Translation (Consultants Bureau, New York, 1964).

50. L. M. Sverdlov, M. A. Kovner, and E. P. Krainov, "Vibrational Spectra of Polyatomic Molecules" (John Wiley and Sons, New York, 1974).

51. M. Gussoni, in "Advances in Infrared and Raman Spectroscopy," R. J. H. Clark and R. E. Hester, Eds. (Heyden, London, 1980), Vol. 6, p. 61.

52. P. L. Prasad and S. Singh, J. Chem. Phys. 67, 4384 (1977).

53. S. Abbate, M. Gussoni, G. Masetti, and G. Zerbi, J. Chem. Phys. 67, 1519 (1977).

54. A. Rupprecht, J. Mol. Spectrosc. 89, 356 (1981).

55. M. Gussoni, C. Castiglioni, and G. Zerbi, J. Phys. Chem. 88 600 (1984).

56. K. B. Wiberg and J. J. Wendoloski, J. Am. Chem. Soc. 100, 723 (1978).

57. J. C. Decius and G. B. Mast, J. Mol. Spectrosc. 70, 294 (1978).

58. W. M. A. Smit and A. J. van Straten, J. Mol. Spectrosc. 65, 202 (1977).

59. J. F. Biarge, J. Herranz, and J. Morcillo, An. R. Soc. Esp. Fis. Quim. A57, 81 (1961).

60. W. B. Person, in "Vibrational Intensities in Infrared and Raman Spectroscopy," W. B. Person and G. Zerbi, Eds. (Elsevier Scientific Publishing Co., Amsterdam, 1982), Chap. 14.

61. W. T. King, in "Vibrational Intensities in Infrared and Raman Spectroscopy," W. B. Person and G. Zerbi, Eds. (Elsevier Scientific Publishing Co., Amsterdam, 1982), Chap. 6.

62. W. T. King, G. B. Mast, and P. P. Blanchette, J. Chem. Phys. 56, 4440 (1972).

63. J. H. Newton and W. B. Person, J. Chem. Phys. 64, 3036 (1976).

64. W. B. Person, S. K. Rudys, and J. H. Newton, J. Phys. Chem. 79, 2525 (1975).

65. W. T. King and G. B. Mast, J. Phys. Chem. 80, 2521 (1976).

66. B. Zilles, Ph.D. Dissertation, University of Florida, 1980.

67. C. A. Coulson, "Valence" (Oxford University Press, London, 1961, 2nd. Edn.).

68. R. S. Mulliken, J. Chem. Phys. 23, 1833, 1841, 2338, 2343 (1955).

69. R. F. Stewart, Acta Cryst. 23, 1102 (1967).

70. R. Ditchfield, W. J. Hehre, and J. A. Pople, J. Chem. Phys. 54, 724 (1971).

71. W. J. Hehre, M. D. Newton, J. S. Binkley, R. A. Whiteside, P. C. Hariharan, R. Seeger, and J. A. Pople, "Gaussian 76 - An ab initio Molecular Orbital Program," as modified by Charles M. Cook, Program No. 391, Quantum Chemistry Program Exchange, Indiana University, Bloomington, IN. (1976).

72. I. Kulakowska, M. Geller, B. Lesyng, and K. L. Wierzchowski, Biochim. Biophys. Acta 361, 119 (1974).

73. P. Pulay, G. Fogarasi, and J. E. Boggs, J. Chem. Phys. 74, 3999 (1981).

74. K. B. Wiberg, V. A. Walters, K. N. Wong, and S. D. Colson, J. Phys. Chem. 88, 6067 (1984).

75. L. Harsanyi and P. Csaszar, Acta Chim. Acad. Sci. Hung. 113, 257 (1983).

76. P. Pulay, in "Applications of Electronic Structure Theory," H. F. Schaefer III, Ed. (Plenum, New York, 1977), p. 153.

77. G. Zerbi, in "Advances in Infrared and Raman Spectroscopy," R. J. H. Clark and R. E. Hester, Eds. (Heyden, London, 1980).

78. A. Mueller and N. Mohan, J. Mol. Spectrosc. 65, 482 (1977).

79. A. A. Chalmers and D. C. McKean, Spectrochim. Acta 22A, 251 (1966).

80. H. C. Allen,Jr. and P. C. Cross, "Molecular Vib-Rotors: The Theory and Interpretation of High Resolution Infrared Spectra" (Wiley, New York, 1963).

81. K. Kuchitsu and L. S. Bartell, J. Chem. Phys. 35, 1945 (1961).

82. S. J. Cyvin, "Molecular Vibrations and Mean Square Amplitudes" (Elsevier, Amsterdam, 1968).

83. D. R. Herschbach and V. W. Laurie, J. Chem. Phys. 40, 3142 (1964).

84. K. Kuchitsu, T. Oka, and Y. Morino, J. Mol. Spectrosc. 15, 51 (1965).

85. D. Steele, "Theory of Vibrational Spectroscopy" (W. B. Saunders Co., London, 1971).

86. T. Shimanouchi, in "Physical Chemistry: An Advanced Treatise," H. Eyring, D. Henderson, and W. Jost, Eds. (Academic Press, New York, 1970).

87. T. Shimanouchi, Y. Ogawa, M. Otha, H. Matsura, and I. Harada, Bull. Chem. Soc. Jpn. 49, 380 (1977).

88. J. L. Duncan, in "Molecular Spectroscopy: A Specialist Periodical Report," R. F. Barrow, D. A. Long, and D. J. Millen, Eds. (The Chemical Society, London, 1975), Vol. 3, Chap. 2.

89. T. Shimanouchi and I. Nakagawa, Ann. Rev. Phys. Chem. 23, 217 (1972).

90. J. Overend, Ann. Rev. Phys. Chem. 21, 265 (1970).

91. G. Zerbi, B. Crawford,Jr., and J. Overend, J. Chem. Phys. 38, 127 (1963).

92. C. D. Needham and J. Overend, Spectrochim. Acta, 22, 1383 (1966).

93. A. J. P. Alix, H. H. Eysel, B. Jordanov, R. Kebabcoglu, N. Mohan, and A. Muller, J. Mol. Struct. 27, 1 (1975).

94. A. Allan, J. L. Duncan, J. Holloway, and D. C. McKean, J. Mol. Spectrosc. 31, 368 (1969).

95. L. H. Jones, R. R. Ryan, and L. B. Asprey, J. Chem. Phys. 49, 581 (1968).

96. K. Machida and J. Overend, J. Chem. Phys. 55, 1157 (1971).

97. P. Pulay, G. Fogarasi, G. Pongor, J. E. Boggs, and A. Vargha, J. Am. Chem. Soc. 105, 7037 (1983).

98. C. E. Blom, L. P. Otto, and C. Altona, Mol. Phys. 32, 1137 (1976).

99. C. E. Blom and C. Altona, Mol. Phys. 33, 875 (1977).

100. C. E. Blom and C. Altona, Mol. Phys. 31, 1377 (1976).

101. G. Banheyi, P. Pulay, G. Fogarasi, J. Mol. Struct. THEOCHEM 89, 1 (1982).

102. S. von Carlowitz, W. Zeil, P. Pulay, and J. E. Boggs, J. Mol. Struct. 87, 113 (1982).

103. J. A. Pople, H. B. Schlegel, R. Krishnan, D. J. DeFrees, and J. S. Binkley, Int. J. Quantum Chem. Symp. 15, 269 (1981).

104. K. B. Wiberg, V. Walters, and S. D. Colson, J. Phys. Chem. 88, 4723 (1984).

105. C. E. Blom and C. Altona, Mol. Phys. 34, 177 (1977).

106. G. Pongor, P. Pulay, G. Fogarasi, and J. E. Boggs, J. Am. Chem. Soc. 106, 2765 (1984).

107. R. G. A. Maia, Ph.D. Dissertation, University of Florida, 1980.

108. O. M. Herrera, M. N. Ramos, and R. E. Bruns, Spectrochim. Acta 39A, 1111 (1983).

109. R. E. Bruns, Y. Hase, and I. M. Brin, J. Phys. Chem. 84, 3593 (1980).

110. J. H. Newton and W. B. Person, J. Chem. Phys. 68, 2799 (1978).

111. W. B. Person and J. Overend, J. Chem. Phys. 66, 1442 (1977).

112. W. G. Golden, D. A. Horner, and J. Overend, J. Chem. Phys. 68, 964 (1978).

113. J. H. Newton and W. B. Person, J. Phys. Chem. 82, 226 (1978).

114. R. O. Kagel, D. L. Powell, M. J. Hopper, J. Overend, M. N. Ramos, A. B. M. S. Bassi, and R. E. Bruns, J. Phys. Chem. 88, 521 (1984).

115. Y. Sugawara, A. Y. Hirakawa, M. Tsuboi, S. Kato, and K. Morokuma, private communication from Professor K. Morokuma.

116. I. Scott, unpublished work at the University of Florida.

117. M. Kitano and K. Kuchitsu, Bull. Chem. Soc. Japan 47, 631 (1974).

118. C. L. Khetrapal and A. C. Kunwar, J. Phys. Chem. 86, 4815 (1982).

BIOGRAPHICAL SKETCH

Ismael Scott-Lebron was born in Yabucoa, Puerto Rico. He attended the public school system in that small town. He then received a B.S. and a M.S. in chemistry from the University of Puerto Rico at Mayaguez Campus. He entered the Graduate School at the University of Florida in September of 1980 and received his Ph.D. in physical chemistry in May, 1986. Currently he is Assistant Professor of chemistry at the Inter American University of Puerto Rico at San German Campus.

Mr. Scott-Lebron is married to the former Evelyn Judith Sanchez, and they have two children: Christian and Krystina.

I certify that I have read this study and that in my opinion it conforms to acceptable standards of scholarly presentation and is fully adequate, in scope and quality, as a dissertation for the degree of Doctor of Philosophy.

Willis B. Person, Chairman
Professor of Chemistry

I certify that I have read this study and that in my opinion it conforms to acceptable standards of scholarly presentation and is fully adequate, in scope and quality, as a dissertation for the degree of Doctor of Philosophy.

Robert J. Hanrahan
Professor of Chemistry

I certify that I have read this study and that in my opinion it conforms to acceptable standards of scholarly presentation and is fully adequate, in scope and quality, as a dissertation for the degree of Doctor of Philosophy.

John R. Eyler
Associate Professor of Chemistry

I certify that I have read this study and that in my opinion it conforms to acceptable standards of scholarly presentation and is fully adequate, in scope and quality, as a dissertation for the degree of Doctor of Philosophy.

James Winefordner
Graduate Research Professor
of Chemistry

I certify that I have read this study and that in my opinion it conforms to acceptable standards of scholarly presentation and is fully adequate, in scope and quality, as a dissertation for the degree of Doctor of Philosophy.

Gar R. Hoflund

Gar Hoflund
Associate Professor of
Chemical Engineering

This dissertation was submitted to the Graduate Faculty of the Department of Chemistry in the College of Liberal Arts and Sciences to the Graduate School, and was accepted as partial fulfillment of the requirements for the degree of Doctor of Philosophy.

May 1986

Dean, Graduate School